KASTAMONU UNIVERSITY JOURNAL OF ENGINEERING AND SCIENCES

e-ISSN 2667-8209

VOL: 10 ISSUE:02

KASTAMONU UNIVERSITY JOURNAL OF ENGINEERING AND SCIENCES

e-ISSN 2667-8209

Kastamonu University Journal of Engineering and Science

Kastamonu University Journal of Engineering and Science publish as blind peer review and two times in a year.

Kastamonu University
Journal of Engineering and Science

Vol: 10 Issue: 2 December 2024 E-ISSN:2667-8209

Kastamonu University
Journal of Engineering and Science

Vol: 10 Issue: 2 December 2024 E-ISSN:2667-8209

Kastamonu University Faculty of Engineering and Architecture 37150 Kastamonu / TÜRKİYE
Tel: +(90)366 2802901 Fax: +(90)366 2802900

Web: https://dergipark.org.tr/tr/pub/kastamonujes
e-mail: kujes@kastamonu.edu.tr

This journal is published two times in a year.
June and December
Kastamonu University Journal of Engineering and Science
Indexed and Abstracted in: Dergipark

Kastamonu University
Journal of Engineering and Science

Vol: 10 Issue: 2 December 2024 E-ISSN:2667-8209

CONTENTS

doi:10.55385/kastamonujes.1555422 KUJES 10(2):52-56, 2024

Kastamonu University
Journal of Engineering and Sciences
e-ISSN 2667-8209
http://dergipark.gov.tr/kastamonujes

Cedrus atlantica's Usability for Reducing and Monitoring the Change in Lithium Pollution in the Air

Şemsettin Kulaç[a, *], Burak Arıcak[b], Ramazan Erdem[c]

[a] Faculty of Forestry, Department of Forest Engineering, Düzce University, Düzce, Türkiye
[b] Faculty of Forestry, Department of Forest Engineering, Bursa Technical University, Bursa, Türkiye
[c] Programs of Forestry and Forestry Products, Arac Rafet Vergili Vocational School Kastamonu University, Kastamonu, Türkiye
***Corresponding Author:** rerdem@kastamonu.edu.tr

Received: **September 24, 2024** ◆ Accepted: **December 10, 2024** ◆ Published Online: **December 25, 2024**

Abstract: The most important and harmful components of air pollution that affect the health and cause the death of millions of people every year around the world are heavy metals. Due to their potential harm, monitoring the change in the concentration of heavy metals in the air and reducing pollution are essential. This study aimed to determine the usability of *Cedrus atlantica* grown in Düzce, where heavy metal pollution is reported to be high, for monitoring and reducing the change in lithium pollution in the air. For this purpose, the change in Li concentration in *Cedrus atlantica* annuals grown in Düzce was evaluated in the 60-year period. As a result of the study, it was determined that Li pollution in the region has increased significantly in the last decade. The highest values were generally obtained in the north direction, and this result was interpreted as Li concentration originating from the highway in this direction, i.e., traffic. As a result of the study, *Cedrus atlantica* is a very suitable species for monitoring and reducing the change in Li pollution.

Keywords: Heavy metal, Lithium, Biomonitor, *Cedrus atlantica*, Düzce

Öz: Dünyada her yıl milyonlarca insanın sağlığına zarar veren ve ölümüne neden olan hava kirliliğinin en önemli ve zararlı bileşenleri ağır metallerdir. Potansiyel zararları nedeniyle havadaki ağır metal konsantrasyonundaki değişimin izlenmesi ve kirliliğin azaltılması esastır. Bu çalışmada, ağır metal kirliliğinin yüksek olduğu bildirilen Düzce'de yetiştirilen *Cedrus atlantica*'nın havadaki lityum kirliliğindeki değişimin izlenmesi ve azaltılmasında kullanılabilirliğini belirlemek amaçlanmıştır. Bu amaçla, Düzce'de yetiştirilen *Cedrus atlantica* yıllıklarındaki Li konsantrasyonundaki değişim 60 yıllık periyotta değerlendirilmiştir. Çalışma sonucunda, bölgedeki Li kirliliğinin son on yılda önemli ölçüde arttığı belirlenmiştir. En yüksek değerler genellikle kuzey yönünde elde edilmiş olup, bu sonuç Li konsantrasyonunun bu yöndeki karayolundan yani trafikten kaynaklandığı şeklinde yorumlanmıştır. Çalışma sonucunda, Cedrus atlantica'nın Li kirliliğindeki değişimin izlenmesi ve azaltılması için oldukça uygun bir tür olduğu ortaya çıkmıştır.

Anahtar Kelimeler: Ağır metal, Lityum, Biomonitor, *Cedrus atlantica*, Düzce

1. Introduction

Today, air pollution is one of the most critical problems worldwide (SOURCE). Air pollution causes approximately 6 million premature births, 3 million low-weight babies, and 7 million premature deaths worldwide [1]. It is stated that approximately 2.5 million living spaces are polluted throughout Europe, 90 percent of the world's population breathes polluted air, and one in every 8 deaths is related to air pollution [1-3]. Air pollution also has an unfavorable impact on global climate change [4]. Moreover, global climate change with urbanization is now defined as irreversible problems [5-6].

The most dangerous and harmful components of air pollution are heavy metals. Therefore, many studies have been conducted on known and widespread heavy metals such as Cr [7], Ni [8], and Cd [9]. However, in recent years, in addition to heavy metals such as Pd [1], Ba [10] and Sb [11], which are extremely harmful even at low concentrations, many studies have been conducted on heavy metals such as Fe [12], Al [13], Cu [14], Mg [15] and Zn [16], which are necessary as nutrients for living things but can be harmful at high concentrations. Studies have shown that heavy metals are harmful to living things above a certain concentration in all cases [17] and become more harmful when taken into the human body through the respiratory tract [3]. Therefore, monitoring the change in heavy metal concentration in the air and reducing pollution is essential.

This study investigated the usability of *Cedrus atlantica* in monitoring the change of lithium (Li) pollution in the air and reducing pollution. Lithium has no known biological use and does not appear to be an essential element for life. The Australia Inventory of Chemical Substances has classified metallic lithium as a health, physiochemical, and/or

ecotoxicological hazard according to the National Occupational Health and Safety Commission (NOHSC) approved criteria for classifying hazardous substances. Lithium, lithium aluminum hydride, and lithium methanolate are hazardous substances found on the Danish list [19]. When the Li element is released, it can very quickly join the food chain. Since it mixes with water and can replace other elements, it can be taken up very quickly by the living body and can threaten living life [19].

2. Material and Method

The study was carried out on a *Cedrus atlantica* growing in Düzce province, one of Europe's 5 most polluted cities, according to the World Air Pollution Report 2021 [7]. The topography and meteorological parameters of Düzce province, located in the Western Black Sea province of Türkiye, play a part in the increased air pollution. The primary pollutants that cause air pollution in Düzce arise from industrial facilities, domestic fuel use, and vehicle traffic load. In 2022, log samples taken outside the vegetation season by determining the north direction were brought to the laboratory, and the surface was smoothed. Annual rings were examined and determined that the tree was 60 years old. Annual rings were grouped over five years, and sawdust samples were taken from each group of wood (WD), as well as the inner bark (IB) and outer bark (OB), with the help of a steel drill. The samples were dried in a 45 °C oven and subjected to pre-combustion. Then, Li concentrations were determined with the ICP-OES device. This method is one of the most frequently used methods in previous studies in this field [20]. Variance analysis was applied to the obtained data with the help of the SPSS package program and evaluated with the Duncan test.

3. Results

The average values and statistical analysis results regarding the changes in Li concentration in cedar based on organs and directions are given in Table 1.

Table 1. Changes in Li concentration (ppb) in cedar based on organs and directions

Organ	North	East	South	West	F	Mean
OB	85478.3 aC	84118.9 B	91137.2 bD	81804.8 A	172.2***	85634.8 A
IB	191371.1 bC	81922.8 A	85328.3 aB	85248.0 B	4057.7***	110967.5 B
WD	107033.7 aB	81331.0 A	88713.0 abA	83586.2 A	12.3***	90353.9 A
F	8.3**	1.1 ns	4.2*	0.2 ns		4.4*
Mean	111518.1 b	81590.9 a	88644.4 a	83577.6 a	16.8***	

*Different letters following each other represent the statistical difference at p≤0.05. Uppercase letters represent from top to bottom direction while lowercase letters from right to left. ns=not significant. *<0.05. **<0.01 ***<0.001. This explanation is valid for all tables*.

When the table results are examined, it is seen that the change in Li concentration in cedar is statistically significant in all organs in direction and directions other than east and west. The highest value was obtained in the inner bark when looking at the organs according to average values. Similarly, the highest value was obtained in the north direction when looking at the directions according to average values. The change in Li concentration by period and direction is given in Table 2.

Table 2. Change in Li concentration (ppb) in cedar by period and direction

Age	North	East	South	West	F	Mean
2018-2022	190299.2 fB	82103.6 bcdA	81897.8 aA	86362.9 cA	1514.0***	110165.9 B
2013-2017	191938.6 fB	81066.2 bcdA	87410.1 bcA	88396.2 cA	5925.1***	122581.6 B
2008-2012	98932.8 eC	72725.9 aA	86722.4 bB	87138.6 cB	87.3***	86379.9 A
2003-2007	93733.1 dD	80069.5 bA	88515.5 cdC	86206.2 cB	166.9***	87131.1 A
1998-2002	92101.6 cdC	80255.7 bA	88929.0 deBC	87291.4 cB	25.4***	87144.4 A
1993-1997	90811.4 bcdC	80395.5 bA	88488.9 cdB	86921.7 cB	51.1***	86654.4 A
1988-1992	88344.6 abB	81862.2 bcA	89026.2 deB	87043.2 cB	11.5**	86569.0 A
1983-1987	89443.8 abcC	83372.5 cdeA	90085.5 efC	86730.1 cB	18.2**	87408.0 A
1978-1982	87859.1 abB	82293.8 bcdeA	91008.7 fgC	86761.8 cB	43.2***	86980.8 A
1973-1977	86463.5 aBC	82884.4 cdeB	90005.0 efC	67305.7 aA	50.6***	81664.6 A
1968-1972	87554.3 abC	84240.9 deB	90962.5 fgD	76294.3 bA	47.5***	84763.0 A
1963-1967	86922.2 aC	84436.5 eB	91504.2 gD	76581.9 bA	113.2***	84861.2 A
F	1318.0***	21.6***	38.2***	27.4***		3.8***

When Table 2 is examined, it is seen that the change in Li concentration in cedar is statistically significant in all periods, directionally and in all directions, period by period. When the periods are examined according to the average values, it is

striking that there has been a significant increase in the last 10 years. When it is examined in terms of direction, it is seen that the highest values are generally obtained in the north direction.

4. Discussion

As a result of the study, it was determined that cedar trees can accumulate significant amounts of Li in both wood and bark. Two significant results were obtained from the current study. The first is that there has been a significant increase in Li concentration in the last decade, and the second is that the highest values were obtained in the north direction. When these results are compared with the studies conducted to date, it can be said that they are generally consistent. Namely, the highest values obtained in the north direction can be interpreted as Li pollution caused by traffic. Because one of the busiest highways in Türkiye passes from the north of the study area, there is a heavy traffic flow. In many studies, it is frequently stated that traffic is one of the most important sources of heavy metal pollution [21, 22].

As a result of the study, it was determined that Li pollution in the air has increased significantly in the last decade. Li has been widely preferred in the innovative industry of recent times. It is used in organic synthesis, glass, plastic, and aluminum production, radio engineering, computers, cameras, phone batteries, electronics, and laser devices. With the increase in Li use in these areas, the amount of Li in the biosphere also increases [23]. Studies have shown that Li accumulation in plants can be caused by traffic [24]. The accumulation of heavy metals in trees, especially in organs such as outer bark and leaves, is associated with particulate matter. After heavy metals leave their source, they infect particulate matter in the air, and particulate matter that becomes a heavy metal sink can lead to serious health problems [25]. Especially in urban areas, the number of people living per unit area is much higher. Since air pollution factors such as heavy metals and particulate matter pollution are also relatively high in these areas, pollution in urban areas directly affects the health of many people [14-26]. According to data from the European Environment Agency, fine particulate pollutants in the atmosphere caused the deaths of more than 400,000 people in 2018. Over 1200 deaths in people under 18 years of age are estimated to be caused by air pollution every year in EEA member and collaborating countries [27]. Many of these deaths are caused by particulate matter contaminated with heavy metals [10].

Particulate matter contaminated with heavy metals also helps heavy metals enter the plant body. As it is known, heavy metals can enter the plant body from leaves, roots, or stem sections [9]. Particulate matter contaminated with heavy metals adheres to the leaves or bark and facilitates the entry of heavy metals into the plant body.

As a result of the current study, Li concentrations in cedar trees were very high. This result shows that cedar can be used effectively to reduce Li pollution. This result is significant because studies show that each tree has a different heavy metal accumulation potential level. Therefore, species that can be used in monitoring and reducing pollution should be determined separately for each heavy metal [10]. Because the potential of plants to absorb and accumulate heavy metals depends on many factors that affect each other. For example, heavy metal accumulation depends on plant physiology, and plant physiology is shaped by the interaction of genetic structure [28-29] and environmental conditions [11-30]. Therefore, all factors affecting plant physiology also affect the entry and accumulation of heavy metals into the plant, which is shaped by the interaction of many interrelated factors such as genetic structure [4], edaphic [31], climatic factors [5-22], stress factors [32].

After heavy metals enter the plant body, the transport of elements within the wood part is primarily related to the cell structure and especially the cell wall (apoplastic pathway). Cell wall proteins (CWP) in plants come into play in various abiotic stresses [11]. Plants frequently face stress factors in their lives. The most common stress factors that plants encounter are high or low temperatures [34] and climatic factors [34]. Drought, in particular, is the factor that stresses plants the most [35], and it is stated that the effects of this factor will be felt more intensely with the impact of global climate change [5-36]. The presence of stress factors changes the environmental conditions where plants grow, thus affecting plant development in many ways. This change also directly affects the process of plants absorbing and accumulating heavy metals.

5. Conclusion and Suggestion

The study resulted in the highest Li concentrations in the north direction, which was interpreted as the Li concentration originating from the highway in this direction, namely traffic. Regarding public health, heavy metal pollution from the highway in question should be prevented from affecting residential areas. For this purpose, it is recommended to place barriers on the sides of the highway and, if possible, to plant live fences. The Li concentration in the species in question was very high in the woods. This result shows that *Cedrus atlantica* can be used effectively to reduce Li pollution. Cultivating *Cedrus atlantica* in areas with high levels of Li pollution can help reduce Li pollution.

Li is a heavy metal yet to be studied sufficiently despite being extremely important for human and environmental health. The study results show that the Li concentration in the air has increased significantly, especially in recent years. Therefore, more research should be done on the effects of the Li element, monitoring and reducing its pollution, and research on the subject should be diversified and continued by increasing.

Conflict of Interest

All authors certify that they have no affiliations with or involvement in any organization or entity with any financial interest or non-financial interest in the subject matter or materials discussed in this manuscript.

Ethics Committee Approval

Ethics committee approval is not required.

Author Contribution

Conceptization: ŞK, BA, RE; methodology and laboratory analyzes: BA, RE; writing draft: ŞK, BA, RE; proof reading and editing. All authors have read and agreed to the published version of manuscript.

Acknowledgements

Not applicable.

5. References

[1] Şevik, H., Yildiz, Y., Ozel, H.B. (2024). Phytoremediation and Long-term Metal Uptake Monitoring of Silver, Selenium, Antimony, and Thallium by Black Pine (Pinus nigra Arnold), BioResources, 19(3). 4824-4837.

[2] Işınkaralar, K., Işınkaralar, Ö., & Şevik, H. (2022). Usability of some landscape plants in biomonitoring technique: an anaysis with special regard to heavy metals. Kent Akademisi, 15(3), 1413-1421.

[3] Sevik, H., Koç, İ. & Cobanoglu, H. (2024). Determination of Some Exotic Landscape Species As Biomonitors That Can Be Used for Monitoring and Reducing Pd Pollution in the Air. Water Air Soil Pollut 235, 615.

[4] Erturk, N., Aricak, B., Sevik, H., & Yigit, N. (2024). Possible Change in Distribution Areas of Abies in Kastamonu due to Global Climate Change. Kastamonu University Journal of Forestry Faculty, 24 (1), 81-91.

[5] Isinkaralar, O., Isinkaralar, K., Sevik, H., & Küçük, Ö. (2024). Spatial modeling the climate change risk of river basins via climate classification: a scenario-based prediction approach for Türkiye. Natural Hazards, 120(1), 511-528.

[6] Cantürk, U., Koç, İ., Özel, H. B., & Şevik, H. (2024). Possible changes of Pinus nigra distribution regions in Türkiye with the impacts of global climate change. BioResources, 19(3), 6190- 6214.

[7] Bayraktar, E. P., Isinkaralar, O., & Isinkaralar, K. (2022). Usability of several species for monitoring and reducing the heavy metal pollution threatening the public health in urban environment of Ankara. World Journal of Advanced Research and Reviews, 14(3), 276-283.

[8] Key, K., Kulaç, Ş., Koç, İ., & Sevik, H. (2023). Proof of concept to characterize historical heavy-metal concentrations in atmosphere in North Turkey: determining the variations of Ni, Co, and Mn concentrations in 180-year-old Corylus colurna L.(Turkish hazelnut) annual rings. Acta Physiologiae Plantarum, 45(10), 120.

[9] Cobanoglu, H., Sevik, H., & Koç, İ. (2023). Do Annual Rings Really Reveal Cd, Ni, and Zn Pollution in the Air Related to Traffic Density? An Example of the Cedar Tree. Water, Air, & Soil Pollution, 234(2), 65.

[10] Koç, İ., Canturk, U., Isinkaralar, K., Ozel, H. B., & Sevik, H. (2024). Assessment of metals (Ni, Ba) deposition in plant types and their organs at Mersin City, Türkiye. Environmental Monitoring and Assessment, 196(3), 282.

[11] Canturk, U., Koç, İ., Ozel, H.B. , Sevik, H. (2024). Identification of proper species that can be used to monitor and decrease airborne Sb pollution. Environ Sci Pollut Res (2024). https://doi.org/10.1007/s11356-024-34939-7

[12] Işınkaralar, Ö., Işınkaralar, K., Şevik, H., & Küçük, Ö. (2023). Bio-climatic Comfort and Climate Change Nexus: A Case Study in Burdur Basin. Kastamonu University Journal of Forestry Faculty, 23(3), 241-249.

[13] Kuzmina, N., Menshchikov, S., Mohnachev, P., Zavyalov, K., Petrova, I., Ozel, H. B., Aricak, B., Onat, S. M., and Sevik, H. (2023). Change of aluminum concentrations in specific plants by species, organ, washing, and traffic density, BioResources 18(1), 792-803.

[14] Istanbullu, S. N., Sevik, H., Isinkaralar, K., & Isinkaralar, O. (2023). Spatial Distribution of Heavy Metal Contamination in Road Dust Samples from an Urban Environment in Samsun, Türkiye. Bulletin of Environmental Contamination and Toxicology, 110(4), 78.

[15] Erdem, R., Koç, İ., Çobanoglu, H., & Şevik, H. (2024). Variation of Magnesium, One of the Macronutrients, in Some Trees Based on Organs and Species. Forestist, 74(1); 84-93

[16] Isinkaralar, O., Isinkaralar, K., & Bayraktar, E. P. (2023). Monitoring the spatial distribution pattern according to urban land use and health risk assessment on potential toxic metal contamination via street dust in Ankara, Türkiye. Environmental Monitoring and Assessment, 195(9), 1085.

[17] Isinkaralar, K., Isinkaralar, O., Koç, İ., Özel, H. B., & Şevik, H. (2024). Assessing the possibility of airborne bismuth accumulation and spatial distribution in an urban area by tree bark: A case study in Düzce, Türkiye. Biomass conversion and biorefinery, 14(18), 22561-22572.

[18] Aral, H., & Vecchio-Sadus, A. (2008). Toxicity of lithium to humans and the environment—a literature review. Ecotoxicology and environmental safety, 70(3), 349-356.

[19] Özel, H. B., Şevik, H., Yıldız, Y., & Çobanoğlu, H. (2024). Effects of Silver Nanoparticles on Germination and Seedling Characteristics of Oriental Beech (Fagus orientalis) Seeds. BioResources, 19(2). 2135-2148.

[20] Isinkaralar, K. (2022). Some atmospheric trace metals deposition in selected trees as a possible biomonitor. Romanian Biotechnological Letters, 27(1), 3227-3236.

[21] Guney, D., Koc, I., Isinkaralar, K., & Erdem, R. (2023). Variation in Pb and Zn concentrations in different species of trees and shrubs and their organs depending on traffic density. Baltic Forestry, 29(2), id661-id661.

[22] Respondek, Z., Isinkaralar, O., Świsłowski, P., Isinkaralar, K., & Rajfur, M. (2024). Biomonitoring with the Use of the Herbal Plant Taraxacum officinale as a Source of Information on Environmental Contamination. Plants, 13(13), 1805.

[23] Kashin VK. (2019). Lithium in soils and plants of Western Transbaikalia. Eurasian Journal of Soil Science, 52(4); 359-369.

[24] Işınkaralar, K., & Erdem, R. (2022). The effect of atmospheric deposition on potassium accumulation in several tree species as a biomonitor. Environmental Research and Technology, 5(1), 94-100.

[25] Isinkaralar, K., Koç, İ., Kuzmina, N. A., Menshchikov, S. L., Erdem, R., & Aricak, B. (2022). Determination of heavy metal levels using Betula pendula Roth. under various soil contamination in Southern Urals, Russia. International journal of environmental science and technology, 19(12), 12593-12604.

[26] Şen, G., Güngör, E., & Şevik, H. (2018). Defining the effects of urban expansion on land use/cover change: a case study in Kastamonu, Turkey. Environmental monitoring and assessment, 190, 1-13.

[27] EEA, 2024, Air pollution, https://www.eea.europa.eu/en/topics/in-depth/air-pollution

[28] Hrivnák, M., Krajmerová, D., Paule, L., Zhelev, P., Sevik, H., Ivanković, M., Goginashvili, N., Paule, J., Gömöry, D. (2024). Are there hybrid zones in Fagus sylvatica L. sensu lato?. Eur J Forest Res 143, 451–464.

[29] Kurz, M., Koelz, A., Gorges, J., Carmona, B. P., Brang, P., Vitasse, Y., ... & Csillery, K. (2023). Tracing the origin of Oriental beech stands across Western Europe and reporting hybridization with European beech–Implications for assisted gene flow. Forest Ecology and Management, 531, 120801.

[30] Özdikmenli, G., Yiğit, N., Özel, H. B., and Şevik, H. (2024). Altitude-dependent Variations in Some Morphological and Anatomical Features of Anatolian Chestnut. BioResources, 19(3), 4635-4651.

[31] Işınkaralar, K., & Erdem, R. (2021). Changes of calcium content on some trees in Kocaeli. Kastamonu University Journal of Engineering and Sciences, 7(2), 148-154.

[32] Koç, İ., & Nzokou, P. (2022). Gas exchange parameters of 8-year-old Abies fraseri (Pursh) Poir. seedlings under different irrigation regimes. Turkish journal of agriculture-food science and technology, 10(12), 2421-2429.

[33] Isinkaralar, K., & Erdem, R. (2021). Landscape plants as biomonitors for magnesium concentration in some species. International Journal of Progressive Sciences and Technologies, 29(2), 468-473.

[34] Çobanoglu, H., Canturk, U., Koc, I., Kulac, S., Sevik, H. (2024). Climate Change Effect on Potential Distribution of Anatolian Chestnut (Castanea sativa Mill.) in the Upcoming Century in Türkiye, Forestist, 73(3), 247-256

[35] Koç, İ. (2022). Determining the biocomfort zones in near future under global climate change scenarios in Antalya. Kastamonu University Journal of Engineering and Sciences, 8(1), 6-17.

[36] Ertürk, N., Arıcak, B., Yiğit, N., & Sevik, H. (2024). Potential changes in the suitable distribution areas of fagus orientalis lipsky in kastamonu due to global climate change. Forestist, 74, 159-165.

doi:10.55385/kastamonujes.1556643 KUJES 10(2):57-62, 2024

Kastamonu University
Journal of Engineering and Sciences
e-ISSN 2667-8209
http://dergipark.gov.tr/kastamonujes

Usage of *Robinia pseudoacacia* and *Cedrus atlantica* in Monitoring and Reduction of Change of Niobium Pollution in Air

Hatice Çobanoğlu [a, *], Ramazan Erdem[b], Şemsettin Kulaç [c]

[a]Department of Forest Engineering, Düzce University, Düzce, Türkiye
[b]Programs of Forestry and Forestry Products, Arac Rafet Vergili Vocational School Kastamonu University, Kastamonu, Türkiye
[c]Department of Forest Engineering, Düzce University, Düzce, Türkiye
***Corresponding Author:** haticecobannoglu@gmail.com

Received: **September 26, 2024** ◆ Accepted: **December 11, 2024** ◆ Published Online: **December 25, 2024**

Abstract: In this study, it was aimed to monitor the change in niobium (Nb) pollution, one of the heavy metals that can be harmful and toxic for human and environmental health, and to determine the usability of *Robinia pseudoacacia* and *Cedrus atlantica* species, which were determined to be biomonitors, in reducing Nb pollution.Within the scope of the study, samples were taken from the main stem of Robinia pseudoacacia and Cedrus atlantica, which grow under similar growing conditions in Düzce province, which is among the 5 most polluted cities in Europe according to the 2021 World Air Pollution report, and Nb concentrations were determined. As a result of the study, it was determined that *Cedrus atlantica* is suitable for monitoring the change in Nb concentration and *Robinia pseudoacacia* is suitable for reducing Nb pollution.

Keywords: Heavy metal, niobium, Atlas cedar, Black locust

Öz: Bu çalışmada, insan ve çevre sağlığı için zararlı ve toksik olabilen ağır metallerden biri olan niyobyum (Nb) kirliliğindeki değişimin izlenmesi ve *Robinia pseudoacacia* ve *Cedrus atlantica*'nın kirliliğin azaltılmasında kullanılabilirliğinin belirlenmesi amaçlanmıştır. Çalışma kapsamında 2021 Dünya Hava Kirliliği raporuna göre Avrupa'da havası en kirli 5 şehir arasında yer alan Düzce ilinde benzer yetişme koşullarında yetişen *Robinia pseudoacacia* ve *Cedrus atlantica*'nın ana gövdesinden örnekler alınarak Nb konsantrasyonları belirlendi. Çalışma sonucunda *Cedrus atlantica*'nın Nb konsantrasyonundaki değişimi izlemek için uygun olduğu, *Robinia pseudoacacia*'nın ise Nb kirliliğini azaltmak için uygun olduğu tespit edilmiştir.

Anahtar Kelimeler: Ağır metal, niyobyum, Atlas sediri, Yalancı akasya

1. Introduction

Air pollution, which has increased in the last century due to anthropogenic sources, especially industrial activities, is one of the most important global problems. It is stated that air pollution causes the death of approximately 7 million people every year [1], 6 million premature births, and 3 million low-weight babies [2]. It is stated that 92 percent of the world's population breathes polluted air, one in every 8 deaths is related to air pollution [3, 4], and air pollution is also one of the most important causes of global climate change [5]. Anthropogenic sources mainly cause air pollution and seriously threaten human health, especially in urban areas with high population density.

Studies conducted in recent years have shown that urbanization, like global climate change, is now an irreversible problem [6, 7]. The fact that more people live per unit area in urban areas and that pollution factors such as traffic, fuel burning, and garbage are very common in these areas causes the environment and especially air pollution, to affect human health more [8, 9].

Heavy metals are the most important and threatening components of air pollution [10]. Moreover, the concentrations of heavy metals in the air, which can be toxic and fatal to living things even at low concentrations, are constantly increasing due to anthropogenic sources [11]. Therefore, monitoring the change in heavy metal pollution in the air and studies on reducing pollution are among the priority research topics [12]. Therefore, many studies have been conducted on known and widely used heavy metals such as Cr [12], Co, Ni [13], and Cd [1]. However, in recent years, in addition to heavy metals such as Ba [4], Pd [14], and Sb [15], which are extremely harmful even at low concentrations, many studies have been conducted on heavy metals such as Fe [8], Mg [16] and Zn [17], which are necessary as nutrients for living things but can be harmful at high concentrations.

However, many elements are still neglected in these studies. One element neglected in heavy metal studies is niobium (Nb). Nb and its compounds can be toxic [18].

Moreover, it is known that heavy metals can be much more harmful when inhaled [19]. Indeed, when Nb is inhaled, it primarily adheres to the lungs and secondarily to the bones and interferes with calcium as an activator of enzyme systems. In laboratory animals, it has been determined that inhalation of niobium nitride and/or pentoxide causes lung scarring at exposure levels of 40 mg/m^3 [18]. Therefore, reducing Nb pollution in the air is of great importance. In this study, the wood of *Robinia pseudoacacia* and *Cedrus atlantica* species, which are frequently grown in urban areas, were examined to determine whether Nb accumulation occurs. In addition, it was aimed to determine the changes in Nb pollution levels until 2022, taking into account the pollution rates in the past years. As a result of the study, it is estimated that these data will increase towards 2022 and will differ according to the directions.

2. Material and Method

The study was carried out on trees growing in the city center of Düzce, among Europe's 5 most polluted cities [20, 21]. Materials taken from the main trunks of *Robinia pseudoacacia* (Black locust) and *Cedrus atlantica* (Atlas cedar) species were used in the study. These species are frequently used in landscape studies in Türkiye and Europe. Log samples were taken at the end of the vegetation season in 2022 by determining the north direction and brought to the laboratory, and the surface was smoothed. When the annual rings were examined, it was determined that the trees were 60 years old.

The annual rings were grouped over five years, and sawdust samples were taken from each group of wood (WD), inner bark (IB), and outer bark (OB) with the help of a steel drill. The study was conducted in 3 replications. Thus, 12 wood and bark samples from each species (12 wood, 1 outer bark, 1 inner bark) * 4 directions * 3 replicates, 144 samples were analyzed. Since there were 2 species in the study, a total of 288 samples were analyzed. The samples were dried in an oven at 45 °C, sorted and pre-burned. After pre-treatment, 65% HNO_3 and 30% H_2O_2 were added to the 0.5 g weighed samples. The chemically treated samples were incinerated at 200 °C. Then pure water was added to the burned samples and after reaching the desired level for measurement, they were analyzed with ICP-OES device and Nb concentrations were determined. This method is one of the most frequently used methods in previous studies in this field [2-21]. Variance analysis was applied to the obtained data with the help of the SPSS package program, and the data was evaluated using the Duncan test, simplified, tabulated, and interpreted.

3. Result

According to the average values and statistical analysis results regarding the change of Nb concentration in *Robinia pseudoacacia* based on organ and direction are given in Table 1.

Table 1. Change of Nb concentration (ppb) in *Robinia pseudoacacia* based on organ and direction

Organ	East	South	West	F	Mean
Ob	54278.1 a	56027.2	53004.4	3.9 ns	54436.6
Ib	56758.8 b	54709.5	52613.6	5.0 ns	54694.0
Wd	53448.7 a	55112.5	52750.8	3.7	53770.6
F	9.5***	0.5 ns	0.0 ns		1.7 ns
Mean	53744.3	55149.0	52759.1	0.2 ns	

*Different letters following each other represent the statistical difference at p≤0.05. Uppercase letters represent from right to left direction while lowercase letters from top to bottom. ns=not significant. *<0.05. **<0.01. ***<0.001. This explanation is valid for all tables.*

As a result of the analyses, all samples' Nb concentrations in the north direction remained below the detectable limits. When the table results are examined, it is seen that the change in Nb concentration in all directions on an organ basis and in all organs on a direction basis is statistically insignificant (p>0.05). The average values and statistical analysis results regarding the change in Nb concentration in *Robinia pseudoacacia* on a period and direction basis are given in Table 2.

Table 2. Change in Nb concentration (ppb) in *Robinia pseudoacacia* on a period and direction basis

Period	East	South	West	F	Mean
2018-2022	54903.7	55044.0	53881.4 cde	0.7 ns	54609.7
2013-2017	52776.9	55440.2	54604.9 e	2.3 ns	54274.0
2008-2012	53829.9	55119.6	52560.7 abc	1.8 ns	53836.7
2003-2007	53481.5	55707.6	54128.1 de	4.6 ns	54439.0
1998-2002	52128.4	54802.6	52065.5 ab	3.2 ns	52998.8
1993-1997	53680.3	55151.2	52926.3 bcd	3.3 ns	53919.3
1988-1992	52484.7 A	55148.3 B	52506.1 abcA	7.3*	53379.7
1983-1987	53279.2	54388.6	52414.4 abc	1.5 ns	53360.7
1978-1982	53639.8	55937.3	52848.0 abcd	4.5 ns	54141.7
1973-1977	53282.6 AB	54805.6 B	52032.2 abA	5.3*	53373.4
1968-1972	53964.8	54063.0	51250.1 a	3.6 ns	53092.6
1963-1967	53932.5 B	55741.5 C	51791.7 abA	5.4*	53821.9
F	1.1 ns	0.3 ns	4.2**		0.9 ns

The change in Nb concentration in *Cedrus atlantica* on an organ and direction basis is given in Table 3. When result is examined, it is seen that the change in Nb concentration in *Robinia pseudoacacia* woods is statistically significant only in the west direction on a period basis and only in the periods 1963-1967, 1973-1977, and 1988-1992 on a direction basis. Therefore, it can be said that the change in Nb concentration in *Robinia pseudoacacia* woods in terms of direction and period is statistically insignificant ($p>0.05$).

Table 3. The change in Nb concentration (ppb) in *Cedrus atlantica* on an organ and direction basis

Organ	North	East	South	West	F	Mean
OB	26418.8 aBC	25960.5 B	26808.4 C	25158.1 A	24.5***	26086.4 A
IB	56873.5 bC	24909.3 A	26191.1 B	25630.4 AB	2234.2***	33401.1 B
WD	31792.7 aB	24857.5 A	26292.0 A	25112.6 A	11.1***	27059.6 A
F	8.3**	1.5 ns	1.0 ns	0.1 ns		4.7*
Mean	33200.3 B	24946.4 A	26321.6 A	25152.8 A	15.7***	

According to Table 3, the change in Nb concentration in *Cedrus atlantica* based on organs is statistically significant only in the north direction. In terms of direction, the change in Nb concentration in all organs is statistically significant, and the highest values in all organs are obtained in the north direction. According to the average values, the data were collected in two groups; all directions were in the first group, while the value obtained in the north direction was in the second group. The change in Nb concentration in *Cedrus atlantica* based on period and direction is given in Table 4.

Table 4. Change in Nb concentration (ppb) in *Cedrus atlantica* based on period and direction

Period	North	East	South	West	F	Mean
2018-2022	56408.6 eB	25208.6 deA	25033.7 aA	25416.9 cA	1241.5***	33017.0 B
2013-2017	56384.6 eB	25119.3 deA	26383.9 bcdA	25845.4 cA	6182.5***	36204.6 B
2008-2012	29895.2 dC	21838.8 aA	26775.5 cdB	26079.1 cB	82.2***	26147.2 A
2003-2007	27173.8 bcC	24453.8 bA	25757.1 bB	26222.4 cB	38.7***	25901.8 A
1998-2002	27290.2 cC	24559.7 bcA	25865.2 bB	26231.2 cB	42.4***	25986.6 A
1993-1997	26727.9 abcB	24536.3 bcA	26099.1 bcB	26346.2 cB	16.8**	25927.4 A
1988-1992	26447.7 abcB	25017.0 cdA	26047.1 bcB	26007.8 cB	8.9**	25879.9 A
1983-1987	26763.4 abcC	25423.4 deA	26441.6 bcdBC	26226.7 cB	17.8**	26213.8 A
1978-1982	25925.5 aB	25255.3 deA	26930.9 dC	26525.8 cBC	15.1**	26159.4 A
1973-1977	26089.8 abB	25465.8 deB	26355.3 bcdB	20188.1 aA	36.4***	24524.7 A
1968-1972	26199.8 abcB	25632.3 efB	26749.0 cdB	23058.3 bA	16.4**	25409.9 A
1963-1967	26205.9 abcB	26042.0 fB	27065.2 dC	23203.1 bA	89.2***	25629.1 A
F	1070.6***	42.7***	6.6***	28.1***		3.8***

The change in Nb concentration in *Cedrus atlantica* is statistically significant in all periods in terms of direction and period. When the periods are examined according to the average values, it is striking that there has been a significant increase in the last 10-year period. Regarding direction, the highest values were generally obtained in the north direction.

4. Discussion

When the results obtained from the current study were evaluated, it was determined that there was a significant difference in Nb concentration among the species included. It was determined that the average Nb concentration, which was 53770.6 ppb in *Robinia pseudoacacia* woods, was 27059.6 ppb in *Cedrus atlantica* woods. This result shows that species' potential for Nb accumulation in woods varies significantly. This result has also been obtained in studies conducted to date, and it has been frequently emphasized that the potential for heavy metal accumulation varies significantly by species [22]. Because the potential of plants to absorb and accumulate heavy metals depends on many factors, such as the structure of the heavy metal and its interaction with the plant, as well as organ structure, weather conditions, and plant habitus [14].

These factors are also linked to other factors and to each other. For example, plant physiology is shaped by genetic structure [23-24] and environmental conditions [25]. Therefore, all factors affecting plant physiology also affect the entry and accumulation of heavy metals into the plant. Plant physiology is also shaped by the interaction of many factors affecting each other, such as genetic structure [26], edaphic [27], climatic [28] factors, stress factors [29]. Each of these factors primarily depends on the plant species and the responses of the plant species to environmental conditions.

As a result of the study, it was determined that there was no significant difference between the Nb concentrations in neighboring cell groups in *Robinia pseudoacacia* woods. At the same time, there was a significant difference between the Nb concentrations in neighboring cell groups in *Cedrus atlantica* woods. This situation can be interpreted as the Nb element can be displaced in *Robinia pseudoacacia* woods, but its displacement is limited in *Cedrus atlantica* woods. After heavy metals enter the plant body, their transport within the wood part is largely related to the cell structure, especially the cell wall (apoplastic pathway). Cell wall proteins (CWP) in plants come into play in various abiotic stresses [4].

Plants frequently face stress factors in their lives. The most common stress factors that plants encounter are high or low temperatures [29] and climatic factors [7]. Drought, in particular, is the factor that stresses plants the most [9, 30]. It is stated that the effects of drought will be felt more intensely with the impact of global climate change [6, 31]. The presence of stress factors changes the environmental conditions where plants grow, thus affecting plant development in many ways. This change directly affects the process of plants absorbing and accumulating heavy metals. These results are consistent with the literature. Studies show that the most important heavy metal sources are mining [3], traffic [17], industrial activities [13], agricultural activities [15] and urbanization [21]. Additionally, many studies are showing that air pollution has increased significantly in recent years [11].

5. Conclusion

As a result of the study, it was determined that there has been a significant increase in Nb concentration in *Cedrus atlantica* woods in the last decade. In addition, the highest Nb values in this species were obtained in the north direction. In the north of the area where the study was conducted, one of the busiest highways in Türkiye has a heavy traffic flow. These results show that the Nb concentration in the air increases due to traffic, and this increase has reached more serious levels in the last decade.

Conflict of Interest

All authors certify that they have no affiliations with or involvement in any organization or entity with any financial interest or non-financial interest in the subject matter or materials discussed in this manuscript.

Ethics Committee Approval

Ethics committee approval is not required.

Author Contribution

Conceptization: HÇ, RE, ŞK; methodology and laboratory analyzes: RE, ŞK; writing draft: HÇ, RE, ŞK; proof reading and editing: All authors have read and agreed to the published version of manuscript.

Acknowledgements

Not appliable.

5. References

[1] Cobanoglu, H., Sevik, H., & Koç, İ. (2023). Do Annual Rings Really Reveal Cd, Ni, and Zn Pollution in the Air Related to Traffic Density? An Example of the Cedar Tree. Water, Air, & Soil Pollution, 234(2), 65.

[2] Şevik, H., Yildiz, Y., Ozel, H.B. (2024). Phytoremediation and Long-term Metal Uptake Monitoring of Silver, Selenium, Antimony, and Thallium by Black Pine (Pinus nigra Arnold), BioResources, 19(3), 4824-4837.

[3] Kuzmina, N., Menshchikov, S., Mohnachev, P., Zavyalov, K., Petrova, I., Ozel, H. B., Aricak, B., Onat, S. M., and Sevik, H. (2023). Change of aluminum concentrations in specific plants by species, organ, washing, and traffic density, BioResources 18(1), 792-803.

[4] Koç, İ., Canturk, U., Isinkaralar, K., Ozel, H. B., & Sevik, H. (2024). Assessment of metals (Ni, Ba) deposition in plant types and their organs at Mersin City, Türkiye. Environmental Monitoring and Assessment, 196(3), 282.

[5] Erdem, R., Aricak, B., Cetin, M., & Sevik, H. (2023). Change in some heavy metal concentrations in forest trees by species, organ, and soil depth. Forestist, 73(3), 257-263.

[6] Isinkaralar, O., & Isinkaralar, K. (2023). Projection of bioclimatic patterns via CMIP6 in the Southeast Region of Türkiye: A guidance for adaptation strategies for climate policy. Environmental Monitoring and Assessment, 195(12), 1448.

[7] Erturk, N., Aricak, B., Sevik, H., & Yigit, N. (2024). Possible Change in Distribution Areas of Abies in Kastamonu due to Global Climate Change. Kastamonu University Journal of Forestry Faculty, 24(1), 81-91.

[8] Key, K., Kulaç, Ş., Koç, İ., & Sevik, H. (2022). Determining the 180-year change of Cd, Fe, and Al concentrations in the air by using annual rings of Corylus colurna L. Water, Air, & Soil Pollution, 233(7), 244.

[9] Cantürk, U., Koç, İ., Özel, H. B., & Şevik, H. (2024). Possible changes of Pinus nigra distribution regions in Türkiye with the impacts of global climate change. BioResources, 19(3), 6190- 6214.

[10] Isinkaralar, K., Isinkaralar, O., Koç, İ., Özel, H. B., & Şevik, H. (2024). Assessing the possibility of airborne bismuth accumulation and spatial distribution in an urban area by tree bark: A case study in Düzce, Türkiye. Biomass conversion and biorefinery, 14(18), 22561-22572.

[11] Özel, H. B., Şevik, H., Yıldız, Y., & Çobanoğlu, H. (2024). Effects of Silver Nanoparticles on Germination and Seedling Characteristics of Oriental Beech (Fagus orientalis) Seeds. BioResources, 19(2), 2135-2148.

[12] Sulhan, O. F., Sevik, H., & Isinkaralar, K. (2023). Assessment of Cr and Zn deposition on Picea pungens Engelm. in urban air of Ankara, Türkiye. Environment, development and sustainability, 25(5), 4365-4384.

[13] Istanbullu, S. N., Sevik, H., Isinkaralar, K., & Isinkaralar, O. (2023). Spatial Distribution of Heavy Metal Contamination in Road Dust Samples from an Urban Environment in Samsun, Türkiye. Bulletin of Environmental Contamination and Toxicology, 110(4), 78.

[14] Sevik, H., Koç, İ. & Cobanoglu, H. (2024). Determination of Some Exotic Landscape Species As Biomonitors That Can Be Used for Monitoring and Reducing Pd Pollution in the Air. Water Air Soil Pollut 235, 615.

[15] Respondek, Z., Isinkaralar, O., Świsłowski, P., Isinkaralar, K., & Rajfur, M. (2024). Biomonitoring with the Use of the Herbal Plant Taraxacum officinale as a Source of Information on Environmental Contamination. Plants, 13(13), 1805.

[16] Erdem, R., Koç, İ., Çobanoglu, H., & Şevik, H. (2024). Variation of Magnesium, One of the Macronutrients, in Some Trees Based on Organs and Species. Forestist, 74(1), 84-93.

[17] Işınkaralar, K., Işınkaralar, Ö., & Şevik, H. (2022). Usability of some landscape plants in biomonitoring technique: an anaysis with special regard to heavy metals. Kent Akademisi, 15(3), 1413-1421.

[18] Evrimagaci, (2024); https://evrimagaci.org/niyobyum-9847 (access date: Sep 15, 2024)

[19] Ghoma, W. E. O., Sevik, H., & Isinkaralar, K. (2023). Comparison of the rate of certain trace metals accumulation in indoor plants for smoking and non-smoking areas. Environmental science and pollution research, 30(30), 75768-75776.

[20] Key, K., Kulaç, Ş., Koç, İ., & Sevik, H. (2023). Proof of concept to characterize historical heavy-metal concentrations in atmosphere in North Turkey: determining the variations of Ni, Co, and Mn concentrations in 180-year-old Corylus colurna L.(Turkish hazelnut) annual rings. Acta Physiologiae Plantarum, 45(10), 120.

[21] Koc, I., Cobanoglu, H., Canturk, U., Key, K., Kulac, S., & Sevik, H. (2024). Change of Cr concentration from past to present in areas with elevated air pollution. International Journal of Environmental Science and Technology, 21(2), 2059-2070.

[22] Guney, D., Koc, I., Isinkaralar, K., & Erdem, R. (2023). Variation in Pb and Zn concentrations in different species of trees and shrubs and their organs depending on traffic density. Baltic Forestry, 29(2), id661-id661.

[23] Isinkaralar, K. (2022). Some atmospheric trace metals deposition in selected trees as a possible biomonitor. Romanian Biotechnological Letters, 27(1), 3227-3236.

[24] Hrivnák, M., Krajmerová, D., Paule, L., Zhelev, P., Sevik, H., Ivanković, M., Goginashvili, N., Paule, J., Gömöry, D. (2024). Are there hybrid zones in Fagus sylvatica L. sensu lato?. Eur J Forest Res 143, 451-464.

[25] Özdikmenli, G., Yiğit, N., Özel, H. B., and Şevik, H. (2024). Altitude-dependent Variations in Some Morphological and Anatomical Features of Anatolian Chestnut. BioResources, 19(3), 4635-4651.

[26] Kurz, M., Koelz, A., Gorges, J., Carmona, B. P., Brang, P., Vitasse, Y., ... & Csillery, K. (2023). Tracing the origin of Oriental beech stands across Western Europe and reporting hybridization with European beech–Implications for assisted gene flow. Forest Ecology and Management, 531, 120801.

[27] Isinkaralar, K., & Erdem, R. (2021). Landscape plants as biomonitors for magnesium concentration in some species. International Journal of Progressive Sciences and Technologies, 29(2), 468-473.

[28] Isinkaralar, O., Isinkaralar, K., Sevik, H., & Küçük, Ö. (2024). Spatial modeling the climate change risk of river basins via climate classification: a scenario-based prediction approach for Türkiye. Natural Hazards, 120(1), 511-528.

[29] Koc, I., & Nzokou, P. (2018). Effects of water stress and cold treatments on the germination of two conifers (Pinus nigra and Pinus brutia) species from Turkey. Hortscience, 53(9), 259-259.

[30] Bayraktar, E. P., Isinkaralar, O., & Isinkaralar, K. (2022). Usability of several species for monitoring and reducing the heavy metal pollution threatening the public health in urban environment of Ankara. World Journal of Advanced Research and Reviews, 14(3), 276-283.

[31] Çobanoglu, H., Canturk, U., Koc, I., Kulac, S., Sevik, H. (2023). Climate change effect on potential distribution of anatolian chestnut (Castanea sativa Mill.) in the upcoming century in Türkiye, Forestist, 73(3), 247-256.

doi:10.55385/kastamonujes.1558417 KUJES 10(2):63-72, 2024

Kastamonu University
Journal of Engineering and Sciences
e-ISSN 2667-8209
http://dergipark.gov.tr/kastamonujes

Examination of the Performance of Spoon-Type Planting Machine in Kastamonu Taşköprü Garlic Planting

Atilla Verep[a], **Hüseyin Güran Ünal**[b,*]

[a]Institute of Science Kastamonu University, Kastamonu, Türkiye
[b]Department of Mechanical Engineering, Faculty of Engineering, Kastamonu University, Kastamonu, Türkiye
***Corresponding author:** gunal@kastamonu.edu.tr

Received: **September 30, 2024** ◆ Accepted: **December 12, 2024** ◆ Published Online: **December 25, 2024**

Abstract: Garlic production and consumption are increasing worldwide, including in Turkey. It has a wide place on tables due to its taste and health benefits. Kastamonu Taşköprü garlic is also a geographically indicated variety known and sought after worldwide due to its sharp aroma. Approximately 20% of garlic in Türkiye is produced in Kastamonu. Garlic is the most important agricultural product in the Kastamonu economy. Thousands of tons of garlic reach consumers unprocessed, in the form of hand-tied garlic, and are placed on tables. Apart from this, netted garlic in markets, peeled garlic, puree, and black garlic, used primarily in sausage-pastırma-pickle-food sectors, are also processed in facilities in Kastamonu and marketed nationwide. Due to the intensive labor requirement in production, production costs and the supply of labor requirements limit garlic production amounts in the region. In recent years, the use of machinery in planting has become widespread. The spoon-type planting machines are used to plant in rows and then facilitate operations such as weeding and uprooting. This study investigated the success of the spoon-type garlic planting machines used in the region with Kastamonu garlic. The field trials revealed planting performance with the sprout spacing measurement and camera image analysis with different speeds, tooth sizes, and field slope variables. As a result of the results obtained, it was seen that the spoon-type machine was far from making precise planting. When plant distribution was evaluated according to the row spacing in all variables, it was determined that the acceptable row spacing rate was insufficient (11.7-79.5%). It is possible to say that it scatters garlic randomly on the row. These machines need to be developed, and losses in garlic planting should be reduced.

Keywords: Garlic, Kastamonu, planting mechanization, resource efficiency, sustainable agriculture

Öz: Sarımsak üretimi ve tüketimi tüm Dünya'da ve Türkiye'de artmaktadır. Gerek lezzeti gerekse sağlık yönünden faydaları sebebiyle sofralarda geniş yer bulmaktadır. Kastamonu Taşköprü sarımsağı da coğrafi işaret sahibi, keskin aroması sebebiyle tüm dünyada tanınan ve aranan bir çeşittir. Türkiye'deki sarımsağın yaklaşık %20 si Kastamonu'da üretilmektedir. Sarımsak, Kastamonu ekonomisinde en önemli tarımsal üründür. Binlerce ton sarımsak işlenmeden, el bağı şeklinde tüketicilere ulaşmakta ve sofralarda yer almaktadır. Bunun dışında marketlerde yer alan filelenmiş sarımsak, başta sucuk-pastırma-turşu-gıda sektörlerinde kullanıma sunulan soyulmuş sarımsak, püre, siyah sarımsak gibi katma değeri yüksek ürünler de Kastamonu'daki tesislerde işlenip yurt geneline pazarlanmaktadır. Üretiminde yoğun işgücü gereksinimi sebebiyle üretim maliyeti ve işgücü ihtiyacının temini yörede sarımsak üretim miktarlarını kısıtlamaktadır. Son yıllarda ekim işlerinde makine kullanımı yaygınlaşmaya başlamıştır. Kullanılan kaşıkçıklı tip ekim makinaları sıraya ekim yapmakta, sonrasında ot alma, söküm gibi işlemlerin yapılmasını da kolaylaştırmaktadır. Bu çalışmada bölgede kullanılan kaşıkçıklı tip sarımsak ekim makinalarının Kastamonu sarımsağı ile kullanıldığındaki ekim başarısı araştırılmıştır. Yapılan tarla denemelerinde farklı hız, diş büyüklüğü, tarla eğimi gibi değişkenlerle filiz aralık ölçümü ve kamera görüntüsü analizi ile ekim performansı ortaya konmuştur. Elde edilen sonuçlar neticesinde kaşıkçıklı tip makinanın hassas ekim yapmaktan oldukça uzak olduğu görülmüştür. Tüm değişkenlerde sıra üzeri mesafeye göre bitki dağılımı değerlendirildiğinde, kabul edilebilir sıra üzeri aralık oranın yetersiz olduğu saptanmıştır (%11.7-79.5). Sıra üzerine gelişi güzel sarımsak döktüğünü söylemek mümkündür. Bu makinaların geliştirilerek sarımsak ekimindeki kayıpların azaltılması gerekmektedir.

Anahtar Kelimeler: Sarımsak, Kastamonu, ekim mekanizasyonu, kaynak verimliliği, sürdürülebilir tarım

1. Introduction

The scientific name for garlic in Latin is *Allium sativum*, which means "a burning plant". Its thin green leaves, white roots, and pungent odor indicate that garlic is a member of the Allium genus, like onions and leeks. Garlic, used as a vegetable, is a plant that has been used in all cultures since ancient times as a condiment and as a medicine [1]**.** Garlic has gone far beyond being a plant that is only used dried or fresh due to its unique qualities. Garlic products available on the market are generally in the form of garlic tablets, garlic vinegar, garlic yogurt, garlic olives, garlic puree, garlic capsules, garlic mustard, (a wide variety) garlic sauces, garlic powder, garlic essential oil, garlic juice (extract), dried garlic, and garlic pickles [2]**,** Kızılaslan and Tokatlı [3], in their study investigating the effects of garlic on human health, stated that

it has anti-inflammatory, antidiabetic, antioncogenic, antimicrobial, antioxidant, cardioprotective, immunomodulatory and hepatoprotective effects and recommended including garlic in daily nutrition. While 28,204,854 tons of garlic were produced in the world in 2021 [4], 0.4% of it was produced in Turkey with 132,617 tons [5]. Approximately 25% of Türkiye's production was produced in Kastamonu, which produced 33,122 tons. Taşköprü garlic, which is the most widely grown garlic variety in Turkey due to its sharp aroma and long-term preservation, is also known as white gold [6]. Garlic is the agricultural product that provides the most employment for Kastamonu Taşköprü District. Approximately 4000 families in Taşköprü sustain their lives with garlic production. This means 75% of the population sustains their lives with garlic income. Since garlic farming requires much labor, it plays an important role in the employment of the population in the Kastamonu-Taşköprü region. For this reason, in Kastamonu, where people emigrate due to limited sources of income, garlic farming has become an important source of income by tying the population to the field [7].

In today's world, where labor supply difficulties and costs are rapidly increasing, agricultural mechanization needs to be increased. The most critical factor in providing equal living space for plants is the precise planting of seeds. Planting precisely with equal distances between rows and on the row also provides convenience in weed control, fertilization, and harvesting processes in the advanced stages of production. Garlic production in Kastamonu requires intensive labor for planting, weed hoeing, harvesting, grading, and cleaning. Planting by hand-sprinkling also makes removing weeds from the randomly scattered seeds difficult. In order to provide equal living space for plants, precision planting machines that control the distances between rows and on the rows are essential. Due to its large and irregular structure, planting garlic cloves with a machine is more complex than other seeds. In recent years, the number of spoon-type garlic planting machines has increased with the search for mechanization in production. In a study conducted in 2008, when producers were asked about their most significant need for mechanization, 61.61% responded that planting and 16.67% responded that seed nipping was the most common [8]. In a study conducted in 2023, 27.8% of producers planted with machines, while 90.9% removed with machines [9]. Although producers have a high need for mechanization, their use of machines remains limited. This is because the planting machines used in the region did not show the expected performance and did not satisfy the users, and the teeth were not placed vertically in the soil as they were planted by hand. Tüfekçi et al. [10] tested the performance of the spoon-type planting machine in a laboratory environment during planting with Kahramanmaraş garlic. Ünal and Keskin [11] made the pneumatic planting machine suitable for garlic planting by changing the planting unit in their study on Taşköprü garlic and conducting a field trial. With this machine whose planting unit was changed, the empty crossing rate was 12.4%, the twinning rate was 6.2%, and the acceptability rate was 81.4%. Feng et al. [12] designed a pneumatic garlic planting machine, and in the trial, they conducted with this machine, they achieved 3.31% twinning, 8.65% empty crossing, and 88.04% acceptability. There is no study on the field performance of spoon-type planting machines, the only machines used in garlic planting in Kastamonu. Kastamonu garlic is used without examining its suitability for these machines. In this study, the spoon-type garlic planting machine used in garlic planting in Kastamonu was tested, and planting performance was examined using sprout spacing measurement and a camera image. Low planting performance leads to major losses due to failure to provide ideal equal living space for plants. The increase in twinning rate causes the cloves falling close to each other not to develop sufficiently and the garlic heads to remain small. The increase in empty crossing causes the field to be filled insufficiently by falling below the ideal number of plants per unit area. For example, a 10% loss leads to approximately 300,000,000 TL in Kastamonu, where 33000 tons of garlic are produced annually. For this reason, it is imperative to analyze the performance of the machines to be used and to improve their success.

2. Material and Method

Biological material used in the experiments

Taşköprü garlic grown in 2023 in the Kastamonu region was used in the study. After the garlic were in a cool warehouse away from sunlight until the planting season, they were separated into cloves in a clove-cutting machine 1 day before planting and divided into 3 classes as large, medium and fine types with the help of a round-hole rotary drum sieve. With the help of the drum sieve, 3 batches of 20 garlic cloves were taken to represent each class according to their sizes and the dimensions of these garlic cloves were measured with a precision of 0.1 mm with the help of a caliper and the averages and standard deviations of their basic dimensions (L: length, W: width, T: thickness) were calculated. In addition, the shape features found with the help of the following relations were also calculated. 20 garlic cloves were taken randomly from the garlic cloves in 3 batches representing each size and weighed on a precision scale. The samples were found to weigh 1000 grains. In addition, in order to calculate the dry matter weights of the same samples, they were separated into sizes and heated in an oven set at 105 degrees for 24 hours [13] and the weights were weighed on a precision scale. All these properties of the seeds used are given in Table 1.

Grain volume (V) *)* $B=\sqrt{WT}$ $V=\frac{\pi B^2 L^2}{6(2L-B)}$ ……. (1) [14]

Sphericity (Ø) $Ø=\frac{(LWT)^{1/3}}{L}$L …….. (2) [15]

Shape ratio (Ra) $Ra = \frac{W}{L}$ …… (3) [16]

Table 1. Characteristics of the seed garlic cloves used

Small clove			**Medium clove**			**Large clove**	
Dimensions (mm)							
W	L	T	W	L	T	W	L
8.9±2	27.2±4	6.9±2	12.6±2	29.1±4	8.8±1	17.0±3	31.2±4
Shape features							
V(mm³)	Ø	Ra	V(mm³)	Ø	Ra	V(mm³)	Ø
505.4	0.4	0.3	1023.8	0.5	0.4	1803.6	0.5
Thousand-grain weight (gr)							
1055±55	1965±280	3050±115	2005±150	1055±55	1965±280	3050±115	2005±150
Dry matter ratio (%)							
43.6	41.22	41.15	41.65	43.6	41.22	41.15	41.65

Garlic planter

A Massey Ferguson 2635 tractor was used as a power source to pull the Çalışkan brand spoon planter used during the study. The planter operates at a fixed 16.5 cm row spacing and 6-8-10 cm row spacing that can be adjusted with the help of gears. The planter specifications are given in Table 2.

Table 2. Planter technical data

Brand	**Calışkan**
Model	HC1-13
Row spacing (cm)	16.5
Number of planting units (pcs)	13
Planting width (cm)	248
Seed storage capacity (kg)	80
Tire size	165 x70 r13
Weight (kg)	800
Power requirement (hp)	70-80hp
Plantable area (m^2/sa)	4500
Transport dimensions (cm)	160 x 276 x 145
above line spacing (cm)	6, 8, 10

Garlic planter seed storage compartmentation

Since the seed storage of the garlic planter we used has a single compartment and 13 rows, the seed storage compartment was divided into compartments with cardboard sheets to examine the planting performance of seeds of different sizes. The seed storage compartment was divided into four compartments with 3-3-3-4 spoon rows to accommodate fine, medium, large, and mixed seeds, respectively (Figure 1).

Figure 1. Seed chamber compartments

Spoonlets

Detailed views of the spoonlets on the 13-row planting machine are given in Figure 2.

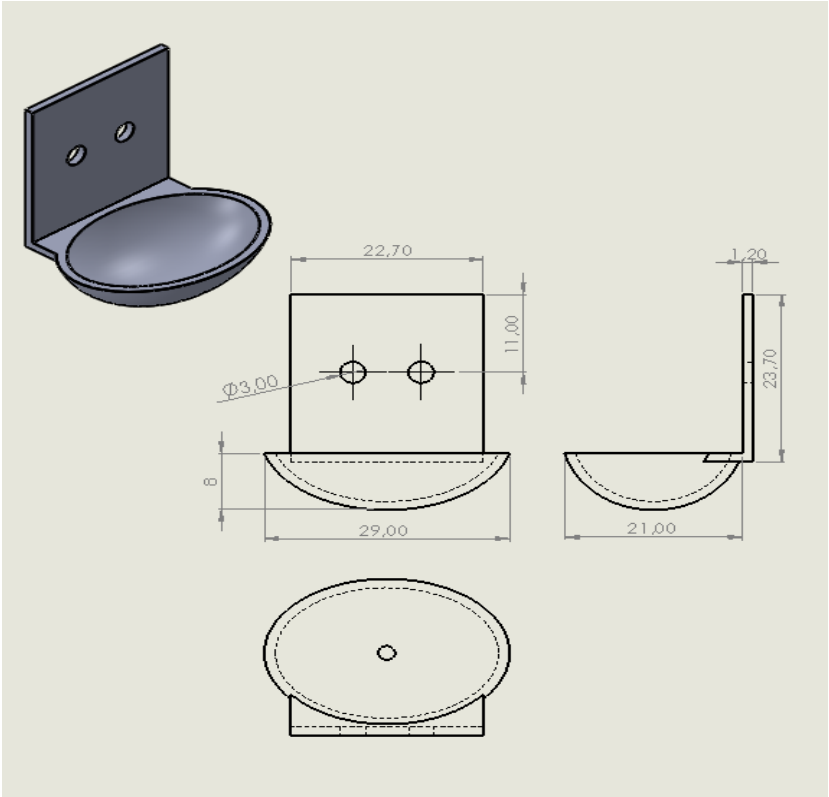

Figure 2. Technical drawings of the spoonlets used in the planting machine

A field where the study was conducted

The study was conducted on February 20, 2024, in the field numbered 106 islands and 16 parcels in the Yukarı Dere location of the Karacaoğlu Neighborhood of Meşeli Village of Taşköprü district of Kastamonu Province. The field is approximately 700 m above sea level and has a slope of approximately 11%. Preparation studies were carried out in the field in the autumn season and before planting the year before planting. Two different slopes were used in this area: downward and upward.

8 cm was preferred as the distance between rows in all trials. Forward speed trials were conducted at three different gears, 1100 rpm engine speed, V1-1.32, V2-2.59, V3-3.62 km/h speeds.

Figure 3. The field where the experiment was conducted

Determination of plant distribution uniformity on the row with sprout spacing measurement

After the field trial conducted on 20.02.2024, the sprouts were expected to emerge completely, and the sprouts were measured on 23.04.2024. The distance on the row was theoretically set to 8 cm during the planting process. Since Z=8 cm was taken, as a result of measuring the sprout spacing, intervals narrower than 4 cm were considered twinning, intervals larger than 12 cm were considered empty crossing, and measurements between 4-12 cm were considered acceptable intervals [16] (Table 3**).**

Table 3. Evaluation of plant distribution according to row spacing [16]

Definition	Plant spacing on row
Twinning	< 0.5 Z
Acceptable spacing	≥0.5Z - ≤1.5Z
Spacing	> 1.5 Z

In order to determine the regularity of the sprouts emerging on the row, the distances between the thin, medium, large, and mixed-sized garlic sprouts planted on the 15 m tracks determined for each speed level were measured. In this process, which was carried out with five repetitions for each size of garlic sprouts on each track, the distances of the plants on the rows within 120 cm randomly selected were measured. The averages obtained were evaluated in Table 4.

Table 4. Evaluation of acceptable twinning and void ratios [16]

Acceptable	Twinning rate	Spacing rate	Evaluation
Plant spacing rate (%)	(%)	(%)	
>99	<0.5	<0.5	very good
>95-99	<0.5-2.5	<0.5-2.5	good
>90-95	<2.5-5.0	<2.5-5.0	average
>80-90	<5.0-10.0	<5.0-10.0	sufficent
<80	>10.0	>10.0	Inadequate

Evaluation with the camera image

A total of 13 spoon bands of the precision planting machine, divided into four different chambers during planting, were recorded with a camera. Camera recordings were made with two mobile phones carried by two people. The recording with one camera is listed on half of the machine's spoons. The camera records were then examined slowly, and the garlic cloves taken with each spoon were counted. While counting the camera images, images of 10 spoons with five replications at different times for each variable were examined. Spoons with more than one tooth were calculated as twinning, spoons with one tooth were calculated as standard, and spoons with no teeth were calculated as empty crossing.

Figure 4. Taking images with a camera during planting

3. Result and Discussion

Twinning rate

The upslope and downslope twinning rates obtained by the measurement of shoot spacing and camera image analysis during the field trial are given in Table 5, respectively.

Table 5. Twinning rates

	According to sprout range measurement twinning rate on upslope (%)				**According to the camera image twinning rate on upslope (%)**			
	Small	Medium	Large	Mix	Small	Medium	Large	Mix
V 1	15.7±15.5	10.2±4.6	8.3±13.1	17.4±13.1	67.1±34.0	8.3±5.0	13.3±10.3	27.3±12.8
V 2	29.7±10	11.4±9.3	14.7±20.9	10.6±8.0	52.9±35.4	15.0±10.0	17.1±13.8	11.8±9.9
V 3	30.5±13.6	6.3±10.3	6.4±3.9	4.2±7.6	31.4±32.8	8.8±9.8	5.7±7.9	11.6±10.7
	Twinning rate on down slope (%)				Twinning rate on down slope (%)			
V 1	33.0±12.0	10.8±14.4	16.3±12.1	8.9±9.9	70.0±34.2	33.8±33.8	40.0±26.1	37.0±24.9
V 2	25.5±7.7	17.5±15.3	3.6±7.9	10.1-12.2	88.3±34.1	24.4±24.0	83.3±23.6	20.0±28.3
V 3	9.5±7.2	28.4±13.7	4±8.9	8.0±11.0	78.3±30.4	8.9±9.3	21.1±10.5	15.0±4.8

Vacancy rate

The upslope and downslope vacancy rates obtained by measuring shoot spacing and camera image analysis during the field trial are given in Table 6.

Table 6. Vacancy rates

	According to sprout range measurement vacancy rate on upslope (%)				**According to the camera image vacancy rate on up slope (%)**			
	Small	Medium	Large	Mix	Small	Medium	Large	Mix
V 1	42.6±24.6	50.4±17.9	79.8±15.4	58.0±17.6	7.9±10.3	26.7±12.9	21.7±34.3	2.5±4.6
V 2	33.0±11.3	65.1±26.7	67.3±29.4	64.6±15.7	10.0±14.6	10.0±15.3	9.2±9.3	13.6±10.3
V 3	27.8±11.5	75.2±18.0	70.5±18.8	78.5±20.7	12.9±14.6	20.0±8.9	14.8±10.7	11.4±13.5
	Vacancy rate on down slope (%)				Vacancy rate on down slope (%)			
V 1	24.2±7.4	69.5±17.3	60.3±13.5	60.8±20.2	5.0±7.9	14.2±13.7	1.7±4.1	8.1±10.7
V 2	33.2±9.9	45.1±11.2	81.4±24.9	57.1±21.3	0.0±0.0	13.3±18.0	0.0±0.0	10.0±14.1
V 3	62.5±20.4	27.3±13.7	71.3±24.1	70.9±17.1	3.3±4.9	36.7±30.4	8.3±7.5	17.5±9.2

Acceptable rates

The acceptable rates of upslope and downslope obtained by the measurement of shoot spacing and camera image analysis during the field trial are given in Table 7, respectively.

Table 7. Acceptable rates

	According to sprout range measurement acceptable rate on upslope (%)				**According to the camera image acceptable rate on upslope (%)**			
	Small	Medium	Large	Mix	Small	Medium	Large	Mix
V 1	41.6±18.6	39.3±15.2	11.9±6.0	24.6±19.1	27.1±23.3	65.0±9.6	65.0±27.4	70.2±13.1
V 2	37.3±14.8	23.5±22.0	18.0±14.3	24.9±12.5	34.3±23.9	75.0±12.9	73.7±11.9	74.6±9.9
V 3	41.6±18.3	18.4±12.5	23.2±17.3	17.3±17.0	55.7±29.5	71.3±14.7	79.5±13.4	77±12.4
	Acceptable rate (%) on down slope				Acceptable rate (%) on down slope			
V 1	42.8±13.2	19.6±16	23.4±12.3	30.3±18.6	25.0±21.2	52.1±23.4	58.3±26.4	54.8±23.6
V 2	41.3±12.9	37.4±18.2	15±20.9	32.8±16.6	11.7±8.2	62.2±23.3	16.7±23.6	70.0±42.4
V 3	28±22	44.3±8.9	20.6±23.1	21±18.9	18.3±9.8	53.3±27.8	63.9±18.8	67.5±12.2

In all variables, twinning was determined as 4.0-33.0% according to the measurement between the sprouts, and 5.7-88.3% according to the image analysis. Vacancy was determined as 24.2-81.4% according to the measurement between the sprouts, and 0.0-36.7% according to the image analysis. According to the measurement between the sprouts, the acceptable was determined as 11.9-44.3%, and 11.7-79.5% according to the image analysis.

When the effect of tractor forward speed is evaluated, in the average of all variables, the acceptable rate is determined as 29.2, 28.8, 26.8% in V1, V2, V3 speeds according to the tiller measurement, and 52.2, 52.3, 60.8% according to the camera image. It is seen that the acceptable rate decreases as the speed increases according to the tiller measurement, and the acceptable rate increases according to the camera image. The results obtained with the tiller spacing measurement values are also consistent with the results of other researchers [17-19]. When the effect of the terrain slope is evaluated, in the average of all variables, the acceptable rate is determined as 26.8% and 30.1% in the up and down slopes according to the tiller measurement, and 64.0% and 45.5% in the up and down slopes according to the camera image, respectively. According to the measurement between the sprouts, the acceptable rate is lower on the upward slope. In contrast, according to the camera image, the acceptable rate is higher on the upward slope. Ünal [20] reported in his study that the seed tube's angle, height, and material are effective in garlic cloves' falling times.

When the effect of garlic clove sizes is examined, in the average of all variables, the acceptable rate was determined as 38.8, 30.4, 18.7, and 25.2% for small, medium, large, and mixed garlic clove sizes according to the measurement between the sprouts, and 28.7, 63.2, 59.5, 69.0% according to the camera image, respectively. It is seen that the acceptable rate decreases as the garlic clove sizes increase according to the measurement between the sprouts, while the acceptable rate increases as the garlic clove sizes increase according to the camera image.

In the average of all variables, the acceptable rate was 28.4% according to the measurement between the sprouts and 54.7% according to the camera image. In general, the acceptable rates obtained with the camera image are higher. These values show the actual filling amount of the spoons. The number of sprout intervals is misleading in showing the spoons' filling performance. It varies depending on falling height, seed tube slope, seed tube material, the possibility of rebound and drifting after falling, and the sprout's emergence direction.

Evaluation of the planter success

According to the sprout spacing measurement and camera image analysis of the planter used in the study, the sufficiency status of garlic seeds in two different slopes, three different progress speeds, and four different sizes is shown in Table 8.

Table 8. Qualification status of the planter

Qualification status according to sprout range measurement																								
	Small						Medium						Large						Mix					
	ye			ae			ye			ae			ye			ae			ye			ae		
	ie	bs	kl	ie	bs	kl	ie	bs	kl	ie	bs	kl	ie	bs	kl	ie	bs	kl	ie	bs	kl	ie	bs	kl
V 1	x	x	x	x	x	x	x	x	x	x	x	x	z	x	x	x	x	x	x	x	x	z	x	x
V 2	x	x	x	x	x	x	x	x	x	x	x	x	x	x	x	o	x	x	x	x	x	x	x	x
V 3	x	x	x	z	x	x	z	x	x	x	x	x	z	x	x	o	x	x	o	x	x	z	x	x
Qualification status according to camera image																								
	Small						Medium						Large						Mix					
	ye			ae			ye			ae			ye			ae			ye			ae		
	ie	bs	kl	ie	bs	kl	ie	bs	kl	ie	bs	kl	ie	bs	kl	ie	bs	kl	ie	bs	kl	ie	bs	kl
V 1	x	z	x	x	z	x	z	x	x	x	x	x	x	x	x	x	i	x	x	i	x	x	z	x
V 2	x	z	x	x	c	x	x	z	x	x	x	x	x	z	x	x	c	x	x	x	x	x	z	x
V 3	x	x	x	x	o	x	z	x	x	z	x	x	z	x	x	x	z	x	x	x	x	x	x	x

ae: downward slope, ye: upward slope, x: insufficient, z: sufficient, o: average, i: good, c: very good, ie: twinning, bs: blank pass, kl: acceptable

When the obtained results regarding twinning, empty crossing, acceptable rates, and precision planting machine trial criteria are examined, it is possible to say that the machine is inadequate in all variables, and the seeds are left randomly on the row rather than precision planting. [10] Tüfekçi et al. determined the acceptable row spacings as 36-47-35%, respectively, with a forward speed of 0.25-0.5-1.0 km/h in laboratory experiments with a spoon-type garlic planter. In this study, in the experiments conducted with Maraş garlic, the row planting performance was found to be insufficient.

The reasons for the negativities can be listed as the inappropriateness of the spoon size and shape to the Kastamonu garlic clove size and shape, the absence of a mixer or a guide towards the spoons in the seed chamber, and the seed tubes being too high and curved. As a result of the producers not liking the performance of the spoon planting machines used in the region, their use remains low at 27.8%. The necessity of 79.6% of garlic cultivation with external labor supply causes farmers to produce in small plots that they can handle with their own families and not to be able to increase their planting areas [9]**.**

In the field trial conducted by Ünal and Keskin [11] with the pneumatic garlic planter they developed, the best results were obtained with 12.4% space ratio, 6.2% twinning ratio, 81.4% normal planting ratio, 94.57% sprouting ratio and 42.79% coefficient of variation at 11.6 cm row spacing and 2.6 km/h machine forward speed.

It was seen in the study that it is not appropriate to determine the suitability of garlic planting machines to the trial criteria by measuring the sprout spacing. Considering the density of the row spacing (8 cm) and the size of the teeth (approximately 3 cm), measurements made according to the position of the sprout tips can be inaccurate, as seen in Figure 3. Even if the centers of the teeth are ideally 8 cm, the spacing of the sprouts on the soil can be closer than 4 cm and be perceived as twinning, or larger than 12 cm and be perceived as empty spacing. The significant difference between the results obtained with camera images and sprout spacing measurements proves this. Ünal and Keskin [11] reported that the method used to evaluate the test results is suitable for demonstrating the performance of existing precision planting machines but that this evaluation is not reliable for plants such as garlic and shallots, which are large, heavy, irregularly shaped, and have differences in the point at which the sprout emerges from the surface, rather than for small and more regular-shaped plant seeds such as sugar beet and corn.

Figure 5. Measurement errors of sprout spacing

Our study was also the first to determine planting performance with camera images during field trials. Although there are studies conducted with camera images and image processing techniques in laboratory environments in existing studies, image analysis was not encountered in field trials.

4. Conclusion and Suggestions

This research has shown that spoon machines used in garlic planting must be developed. With its current structure, it is impossible to say that it leaves seeds at equal intervals on the row; it is more appropriate to say that it pours them randomly on the row. It is necessary to approach the distances on the row to the ideal size, reduce twinning and empty crossing rates, and increase acceptable rates.

For this purpose, technical arrangements that can be made can be listed as follows:

i) Spoonlet shape and dimensions should be revised for Kastamonu garlic.

ii) Modifications should be made in the warehouse, such as adding a mixer or a vibration provider to ensure that the cloves are directed to the spoons.

iii) A mechanism should be worked on to ensure that the excess seeds in spoons that hold more than one garlic clove are dropped and singulated.

iv) The point where the garlic falls from the spoonlets should be brought as close to the soil as possible, the drop pipe used in between should be shortened, and it should be ensured to be straight and vertical. Studies have shown that pneumatic machines used in garlic planting give better results. Such machines' development and widespread use will also contribute to a more uniform planting.

This research also showed that determining planting performance according to sprout spacing in garlic is misleading. Camera image examination provides more realistic results. Work on production mechanization, especially planting Taşköprü garlic, the largest agricultural production in Kastamonu province, and providing a living for hundreds of families, should be encouraged and increased.

Conflict of Interest

The authors declare that they have no competing interests.

Ethics Committee Approval

Ethics committee approval is not required.

Author Contribution

Conceptization: AV, HGÜ; methodology and laboratory analyzes: AV, HGÜ; writing draft: AV, HGÜ; supervision: HGÜ, proof reading and editing: All authors have read and agreed to the published version of manuscript.

Acknowledgements

This publication was prepared by using a part of the master's thesis study of Atilla Verep, Kastamonu University, Institute of Science, Department of Mechanical Engineering.

5. References

[1] Rebecca L. J. & Stewen F. (2016) National Geographic Encyclopedia of Medicinal Plants:152-157.

[2] Koyuncu, M. (2012). Garlic and Taşköprü Garlic. Taşköprü Garlic Panel Proceedings, (pp:11-20), 6 February 2012. Kastamonu.

[3] Kızılaslan, N. & Tokatlı, K. (2021). Effects of garlic on human health. TOGÜ Journal of Health Sciences, 1(2), 62-71.

[4] FAO, (2024). Statistical data of FAO. Retrieved from: http://faostat.fao.org/site/567/default.asp (access date: May 8, 2024).

[5] TÜİK, (2024). Production statistics, https://biruni.tuik.gov.tr/medas/?kn=92&locale=tr (access date: August 11, 2024).

[6] Ipek M, Ipek A, Simon PW. 2008. Molecular characterization of Kastamonu garlic: An economically important garlic clone in Turkey. Scientia Horticulturae, 115(2), 203-208.

[7] Çetin, T. & Karakuş, U. (2005). Population Movements in Taşköprü (Kastamonu) District Center. Istanbul University and Turkish Geographical Society National Geographical Congress, 29-30 September 2005, Proceedings Book p.523-532.

[8] Ünal, H.G., Saçılık, K. & Yurtlu, Y.B. (2010). A study on the determination of agricultural practices and approaches in Taşköprü garlic, 26. National Congress of Agricultural Mechanization, (pp. 263-271), Hatay, Turkey, (October 2010)

[9] Ünal, H.G. (2024). Production Habits and Problems in Taşköprü Garlic, Turkish Journal of Agriculture - Food Science and Technology, 12(7), 1156-1161.

[10] Tüfekçi Y., Çakır B. & Akdemir B. (2018). Investigation of the Effect of Spoonlet Type on Planting Performance and the Suitable Spoonlet Type in Garlic Planters, Journal of Agricultural Machinery Science, 14(3), 179-187.

[11] Ünal H.G. & Keskin R. (2005). Development of garlic planting machine prototype, Journal of Agricultural Sciences 11(3), 303-310.

[12] Feng D., Li H., Qi X., Sun X, Wang J & Nyambura M.S. (2024). Design and laboratory experiments of a pneumatic disc-type garlic precision seed-metering device, American Society of Agricultural and Biological Engineers. 67(2), 451-460.

[13] AOAC, (2000). Official Method of Analysis, Association of Official Analytical Chemists (No. 934.06), Washington, DC.

[14] Al-Mahasneh, M. A. & Rababah, T. M. (2007). Effect of moisture content on some physical properties of green wheat. Journal of food engineering, 79(4), 1467-1473.

[15] Dursun, E. & Dursun, I. (2005). Some physical properties of caper seeds. Biosystems Engineering, 92(2), 237-245.

[16] Anonymous (1999). Agricultural mechanization tools testing principles and methods, Ministry of Agriculture and Rural Affairs p: 246, Ankara.

[17] Karayel, D. & Özmerzi A. (2001). Effect of the distance and sowing speed in the row on the evenness of sowing in melon and cucumber planting with an air-suction single-grain planter system, Journal of Akdeniz University Faculty of Agriculture, 14(2), 63-67.

[18] Ünal H.G. (2006). A study on the possibilities of planting shallots with a garlic planting machine prototype, Journal of Agricultural Sciences, 12(1), 37-43.

[19] Karagülmez A., Konak M. & Özbek O. (2018). Effect of some operating parameters on the evenness of seed distribution in the row in a horizontal plate mechanical precision planter system, Selçuk Journal of Agriculture and Food Sciences, 32(3), 350-354.

[20] Ünal H.G. (2003). Determination of the effect of seed tube material, falling angle and seed size on falling time in garlic, Journal of Agricultural Sciences, 10(3), 287-290.

doi:10.55385/kastamonujes.1559603 KUJES 10(2):73-80, 2024

Kastamonu University
Journal of Engineering and Sciences
e-ISSN 2667-8209
http://dergipark.gov.tr/kastamonujes

Modeling of Triaxial Pressure Tests with Uniform Granular Materials Discrete Particle Method

Mehmet Uğur Yılmazoğlu

Department of Civil Engineering, Faculty of Engineering and Architecture, Kastamonu University, Kastamonu, Türkiye
Corresponding Author: myilmazoglu@kastamonu.edu.tr

Received: **October 1, 2024** ◆ Accepted: **December 13, 2024** ◆ Published Online: **December 25, 2024**

Abstract: Predicting the mechanical behavior of the soils on which the structures and facilities are built is crucial in civil engineering. Although solutions are made by modeling the soils as continuous homogeneous environments due to their ease and fast solutions, the soil is the combination of particles in a multiphase environment. Therefore, the Discrete Element Method, which offers a closer approach to the soil properties, was used in the study. This study modeled the behavior of homogeneous granular materials under triaxial compression tests using the Discrete Element Method (DEM). DEM, an ideal numerical technique for simulating particle environments, was used to investigate the mechanical responses of granular assemblies when subjected to varying confining pressures. The research focused on the effects of particle shape, size distribution, and contact mechanics on the material's stress-strain relationship and deformation behavior during the test. Using the DEM approach and PFC3D, the triaxial compression test of uniform sands was modeled to estimate the Poisson's ratio, Young's modulus, and bearing capacity.

Keywords: Discrete element method, PFC3d, triaxial pressure test

Öz: Yapı ve tesislerin üzerine inşa edildiği zeminlerin mekanik davranışların tam ve doğru olarak tahmin edilmesi inşaat mühendisliği açısından çok önemlidir. Günümüzde gerek kolaylığı gerekse hızlı çözümler sunduğu için zeminler sürekli homojen ortamlar gibi modellenerek çözümler yapılsa da zemin parçacıkların çok fazlı ortamda birleşmesidir. Bu nedenle çalışmada zemin özelliğine daha yakın yaklaşım sunan Discrete Element Method kullanılmıştır. Bu çalışmada, üç eksenli basınç testleri altında homojen granüler malzemelerin davranışı Ayrık Eleman Yöntemi (DEM) kullanılarak modellenmiştir. Partikül ortamları simüle etmek için ideal bir sayısal teknik olan DEM, granüler düzeneklerin değişen sınırlayıcı basınçlara maruz kaldığında mekanik tepkilerini araştırmak için kullanılmıştır. Araştırma, parçacık şeklinin, boyut dağılımının ve temas mekaniğinin, test sırasında malzemenin gerilim-şekil değiştirme ilişkisi ve deformasyon davranışı üzerindeki etkilerine odaklanmıştır. DEM yaklaşımı ve PFC3D kullanılarak üniform kumların üç eksenli basınç testi modellenerek poisson oranı, young modülü ve taşıma kapasitesi tahmin edilmeye çalışılmıştır.

Anahtar Kelimeler: Ayrık eleman yöntemi, PFC3d, üç eksenli basınç testi

1. Introduction

Granular materials are commonly encountered in fields such as soil mechanics and civil engineering. These materials consist of individual particles in contact with each other, and their mechanical properties can vary greatly depending on the particles' size, shape, distribution, and interactions. Understanding the mechanical behavior of granular materials is critical to ensuring structural safety in geotechnical engineering [1]. However, due to the complex structure of such materials, classical continuum theories may not be sufficient to reflect the behavior of granular materials fully. Therefore, numerical modeling techniques such as the Discrete Element Method (DEM) have been developed to investigate the mechanical properties of granular materials in more detail [2].

DEM is a powerful method that simulates the interactions of particles forming granular materials by considering them separately. DEM was first developed by Cundall [1] to analyze rock mechanics problems and later applied to soils by Cundall and Strack [1, 3]. The analysis algorithm includes two stages. First, the interaction forces are calculated when the elements penetrate each other slightly. This force-displacement formulation is usually called the "Smooth contact" or the "Force-Displacement" method. As stated by Cundall and Hart [4], it really represents the relative deformation of the surface layers of the elements [4]. In the second stage, Newton's second law is used to determine the acceleration occurring in each particle, and new particle positions are found using these acceleration data integrated with time. This process is repeated until the fracture is achieved.

This method, developed by Cundall and Strack [1], is widely used to accurately model granular materials' deformation, fracture, and shear behavior [1, 5–10]. The micro-scale analysis capability provided by DEM allows for a detailed

examination of particle displacements and interactions. This has made it possible to develop a deeper understanding of the mechanical behavior of granular materials.

In the discrete element method, other numerical methods include possible deformation between particles, i.e., one-sided contact. These methods are called "non-smooth contact" methods. There are two main classes of numerical integration for these methods: event-driven integrations, known as the "Event-Driven Method" (EDM) [11], and contact dynamics time integrations, known as the "Contact Dynamics Method" (CD) [12–15].

In the EDM method, when two solid particles touch each other, a collision (Event) occurs, and the velocity and angular velocities after the collision are determined by a collision operator [16, 17]. Since the method considers single-point contact, it transmits only one force, which is unsuitable for systems with many contact points (contacts) such as soil, rock, or concrete.

The CD method works with the integral of the contact forces as in EDM. Still, this method works on the non-accelerated movements and effects that are integral to the contact forces, not the forces themselves. Since DEM, EDM, or CD consider soil particles as non-deformable objects in time element numerical analyses, they offer limited performance when the deformation and stress of the components (particles) must be regarded as in a static framework.

A triaxial compression test is a laboratory test widely used to determine granular materials' shear strength and deformation properties. During the test, pressure is applied to the sample in three axes to examine the material's behavior under different pressure conditions [18, 19]. While traditional experimental methods reveal the general trends of these behaviors, DEM-based simulations contribute to a more accurate interpretation of the experimental results by examining the microscopic interactions between particles in more detail [20, 21].

DEM has been used in geomechanics in various fields in recent years, from soils to intact rocks. Its applications have spread to many fields, including rock engineering, soil mechanics, mining, and petroleum engineering. DEM codes are primarily used in two-dimensional studies such as disks, ellipses, and polygons [22], whereas today, with the help of three-dimensional DEM computer programs, analyses can be made by summing up particles such as balls, ellipsoids and even polytropes [4]. The DEM method is applied to study the behavior of cohesionless and granular materials. However, the lack of testing capabilities to determine particle model parameters at the particle scale is a significant limitation in using DEMs. Therefore, the selection of parameters is based on trial and error by approximating the simulation results to laboratory results.

This study discusses the DEM modeling of the triaxial compression test on uniform granular materials. First, the properties of uniform granular materials and the theoretical basis of DEM simulations are examined. Then, the modeling of triaxial compression tests is evaluated in light of previous studies in the literature. By modeling uniform sands with a diameter range of 0.075 to 1.0 mm with PFC 3d (Particle Flow Code in three dimensions, version 3.0), the effects of particle model parameters on the stress-strain curve, shear strength, and elastic modulus of the sample are investigated, and the bearing capacity is calculated [23]. The success of DEM in predicting the mechanical behavior of granular materials is discussed.

2. Material and Method

For numerical analysis, uniform sands with diameters between 0.075 and 1.0 mm were simulated by modeling with PFC 3d (Particle Flow Code in three dimensions, version 3.0). The sample generation procedure with PFC3d is formed in four main steps. For each contact, the material strength is selected from a Gaussian distribution specified by the mean value and standard deviation. In programming, the FISH language is used to generate the three-axis test code in the PFC3D environment [23].

Step 1: Particle production and initial compaction

At the beginning of this step, a cylinder sample consisting of arbitrarily placed particles confined by three walls (top, bottom plates, and side cylinder wall) is produced by an expansion compaction method. To prevent particles from penetrating the walls, the average hardness of the walls is set equal to β times the average particle's typical hardness. The size distribution of the particles conforms to a uniform distribution characterized by the minimum and maximum particle radii. The porosity is set to 0.22 to calculate the number of particles that can be produced in the initially specified region.

Step 2: Loading the Specimen with the Specified Isotropic Stress

This step aims to reduce the magnitude of the locked-in stress that will develop after bonding (STEP 4). The magnitude of the locked-in contact forces caused by the particle deformation in STEP 1 will be close to the compressive forces during bonding. The isotropic stress, defined as the average of the three direct stresses in the main direction, is obtained by changing the radii of all particles equally at that time. To reduce the effect of the locked-in stress, the specified

isotropic stress is typically set to a relatively low value against the material strength. The isotropic stress present in the assembly is calculated using the FISH code.

Step 3: Reducing the number of floating particles

Due to the characteristics where the irregular radius particles are randomly placed and mechanically compressed, fewer than three floating particle contacts may be present. All floating particles should be eliminated in the following surface placement stages to create a more realistic and dense bonding contact.

Step 4: Bond installation

Particles are allowed to stick together at the contacts to simulate material fusion. There are two bonding models in PFC3D. The contact bond model can be envisioned as two particles bonded over a small area at the point of contact only. The parallel bond model can be viewed as a finite-size plate-shaped contact acting on a circular cross-section extending in the plane of contact. Only forces can be transmitted through a force contact model.

A force and a moment can be transferred from the parallel bond model. While a particle cannot be attached to a wall, only particles can be connected. The bonds between particles are never renewed after they are broken. Parallel bonds are placed on all particles in physical contact throughout the sample, and then the μ friction coefficient of all particles is determined. The study created parallel bonds between the modeled particles, and their behaviors were investigated. The main material parameters used in PFC3d are shown in Table 1, and the particle model parameters are shown in Table 2. The model created using PFC3d is shown in Figure 1.

Table 1. Material properties used in PFC3d

Property	**Value**	**Symbol and Unit**
Density	1500	ρ, kg/m^3
Ultimate soil porosity	0,30	n
Parallel Bond Axial Stress	1x10^7	pb_nstren, N/m^2
Parallel Bond Shear Stress	1x10^7	pb_sstren, N/m^2

Table 2. Mineralogical properties of the RHA

Symbol	**Analysis 1**	**Analysis 2**	**Analysis 3**	**Analysis 4**
$k_n = k_s$ *(N/m)*	1x10^8	5x10^8	10x10^8	15x10^8
k_n / k_s	1	3	6	10
F_s (ratio)	0.5	1.0	2.0	3.0
pb_kn = pb_ks (N/m)	6x10^9	8x10^9	10 x10^9	12 x10^9

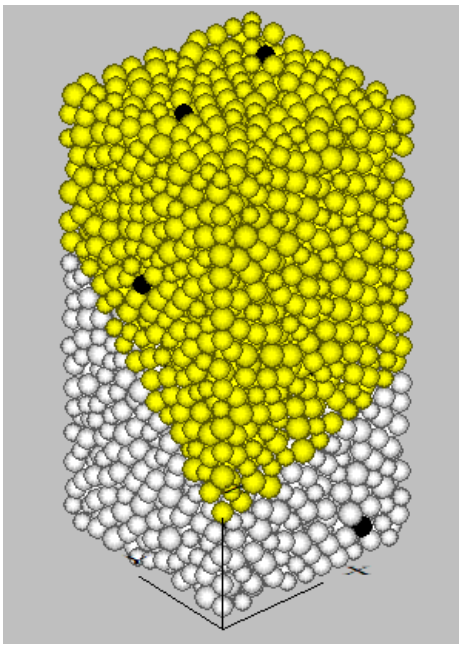

Figure 2. The model created using PFC3d.

3. Result

The elastic properties of the specimen can be determined by performing a loading/unloading test under elastic conditions (high bond strength and friction). Since the confining stress is constant (σ_d=σ_a), the test measured the initial Young's modulus and Poisson's ratio. The elastic properties of the specimen can be determined by performing a loading/unloading test under elastic conditions (high bond strength and friction). Since the confining stress is constant (σ_d=σ_a), the test measured the initial Young's modulus and Poisson's ratio. Equations 1 and 2 calculated the modulus of elasticity and Poisson's ratio as 230.08 MPa and 0.096, respectively.

$$E = \frac{\Delta\sigma_a}{\Delta\varepsilon_a} = \frac{\Delta\sigma_d}{\Delta\varepsilon_a} = \frac{1.349*10^6}{5.846*10^{-3}} = 230.8MPa \quad (1)$$

$$\upsilon = \frac{\frac{1}{2}(\Delta\varepsilon_x+\Delta\varepsilon_y)}{\Delta\varepsilon_a} = \frac{1}{2}\left(1-\frac{\Delta\varepsilon_v}{\Delta\varepsilon_a}\right) = \frac{1}{2}\left(1-\frac{4.694*10^{-3}}{5.846*10^{-3}}\right) = 0.096 \quad (2)$$

For the sample model without contact bond, axial stress and axial deformation analysis against confining stress were performed and presented graphically in Figure 3. The analyses kept the density at 1500 kg/m^3, porosity at 0.3, friction angle 0.5 and particle diameters at 0.075-10 mm. The effect of particle axial hardness on soil behavior was investigated and analyzed.

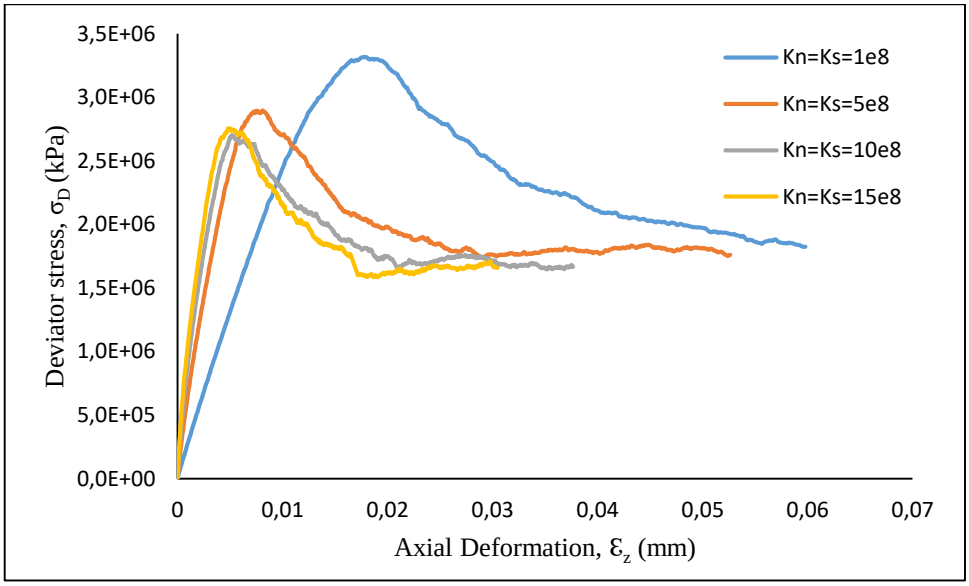

Figure 3. Analysis of axial deformation versus deviator stress for the sample model without contact bond.

In the analyses where the effect of the ratio of particle axial hardness to shear hardness of the parallel bonded model was investigated, particle axial hardness was used as 10e8 N/m, internal friction angle as 0.5, parallel bond axial hardness as 8e9 N/m^3 (pb_kn), parallel bond shear hardness as 1e9 N/m^2 (pb_ks), parallel bond axial tensile strength as 1e7 N/m^2 (pb_nstren), parallel bond shear tensile strength as 1e7 N/m^2 (pb_sstren).

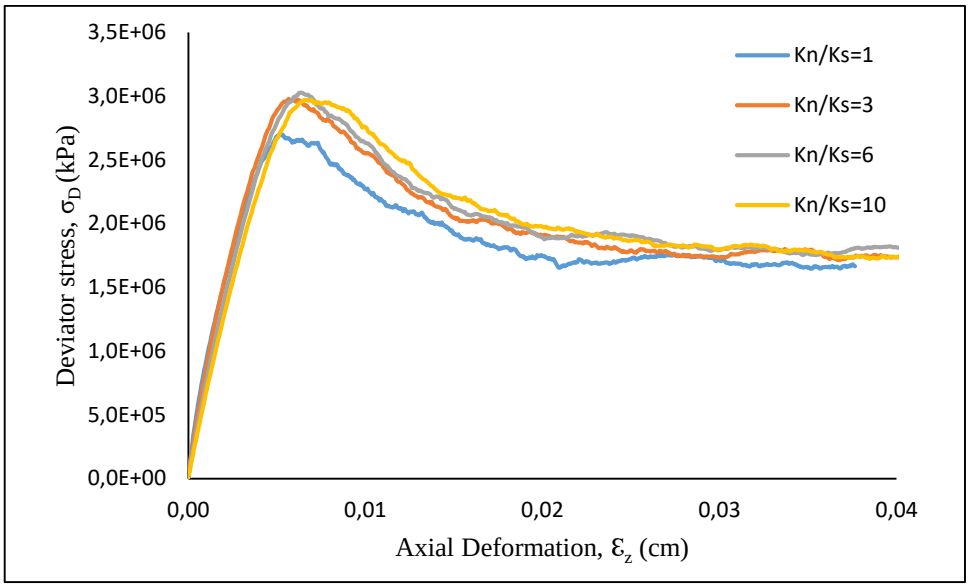

Figure 4. Effect of the ratio of particle axial hardness to shear hardness

In the analyses where the effect of the particle friction coefficient of the parallel-bonded model was examined, particle axial hardness 10e8 N/m (kn=ks), parallel bond axial hardness 8e9N/m^3 (pb_kn), parallel bond shear hardness 1e9N/m^2 (pb_ks), parallel bond axial tensile strength 1e7N/m^2 (pb_nstren), parallel bond shear tensile strength 1e7 N/m^2 (pb_sstren) were used.

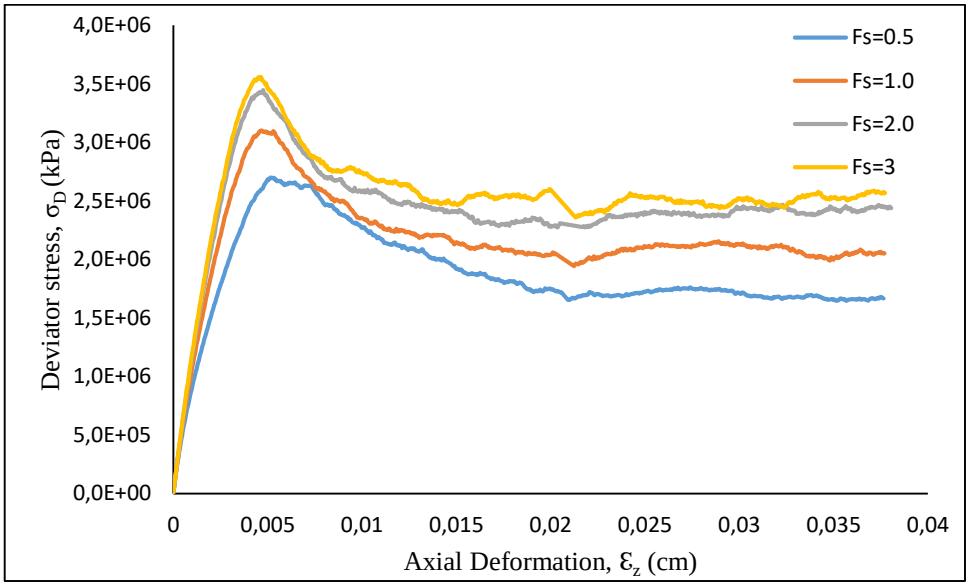

Figure 5. Effect of friction coefficient

In the analyses where the effect of parallel bond stiffness of the parallel bonded model was examined, particle axial stiffness 10e8 N/m (kn=ks), friction angle 0.5, parallel bond axial tensile strength 1e7N/m2 (pb_nstren), parallel bond shear tensile strength 1e7 N/m2 (pb_sstren) values were used.

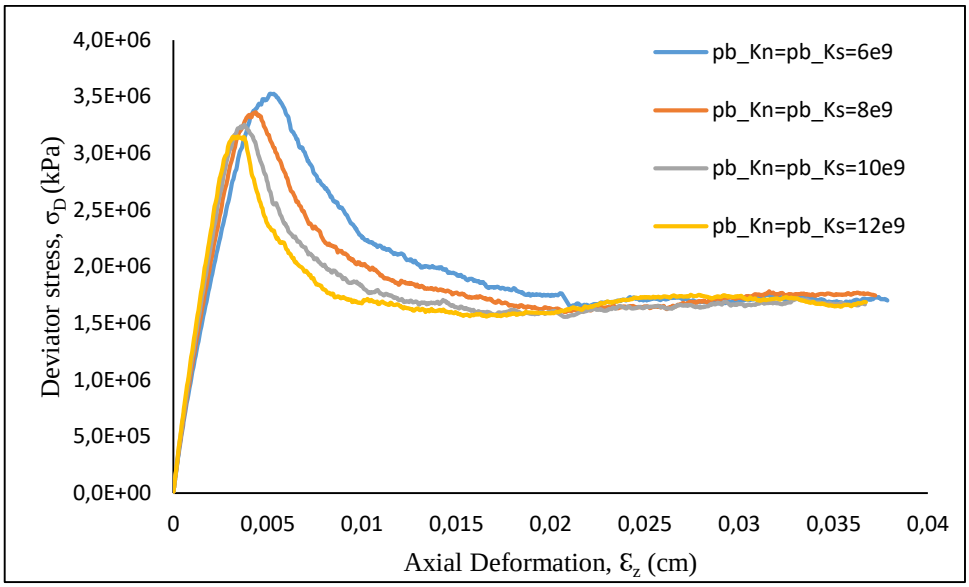

Figure 6. Effect of parallel bond stiffness

4. Discussion and Conclusion

As it is known, in this century the most important problems on a global scale are global climate change [24], pollution [25] and urbanization [26-28] is expressed. One of these problems is urbanization, which has increased rapidly in the last century, It is a problem that requires more people to live per unit area. To make it possible for more people to live per unit area in urban areas, is possible with the construction of high-rise and durable buildings, the foundation of which is building block is concrete [29-32]. Concrete is so widely used today that It is the most widely used building material after water and is an important part of building costs of the environmental pollution [33]. Therefore, in recent years, environmental pollution various waste materials as concrete admixtures. A large number of studies have been conducted on its usability. In these studies especially how admixtures affect the mechanical properties of concrete to determine the effects of the construction on the buildings and facilities [34-37]. In this study, it was also tried to be determined It is aimed to predict the mechanical behavior of the soils on which they are built. In order to provide an easier comparison of the analysis results, deviator stress and axial deformation results for different bond models are shown in Table 3.

Table 3. Deviator stress and axial deformation results obtained by analysis

Type of Bond Between Soil Particles	**Deviator Stress** kN/m^2	***Axial Deformation*** ***cm***
No contact bond	$1.672*10^6$	1.202
Particle contact bond bond strength: 0.05MN	$3.235*10^6$	1.170
Particle contact bond bond strength: 0.10MN	$5.833*10^6$	1.171
Parallel bond between particles	$3.630*10^6$	$7.572*10^{-1}$

In the laboratory, a sample with a diameter of 3.5 and a height of 7 cm was subjected to a triaxial compression test., The deviator load and axial deformation were measured at 3.15 MPa and 12 mm, respectively. The analysis showed that the contact bond condition is essential when uniform granular soils are modeled using the discrete element method. This method indicates that the parallel bond model gives close to actual results in modeling uniform sands.

In the study, the formation of peak stresses in analyzing triaxial compression tests is considered an essential point in understanding the mechanical behavior of granular materials. In particular, the effects of contact bonds and parallel bond models between particles on the peak stress are investigated.

When the parallel bond model was used, higher peak stresses were achieved because both force and moment transmission was provided between the particles. This model provided results that were particularly close to laboratory tests and allowed accurate prediction of peak stress values.

Since only the forces at the contact points were considered in the contact bond model, the peak stress values remained lower than in the parallel bond model. However, it was still helpful in providing information about the resistance capacity of the soil.

These differences were made more apparent by adjusting parameters such as soil particle hardness, friction angle, and bond strength. For example, the study showed that peak stress levels increased significantly by increasing axial stiffness and parallel bond axial tensile strength.

In this context, it was concluded that the peak stress values obtained accurately represent the bearing capacity and deformation properties of granular materials and provide critical data for the ground stability of structures.

Conflict of Interest

The author declares no conflict of interest.

Ethics Committee Approval

Ethics committee approval is not required.

Author Contribution

Writing-original draft, conceptualization, M.U.Y.

Acknowledgements

Not applicable.

5. References

[1] Cundall, P. A., & Strack, O. D. (1979). A discrete numerical model for granular assemblies. geotechnique, 29(1), 47-65.

[2] Luding, S. (2008). Introduction to discrete element methods: basic of contact force models and how to perform the micro-macro transition to continuum theory. European journal of environmental and civil engineering, 12(7-8), 785-826.

[3] Cundall, P. A. (1971). A computer model for simulating progressive, large-scale movement in blocky rock system. In Proceedings of the international symposium on rock mechanics (Vol. 8, pp. 129-136).

[4] Cundall, P. A., & Hart, R. D. (1993). Numerical modeling of discontinua. In Analysis and design methods (pp. 231-243). Pergamon.

[5] Bourrier, F., Kneib, F., Chareyre, B., & Fourcaud, T. (2013). Discrete modeling of granular soils reinforcement by plant roots. Ecological Engineering, 61, 646-657.

[6] Jiang, M. J., Yu, H. S., & Harris, D. (2006). Discrete element modelling of deep penetration in granular soils. International journal for numerical and analytical methods in geomechanics, 30(4), 335-361.

[7] Gu, X., Lu, L., & Qian, J. (2017). Discrete element modeling of the effect of particle size distribution on the small strain stiffness of granular soils. Particuology, 32, 21-29.

[8] Ma, X., Lei, H., & Kang, X. (2022). Effects of particle morphology on the shear response of granular soils by discrete element method and 3D printing technology. International Journal for Numerical and Analytical Methods in Geomechanics, 46(11), 2191-2208.

[9] Zhang, T., Li, S., Yang, H., & Zhang, F. (2024). Prediction of constrained modulus for granular soil using 3D discrete element method and convolutional neural networks. Journal of Rock Mechanics and Geotechnical Engineering.

[10] Nasirpur, O., Çelik, S., & Karimi, B. (2024). Modeling the Behavior of Granular Soils with Different Shape Characteristics Behind a Retaining Wall with Discrete Element and PIV Method. Iranian Journal of Science and Technology, Transactions of Civil Engineering, 48(3), 1609-1626.

[11] Luding, S. (1998). Collisions & contacts between two particles. In Physics of dry granular media (pp. 285-304). Dordrecht: Springer Netherlands.

[12] Raous, M., Jean, M., & Moreau, J. J. (Eds.). (1995). Contact mechanics. New York: plenum Press.

[13] Moreau, J. J. (1994). Sorne numerical methods in multibody dynamics: application to granular materials. European Journal of Mechanics-A/Solids, 13(4-suppl), 93-114.

[14] Moreau, J. J. (1995). Numerical experiments in granular dynamics: Vibration-induced size segregation. In Contact Mechanics (pp. 347-358). Boston, MA: Springer US.

[15] Jean, M. (1995). Mechanics of geometrical interfaces.

[16] Rapaport, D. C. (1980). The event scheduling problem in molecular dynamic simulation. Journal of Computational Physics, 34(2), 184-201.

[17] Walton, O. R., & Braun, R. L. (1986). Viscosity, granular-temperature, and stress calculations for shearing assemblies of inelastic, frictional disks. Journal of rheology, 30(5), 949-980.

[18] Wu, K., Sun, W., Liu, S., & Zhang, X. (2021). Study of shear behavior of granular materials by 3D DEM simulation of the triaxial test in the membrane boundary condition. Advanced Powder Technology, 32(4), 1145-1156.

[19] Wang, X., & Li, J. (2014). Simulation of triaxial response of granular materials by modified DEM. Science China Physics, Mechanics & Astronomy, 57, 2297-2308.

[20] Gong, J., Pang, X., Tang, Y., Liu, M., Jiang, J., & Ou, X. (2024). Effects of particle shape, physical properties and particle size distribution on the small-strain stiffness of granular materials: A DEM study. Computers and Geotechnics, 165, 105903.

[21] Nguyen, H. B. K., Rahman, M. M., & Fourie, A. B. (2020). Effect of particle shape on constitutive relation: DEM study. Journal of Geotechnical and Geoenvironmental Engineering, 146(7), 04020058.

[22] Ng, T. T. (1994). Numerical simulations of granular soil using elliptical particles. Computers and geotechnics, 16(2), 153-169.

[23] Itasca, C. G. I. (2005). PFC3D (Particle Flow Code in Three Dimensions). Minneapolis, Minnesota, USA.

[24] Cantürk, U., Koç, İ., Özel, H. B., & Şevik, H. (2024). Possible changes of Pinus nigra distribution regions in Türkiye with the impacts of global climate change. BioResources, 19(3), 6190- 6214.

[25] Işınkaralar, K., Işınkaralar, Ö., & Şevik, H. (2022). Usability of some landscape plants in biomonitoring technique: an anaysis with special regard to heavy metals. Kent Akademisi, 15(3), 1413-1421.

[26] Şen, G., Güngör, E., & Şevik, H. (2018). Defining the effects of urban expansion on land use/cover change: a case study in Kastamonu, Turkey. Environmental monitoring and assessment, 190(8), 454.

[27] Yılmazoğlu, M. U., & İnce, G. Ç. (2022). Investigation of the soil behaviour of Fethiye District, Mesudiye, Muğla, by one-dimensional equivalent linear analysis method. Arabian Journal of Geosciences, 15(9), 813.

[28] İnce, G. Ç., & Yılmazoğlu, M. U. (2021). Probabilistic seismic hazard assessment of Muğla, Turkey. Natural Hazards, 107(2), 1311-1340.

[29] Memiş, S., Mütevelli, İ. G., & Yılmazoğlu, M. U. (2016). Sinop İlinde Üretilen Hazır Betonların İstatistiksel Olarak Değerlendirilmesi. Engineering Sciences, 11(4), 83-92.

[30] Özkan, İ. G. M., Aldemir, K., Alhasan, O., Benli, A., Bayraktar, O. Y., Yılmazoğlu, M. U., & Kaplan, G. (2024). Investigation on the sustainable use of different sizes of sawdust aggregates in eco-friendly foam concretes: Physico-mechanical, thermal insulation and durability characteristics. Construction and Building Materials, 438, 137100.

[31] Kaplan, G., Bayraktar, O. Y., Li, Z., Bodur, B., Yılmazoglu, M. U., & Alcan, B. A. (2023). Improving the eco-efficiency of fiber reinforced composite by ultra-low cement content/high FA-GBFS addition for structural applications: Minimization of cost, CO2 emissions and embodied energy. Journal of Building Engineering, 76, 107280.

[32] Memiş, S., Yılmazoğlu, M. U., & Mütevelli, İ. G. (2016). Kastamonu İlinde Kullanılan Betonların Nicel Analizi. Düzce Üniversitesi Bilim ve Teknoloji Dergisi, 4(2), 756-764.

[33] Bayraktar, O. Y., Yılmazoğlu, M., Mütevelli, İ., Çetin, M., Çitoğlu, G. S., Dadula, C. P., & Dadula, D. P. (2022). Usability of organic wastes in concrete production; Palm leaf sample. Kastamonu University Journal of Engineering and Sciences, 8(1), 69-77.

[34] Yaprak, H., Memis, S., Kaplan, G., Yilmazoglu, M. U., & Ozkan, I. G. M. (2018). Effects on compressive strenght of accelerated curing methods in alkali activated mortars. Int J Sci Technol Res, 4.

[35] Memis, S., Kaplan, G., Yaprak, H., Yilmazoglu, M. U., & Mütevvelli Özkan, I. G. (2018). Some durability properties of alkali activated materials (AAM) produced with ceramic powder and micro calcite. Ceram. Silik, 62, 342-354.

[36] Memiş, S., Özkan, İ. M., Yılmazoğlu, M. U., Kaplan, G., & Yaprak, H. (2018). Behavior of mortar samples with waste brick and ceramic under freeze-thaw effect. In Proceedings of 3rd International Sustainable Buildings Symposium (ISBS 2017) Volume 2 3 (pp. 189-202). Springer International Publishing.

[37] Yilmazoğlu, M. U. (2024). Effect of Bone Ash and Rice Husk Ash on the Unconfined Compressive Strength of Silt Soil. Kastamonu University Journal of Engineering and Sciences, 10(1), 22-28.

doi:10.55385/kastamonujes.1560664 KUJES 10(2):81-94, 2024

Kastamonu University
Journal of Engineering and Sciences
e-ISSN 2667-8209
http://dergipark.gov.tr/kastamonujes

Integrated Ergonomic Risk Analysis by Using REBA, RULA, OWAS, and AHP in the Furniture Manufacturing Line

Dilara Güray[a], Dilber İnal[a], Ahmet Al-Ahdal[a], Mustafa Sekmen[b], Fatih Yapıcı[a,*]

[a] Department of Industrial Engineering, Faculty of Engineering, Ondokuz Mayıs University, Samsun, Türkiye
[b] Department of Occupational Health and Safety Program, Havza Vocatioanal School, Ondokuz Mayıs University, Samsun, Türkiye
***Corresponding Author:** fatih.yapici@omu.edu.tr

Received: **October 3, 2024** ◆ Accepted: **December 20, 2024** ◆ Published Online: **December 25, 2024**

Abstract: Ergonomic risk is defined as the existence or potential of factors that may negatively affect the health and safety of employees in the workplace. The main source of ergonomic risks may be unsuitable working body posture, carried loads or applied forces at the workplaces. In order to protect employee health, ergonomic risk assessments must be carried out in workplaces to determine risk levels and take necessary precautions. This study was carried out in a company that produces furniture in the furniture sector. 42 working postures were evaluated in the study. Ergonomic risk levels of employees were determined by using REBA, RULA, OWAS and MURI methods. Since the risk score levels of each of these methods are different, the AHP method was applied to obtain an integrated risk score. Risk values were ranked using the criteria weights determined by the AHP method. While applying the AHP method, 3 decision makers were employed. Decision makers compared each ergonomic risk assessment method and determined their importance levels. According to the integrated risk scores, the highest risk levels of operations were determined to be taping the box (58%), sewing (45%), putting the finished parts (43%), removing the feet (43%), closing the box lids (42%) and removing the bases of parts (40%), respectively, and necessary remedial suggestions were presented.

Keywords: Ergonomics, risk Analysis, REBA, RULA, AHP

Öz: İşyerlerinde çalışanların sağlığını ve güvenliğini olumsuz etkileyebilecek faktörlerin varlığı veya potansiyeli ergonomik risk olarak tanımlanmaktadır. İşyerlerindeki ergonomik risklere, uygun olmayan vücut pozisyonları, taşınan yükler veya uygulanan aşırı ve sık tekrarlı kuvvetler gibi vb. unsurlar neden olabilir. Çalışan sağlığını korumak için işyerlerinde gerekli ergonomik risk değerlendirmeleri yapılmalı, olası risk seviyelerinin tespit edilerek ve gerekli önlemlerin alınması sağlanmalıdır. Bu çalışmada, mobilya sektöründe üretim yapan bir işletmede üretim süreçleri dikkate alınak çalışanların ergonomik risk seviyeleri REBA, RULA, OWAS ve MURI yöntemleri belirlenmiştir. Bu yöntemlerin her birinin risk skorları farklı olduğundan bütünleşik sonuç elde edebilmek için AHP yöntemi uygulanmıştır. AHP yöntemi ile belirlenen kriter ağırlıkları kullanılarak sıralama yapılmıştır. AHP yöntemi uygulanırken 3 karar verici ile çalışılmıştır. Karar vericiler her bir ergonomik risk değerlendirme yöntemlerini ikili olarak karşılaştırarak birbirlerine göre önem düzeyleri belirlenerek yüksek risk düzeyine sahip süreçler tepit edilmiştir. Bütünleşik risk skorlarına göre en yüksek riske sahip işlemlerin sırasıyla kutuyu bantlama (%58), dikim işlemi (%45), biten parçaları kenara koyma (%43), ayakları alma (%43), kutunun kapaklarını kapatma (%42) ve altlıkları alma (%40) şeklinde olduğu belirlenerek gerekl iyileştirici öneriler sunulmuştur.

Anahtar Kelimeler: Ergonomi, risk Analizi, REBA, RULA, AHP

1. Introduction

Machines have become widely used in today's production system. Although mechanization and automation increase the speed of production, the need for physical manpower is present in many areas. Especially in businesses with labor-intensive production system, employees are faced with intense musculoskeletal system disorders (MSDs). MSDs is one of the most common health problems in the world. This disease occurs in joints, discs, muscles, ligaments, nerves and tendons while performing ordinary body movements such as bending, straightening, holding, grasping, twisting and reaching [1]. According to the Global Burden of Disease results, it has been reported that MSDs increased by 38.4% from 1990 to 2007 and by 19.9% from 2007 to 2017 in 195 countries examined. MSD accounts for 50% of new cases in work-related diseases. In Turkey, MSD ranks second in disability-adjusted life years lost with 37% [2]. These disorders generally result from physical and environmental factors such as repetitive movements, incorrect body postures, static working conditions, excessive workload, and heavy lifting in the workplace [3]. MSD develops over time and mostly affects the upper body parts (such as neck, shoulder, elbow, wrist and waist). This situation causes fatigue, pain and eventually work accidents in the employee and reduces the labor productivity of factory [4]. Improving working conditions is very important for employee health and workforce productivity. The most important way to prevent MSDs is to determine ergonomic risks in the workplace. Ergonomics is an interdisciplinary branch of science that establishes a

relationship between employees and working conditions. Ergonomics seeks solutions on how to organize the work environment and adapt it to workers in order to eliminate health problems caused by work and increase productivity [5]. As a result of ergonomic risk assessment analyses, risk scores and the improvements to be made in working conditions are determined accordingly [6]. There area many methods used to assess ergonomic risks. These methods are designed by considering the posture of the worker or the nature of the work. For this reason, it is important to choose the appropriate methods for the job [7].

Beliveau et al. [8] presented a web-based survey study that revealed the level of awareness levels of about MSD risk assessment tools in Canada. Zengin and Asal [9] analyzed 39 working postures of construction industry workers with 3 different ergonomic risk assessment methods suc as REBA, OWAS and QEC. As a result of this analysis, it was seen that the results of the QEC method were different from the other methods. Hawari et al. [10] conducted ergonomic risk analysis with QEC and REBA methods for cutting, lifting and assembly operations in three woodworking workshops. Erginel et al. [11] examined the work postures of workers in a furniture factory with the Fuzzy REBA method. Ekinci and Can [12] analyzed work postures using the REBA method in a fruit juice production line and determined ergonomic risk levels. Akalp et al. [13] analyzed the work postures of agricultural workers during olive harvest with the REBA method and offered some solutions for risky processes. Koç and Testik [14] analyzed 40 tasks in modular and upholstery units of a furniture manufacturing factory with the REBA method. Polat et al. [15] evaluated 32 working postures in a furniture factory with REBA, identified high-risk jobs, and they made recommendations to reduce the identified risks. Costa et al. [16] conducted an ergonomic analysis of an industrial kitchen. In this context, the most critical activities were analyzed with RULA, REBA and OWAS methods and the results were compared. Kahya et al. [17] analyzed 20 different processes performed by using the REBA, NERPA, QEC, OWAS and MURI methods in a company which produces metal parts. According to risk scores they suggested to remedial developments for the first 5 processes with the highest integrated risk scores. Delice et al. [18] performed ergonomic risk assessment analyses with REBA, OWAS, QEC and MANTRA methods in a tube production factory and obtained an integrated result with the AHP method.

In the literature, various analyses have been conducted for ergonomic risk assessment in many different sectors such as textiles, furniture, metal, manufacturing, and construction. It has been observed that methods such as REBA, RULA, NISOH, OCRA, QEC, NERPA, ManTRA, and OWAS are commonly used in the differents manufacturing area. It has also been noted that different methods used for the same tasks in different working conditions may occurred different results. In this case, determining integrated risk scores is important in evaluating the same processes. In this study, it was aimed to determine the integrated risk scores of 42 working postures that can represent the all-production processes, especially in a labor-intensive furniture production, using REBA, RULA, OWAS, MURI and AHP methods. As a result of the analyses, the risk scores for each position of body posture were determined, and risk score weights were established by using the AHP method, considering the views of three decision-makers. Detailed examinations were conducted for the job position with the highest risk score, and ergonomic improvement suggestions were developed.

2. Material and Method

2.1. Material

This study was carried out in a furniture manufacturing company with labor-intensive production. The company is located in the Black Sea Organized Industrial Zone. The product group that is most produced in the company for risk analysis was called as the name A. The production processes of product A consist of 7 steps. These steps can be listed as face fabric sewing, frame laying, polyurethane sponge laying, lining, assembly, foot attachment and packaging. The movements of the workers working at each stage were examined and ergonomic risk analysis was performed according to the REBA, RULA, OWAS and MURI methods. In addition, since the risk scores of each of these methods may give different results, the AHP method was applied in order to obtain an integrated result. Decision makers were selected from experts who have sufficient knowledge about the risk assessment methods used in the study, such as REBA, RULA, OWAS and MURI, as well as the AHP method and the production processes to be examined in the study. Table 1 shows the ergonomic risk assessment method, risk scores and action cases.

Table 1. Risk scores and action statuses depending on risk methods.

Technique	Risk Score	Action
REBA [19]	1	No action required
	2-3	Modification may be needed
	4-7	Further investigation may be needed
	8-10	Modification is required
	>11	Modification is required immediately
RULA [20]	1-2	No action is needed.
	3-4	Measures should be taken, but not in the short term.
	5-6	Measures should be taken in the short term.
	7+	Urgent action must be taken.
OWAS [21]	1	No action required
	2	Ergonomic arrangement should be done soon
	3	Ergonomic arrangement should be done soon
	4	Ergonomic arrangement should be done immediately
MURI [22]	0-10	Green
	11-15	Yellow
	16+	Red

2.2. Analytic Hierarchy Process (AHP)

The AHP method is a Multi-Criteria Decision-Making (MCDM) method that assists decision-makers by providing results that are easy to understand and reliable. This method enables the numerical ranking of alternatives and criteria and contributes to solving complex problems. Problems to be solved using the AHP method should be defined in as much detail as possible and structured according to a specific priority hierarchy. At the top level of the hierarchy is the main goal, while at the lowest level are the decision alternatives [23]. The AHP method generally consists of certain stages, which are detailed below.

Building the hierarchical model: At the top is the main goal to be achieved, while the criteria used to reach this goal are located at the middle level. At the lowest level are the alternatives evaluated in the decision-making process. An example of a three-level hierarchical structure is provided in Figure 1.

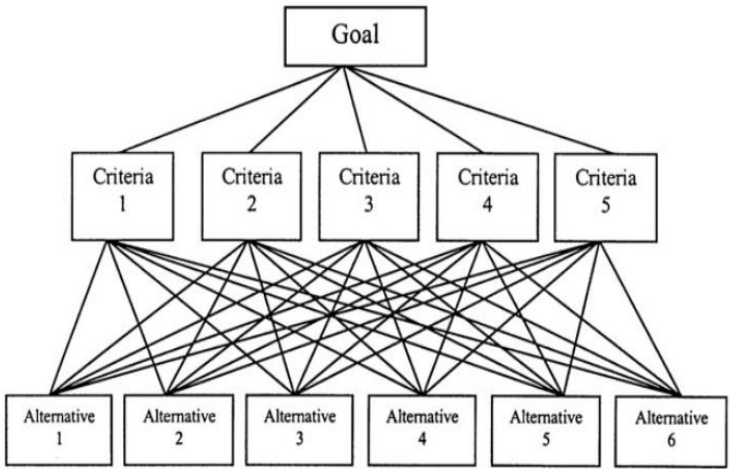

Figure 1. Example AHP model

Preparation of Pairwise Comparison Matrices: After building the hierarchical model, pairwise comparison matrices are prepared to determine the relative importance of each element. In these matrices, decision-makers determine the importance levels for each pair. When criterion i is compared with criterion j, the 1-9 scale proposed by Saaty [24] is used to determine the degree to which criterion i is preferred over criterion j. This comparison scale is provided in Table 2.

Table 2. Comparison scale of AHP method

Severity Level	Definition	Explanation
1	Equal importance	Two activities have equal contribute to the objective
3	Moderate importance	Experience and judgment slightly favor one activity over another
5	Strong importance	Experience and judgment strongly favor one activity over another
7	Very strong importance	An activity is favored very strongly over another
9	Extreme importance	The evidence favoring one activity over another is of the highest possible order of affirmation
2, 4, 6, 8	Intermediate values	Sometimes one needs to interpolate a compromise judgment numerically

With the judgments converted into numerical values by means of the comparison scale, the pairwise comparison matrix, whose general representation is provided in Equation 1, is constructed.

$$\boldsymbol{A_{ij}} = \begin{bmatrix} \boldsymbol{a_{11}} & \boldsymbol{a_{12}} & \dots & \boldsymbol{a_{1n}} \\ \boldsymbol{a_{21}} & \boldsymbol{a_{22}} & \dots & \boldsymbol{a_{2n}} \\ \boldsymbol{a_{n1}} & \boldsymbol{a_{n2}} & \dots & \boldsymbol{a_{nn}} \end{bmatrix} \quad (1)$$

Pairwise comparisons are made for the upper triangular part of a matrix whose diagonal elements are equal to 1. That is, the diagonal elements of A (a_{ij}) must take the value of 1. If A_{ij} represents the pairwise comparison value of criterion *i.* and *j.* then A_{ij} is obtained by the equality $A_{ij} = 1/A_{ij}$.

To make decisions using the AHP method, the comparison matrix A, which is formed in the case where n criteria exist, will have a size of $n \times n$. If there is more than one decision-maker, the pairwise comparison matrices must be transformed into a single pairwise matrix using the geometric mean method. Therefore, the comparison of criterion i and criterion j by decision-maker kk is expressed as a_{ij}^k, and the common decision regarding the criterion made by n decision-makers is transformed into a single pairwise comparison matrix using the geometric mean method with the formula given in Equation 2.

$$\boldsymbol{a_{ij}^k} = (\boldsymbol{a_{ij}^1} * \boldsymbol{a_{ij}^2} * \dots * \boldsymbol{a_{ij}^n})^{\boldsymbol{1/n}} \quad (2)$$

Calculation of the normalized pairwise comparison matrix: The values in the initial A_{ij} matrix, which is prepared based on the judgments of the decision-makers, are determined as numbers between 0 and 1 using Equation 3.

$$\boldsymbol{b_{ij}} = \frac{\boldsymbol{a_{ij}}}{\sum_{\boldsymbol{i=1}}^{\boldsymbol{n}} \boldsymbol{a_{ij}}} \quad (3)$$

This operation is performed by dividing each element of the initial A_{ij} matrix by the sum of its respective column. This process is repeated for each column. The new matrix obtained is the normalized pairwise comparison matrix N_{ij} , as shown in Equation 4.

$$\boldsymbol{N_{ij}} = \begin{bmatrix} \boldsymbol{b_{11}} & \boldsymbol{b_{12}} & \dots & \boldsymbol{b_{1j}} \\ \boldsymbol{b_{21}} & \boldsymbol{b_{22}} & \dots & \boldsymbol{b_{2j}} \\ \boldsymbol{b_{i1}} & \boldsymbol{b_{i2}} & \dots & \boldsymbol{b_{ij}} \end{bmatrix} \quad (4)$$

Calculation of the Weight Matrix: The b_{ij} values in the normalized matrix obtained in Step 3 are averaged row-wise using the formula in Equation 5.

$$\boldsymbol{W_i} = \frac{\sum_{\boldsymbol{j=1}}^{\boldsymbol{n}} \boldsymbol{b_{ij}}}{\boldsymbol{n}} \quad (5)$$

The obtained values for each row form the weight matrix W_i , as shown in Equation 6. The W_i matrix represents the percentage importance distribution of the criteria.

$$\boldsymbol{W_i} = \begin{bmatrix} \boldsymbol{W_1} \\ \boldsymbol{W_2} \\ . \\ \boldsymbol{W_n} \end{bmatrix} \quad (6)$$

Performing Consistency Test Procedures: The matrices formed by decision-makers must be consistent. Here, consistency refers to the mutual compatibility of the pairwise comparisons of criteria and alternatives. If Equation 7 is satisfied for all i, j, k it indicates that the pairwise comparison matrix A is consistent.

$$a_{ij} * a_{jk} = a_{ik} \quad (7)$$

As a result, the matrix N, where all rows and columns will be equal in the pairwise comparison matrix A accepted as consistent, is calculated as shown in Equation 8.

$$\boldsymbol{N} = \begin{bmatrix} \boldsymbol{W_1} & \boldsymbol{W_1} & \boldsymbol{W_1} \\ \boldsymbol{W_2} & \boldsymbol{W_2} & \boldsymbol{W_2} \\ \boldsymbol{W_n} & \boldsymbol{W_n} & \boldsymbol{b_{ij}} \end{bmatrix} \quad (8)$$

After this stage, the symmetric matrix A is obtained by dividing the elements in the iii-th column of the matrix N by W_i. Thus, the matrix given in Equation 9 is obtained.

$$\boldsymbol{A} = \begin{bmatrix} \boldsymbol{1} & \boldsymbol{W_1/W_2} & \cdots & \boldsymbol{W_1/W_n} \\ \boldsymbol{W_2/W_1} & \boldsymbol{1} & \cdots & \boldsymbol{W_2/W_n} \\ \vdots & \vdots & \vdots & \vdots \\ \boldsymbol{W_n/W_1} & \boldsymbol{W_n/W_2} & \cdots & \boldsymbol{1} \end{bmatrix} \quad (9)$$

By continuing with the definition of A, the matrix provided in Equation 10 is obtained.

$$\begin{bmatrix} 1 & W_1/W_2 & \cdots & W_1/W_n \\ W_2/W_1 & 1 & \cdots & W_2/W_n \\ \vdots & \vdots & \vdots & \vdots \\ W_n/W_1 & W_n/W_2 & \cdots & 1 \end{bmatrix} * \begin{bmatrix} W_1 \\ W_2 \\ W_3 \\ \vdots \\ W_n \end{bmatrix} = \begin{bmatrix} n * W_1 \\ n * W_2 \\ n * W_3 \\ \vdots \\ n * W_n \end{bmatrix} = n * \begin{bmatrix} W_1 \\ W_2 \\ W_3 \\ \vdots \\ W_n \end{bmatrix} \quad (10)$$

In summary, *A* can only be considered consistent if the equation given in Equality 11 is satisfied.

$$A * w = n * W \quad (11)$$

The *w* w_i in Equation 11 represents the column vector of relative weights for *i= 1,2,3,…n*. Moreover, when the size of the normalized pairwise comparison matrix given in Equation 4 is greater than 2×2 , the column values of the relevant matrix can be checked to determine whether the matrix is identical. As a result of this check, if there is a normalized pairwise comparison matrix where the column values are identical, the relative importance weights will remain the same regardless of how the pairwise comparison was conducted, and a consistency test will not be necessary. The A_{ij} matrix given in Equation 1 and the W_i weight matrix given in Equation 6 are multiplied according to the rules of matrix multiplication (as per Equation 11). The column sums of the resulting matrix represent the *n*_max value [23] (Karaburun, 2018). If the despite all the checks, the equality in the columns of the normalized pairwise comparison matrix specified in Equation 4 is not achieved, the CR (Consistency Ratio) is calculated using the formula shown in Equation 12.

$$CR = \frac{CI}{CR} \quad (12)$$

The *CI* in Equation 12 is the Consistency Index, and RI is the Random Index. The calculation of *CI* and *RI* is carried out using the formulas in Equations 13 and 14.

$$CI = \frac{n_{max}-n}{n-x} \quad (13)$$

$$RI = \frac{1{,}98(n-2)}{n} \quad (14)$$

In the calculation of *CR*, the Random Index (*RI*) table, which contains fixed values based on the number of criteria (*n*) used in the pairwise comparison, is provided in Table 3.

Table 3. Random Indices

n	1	2	3	4	5	6	7	8	9	10	11	12	13	14	15
RI	0	0	0.6	0.9	1.1	1.2	1.3	1.4	1.5	1.5	1.5	1.5	1.6	1.6	1.6

After calculating the CR value, some comments can be made based on the result. These are: If *CR*≤ 0,1 it can be said that the consistency level of the pairwise comparison matrix *A* is at an acceptable level.

If *CR*> 0,1 it is understood that the consistency level of the pairwise comparison matrix *A* is not at an acceptable level. In the case of inconsistency, the decision-maker needs to review their judgments, reconstruct the pairwise comparison matrix *A*, and repeat the process.

3. Findings and Discussion

3.1. Findings on Classical Risk Scores

When the literature is reviewed, it is seen that methods such as REBA, RULA, OWAS, and MURI have been successfully applied in various sectors. Some of these studies include; Akay et al. [3] conducted a risk analysis using the OWAS method in auto-service stations and proposed corrective recommendation, Atıcı et al. [25] conducted a risk analysis using the REBA method in a cable manufacturing facility, Ülker and Buldurlu [26] performed measurements using the OWAS method in a furniture enterprise and identified risk values, Kahraman [27] conducted analyses in a marble enterprise using REBA, RULA, and AHP methods; and in a study by Kılıç Delice et al. [28], ergonomic risk assessments were carried out using REBA, OWAS, QEC, and MANTRA methods in a tube production enterprise categorized as heavy and hazardous work. In the literature, there are various methods with different characteristics for evaluating ergonomic risks. These methods are generally designed to assess the worker's posture (changes in joint positions) during work. It is crucial to select the appropriate method for the specific job while evaluating ergonomic risks [7]. The enterprise where the ergonomic risk analyses were conducted is a furniture manufacturing company located in the Karadeniz Organized Industrial Zone. For the risk analysis, the most commonly produced product group in the enterprise has been anonymized under the name Product A. The production processes for Product A consist of seven main stages: sewing the fabric cover, upholstering the frame, foam padding, lining, assembly, attaching the legs, and packaging. In each production process

(including sub-processes), workers' movements were examined, and ergonomic risk analyses were performed using the REBA, RULA, OWAS, and MURI methods. The results obtained are presented in Table 4.

Table 4. Risk scores of operations according to methods

Process	Process steps	REBA	RULA	OWAS	MURI
Sewing the face fabric	(1) Reach for the part	3	3	1	10
	(2) Sewing	5	4	2	11
	(3) Cutting	4	4	1	11
	(4) Reach for the machine	4	3	1	9
	(5) Drop the part	3	3	1	10
	(6) Change the thread and spool	2	4	1	9
Sponge laying	(7) Take the sponges	4	3	1	12
	(8) Take the bases	3	4	2	12
	(9) Reach for the glue gun (600gr)	2	3	1	10
	(10) Apply glue	3	3	1	10
	(11) Put down the glue gun	1	3	1	9
	(12) Stick the base to the sponge	3	3	2	11
	(13) Put the finished items aside	3	3	2	12
Priming / lining	(14) Take the sponge	4	3	1	11
	(15) Adjust the primer lining	2	3	1	12
	(16) Reach for the scissor	3	3	2	11
	(17) Cut the primer lining material	3	3	2	10
	(18) Reach for the stapler	3	3	2	9
	(19) Stapling	4	3	2	10
	(20) Reach for the knife	3	4	2	10
	(21) Open the mechanism	3	2	2	9
	(22) Put the finished items aside	3	3	2	10
Framework laying	(23) Take the frame	3	3	1	10
	(24) Take the cover	3	3	2	9
	(25) Put on the cover	3	3	1	10
	(26) Fix of the cover	5	3	1	11
	(27) Put the finished parts in the box	3	2	2	10
Wheel fitting	(28) Bring the materials to the table	3	2	1	10
	(29) Attach the wheel	4	2	1	9
	(30) Take the hub ring	3	3	2	12
	(31) Install the hub ring	4	2	2	9
	(32) Put the finished parts aside	5	4	1	9
Assembly process	(33) Take the bottom cover	1	4	1	9
	(34) Assemble the bottom cover	4	3	2	11
	(35) Take the mechanism	1	2	1	9
	(36) Assemble the mechanism	4	3	2	10
	(37) Leave the finished ones in the box	2	3	2	10
Packaging	(38) Take the legs	6	3	2	13
	(39) Put the legs in the box	4	3	2	11
	(40) Install the shock absorber	4	4	2	9
	(41) Close the box lids	6	3	2	10
	(42) Tape the box	7	5	2	13

As seen in Table 4, the highest risk level, according to the REBA and RULA methods, is the box taping process (scores of 7 and 5), while according to the MURI method, the box taping and foot retrieval processes have the highest risk (score of 13). According to the OWAS method, 23 processes have the highest equivalent score.

For processes with medium and higher risk levels:

The REBA method identified 17 processes,

The MURI method identified 15 processes,

The RULA method identified 1 process,

The OWAS method identified no processes with medium or higher risk.

As is known, improvements should be made for medium-level risks, while for high-risk levels, improvements are recommended to be made as soon as possible. In ergonomic risk assessment, when different methods are used, different

risk scores can be obtained even for the same processes. Therefore, it is important to use a method that is suitable for the work processes or to determine integrated risk scores obtained from multiple methods.

3.2. Results on Determining Risk Scores as Percentages (%)

The structure of each ergonomic risk assessment method used in practice is different from one another. (For example, the maximum risk score in the OWAS method is 4, while it is 15 in the REBA method.) To express risk scores in a common language, they can be converted to the same unit. For this, the percentage (%) value per 1 unit of risk score can be determined. For example, for the RULA score, since the maximum risk score is 7, the value for 1 risk score is calculated as 14.30% (Table 5).

Table 5. Comparison scale

Method	Mak.Score	Score (%)
REBA	15	6.70
RULA	7	14.30
OWAS	4	25
MURİ	27	3.7

In this case, for Process 1 (the reaching movement for the part), the risk scores in percentage (%) terms would be calculated as 20.10% (3x6.7) for REBA, 42.90% (3x14.30) for RULA, 25% (1x25) for OWAS and 37% (10x3.7) for MURI.

If it is assumed that the integrated risk scores of the four methods used have an equal impact (equal weight of 25%), the risk score of Process 1 (the reaching movement for the part) would be calculated as approximately ~%31 [%25. (%20,10+ %42,90+ %25+ %37)] it would have been calculated as. According to this calculation, the integrated risk scores of all movements are given in Table 6.

Although ergonomic risk assessment methods consider body posture and positioning when identifying risks in work processes, the evaluation procedures and risk score classifications of each method differ. In other words, when the same work processes are evaluated using different methods, they may yield risk levels with varying priorities. Sometimes, to obtain more consistent risk scores in the analyzed work processes, an integrated risk score can be calculated by using multiple methods.

Under the assumption that the impact of the methods on the integrated risk score is considered equal, it is assumed that each method has the same influence. However, this assumption may not be consistent due to the differing criteria considered by each risk analysis method. Therefore, obtaining an integrated risk score by weighting each method according to decision-makers' evaluations would provide more reliable results. In this study, the ergonomic risk assessment methods used were weighted using the AHP (Analytic Hierarchy Process), and integrated risk scores were obtained.

Table 6. Integrated risk scores in the case where the weights of methods are assumed to be equal

Process	Process steps	REBA	RULA	OWAS	MURI	REBA%	RULA%	OWAS %	MURI %	Risk Skoru%
Sewing the face fabric	(1) Reach for the part	**3**	**3**	**1**	**10**	**20**	**43**	**25**	**37**	**31**
	(2) Sewing	5	4	2	11	34	57	50	41	45
	(3) Cutting	4	4	1	11	27	57	25	41	37
	(4) Reach for the machine	4	3	1	9	27	43	25	33	32
	(5) Drop the part	3	3	1	10	20	43	25	37	31
	(6) Change the thread and spool	2	4	1	9	13	57	25	33	32
Sponge laying	(7) Take the sponges	4	3	1	12	27	43	25	44	35
	(8) Take the bases	3	4	2	12	20	57	50	44	43
	(9) Reach for the glue gun (600gr)	2	3	1	10	13	43	25	37	30
	(10) Apply glue	3	3	1	10	20	43	25	37	31
	(11) Put down the glue gun	1	3	1	9	7	43	25	33	27
	(12) Stick the base to the sponge	3	3	2	11	20	43	50	41	38
	(13) Put the finished items aside	3	3	2	12	20	43	50	44	39
Priming or lining	(14) Take the sponge	4	3	1	11	27	43	25	41	34
	(15) Adjust the primer lining	2	3	1	12	13	43	25	44	31
	(16) Reach for the scissor	3	3	2	11	20	43	50	41	38
	(17) Cut the primer lining material	3	3	2	10	20	43	50	37	38
	(18) Reach for the stapler	3	3	2	9	20	43	50	33	37
	(19) Stapling	4	3	2	10	27	43	50	37	39
	(20) Reach for the knife	3	4	2	10	20	57	50	37	41
	(21) Open the mechanism	3	2	2	9	20	29	50	33	33
	(22) Put the finished items aside	3	3	2	10	20	43	50	37	38
Framework laying	(23) Take the frame	3	3	1	10	20	43	25	37	31
	(24) Take the cover	3	3	2	9	20	43	50	33	37
	(25) Put on the cover	3	3	1	10	20	43	25	37	31
	(26) Fix of the cover	5	3	1	11	34	43	25	41	36
	(27) Put the finished parts in the box	3	2	2	10	20	29	50	37	34
Wheel fitting	(28) Bring the materials to the table	3	2	1	10	20	29	25	37	28
	(29) Attach the wheel	4	2	1	9	27	29	25	33	28
	(30) Take the hub ring	3	3	2	12	20	43	50	44	39
	(31) Install the hub ring	4	2	2	9	27	29	50	33	35
	(32) Put the finished parts aside	5	4	1	9	34	57	25	33	37
Assembly process	(33) Take the bottom cover	1	4	1	9	7	57	25	33	31
	(34) Assemble the bottom cover	4	3	2	11	27	43	50	41	40
	(35) Take the mechanism	1	2	1	9	7	29	25	33	23
	(36) Assemble the mechanism	4	3	2	10	27	43	50	37	39
	(37) Leave the finished ones in the box	2	3	2	10	13	43	50	37	36
Packaging	(38) Take the legs	6	3	2	13	40	43	50	48	45
	(39) Put the legs in the box	4	3	2	11	27	43	50	41	40
	(40) Install the shock absorber	4	4	2	9	27	57	50	33	42
	(41) Close the box lids	6	3	2	10	40	43	50	37	43
	(42) Tape the box	7	5	2	13	47	72	50	48	54

3.3. Results of the AHP Method

The AHP method was applied with the involvement of three decision-makers. The decision-makers conducted pairwise comparisons of each ergonomic risk assessment method to determine their relative importance.

The pairwise comparison matrices created by the decision-makers were combined using the geometric mean. The Combined Decision Matrices of the three decision-makers are presented in Table 7, and the Normalized Matrices are presented in Table 8.

Table 7. Combined Decision Matrices

Method	REBA	RULA	OWAS	MURİ
REBA	1.000	0.693	7.612	4.217
RULA	1.442	1.000	3.557	4.932
OWAS	0.131	0.281	1.000	0.523
MURİ	0.237	0.203	1.913	1.000
Total	2.811	2.177	14.081	10.672

Table 8. Normalized Matrix

Method	REBA	RULA	OWAS	MURI
REBA	0.356	0.318	0.541	0.395
RULA	0.513	0.459	0.253	0.462
OWAS	0.047	0.129	0.071	0.049
MURI	0.084	0.093	0.136	0.094

The combined priority weights of the four methods used were calculated, and these calculated values are presented in Table 9.

Table 9. Combined with priority values (Weights) (%)

Method	Values of weight (%)
REBA	40.2
RULA	42.2
OWAS	7.4
MURI	10.2

The consistency ratio was determined to be 0.054. Since this value is less than 0.1, the matrix is considered consistent. While coefficients in mathematical programming problems are explicitly known, in real-world business operations, coefficients are not always numerically defined. In such cases, efforts are made to determine the ranges of these coefficients, which is referred to as sensitivity analysis [29].

Sensitivity analysis shows how well the alternatives perform for each objective and how sensitive they are to changes in the importance of the objectives. Determining the impact of changes in the values assigned by decision-makers during the relative evaluation of the methods used in the study is important for finding the optimal solution. Using the values in Table 9, the integrated risk scores of the analyzed work processes were obtained (Table 10). This approach enabled the systematic and objective evaluation of risk levels, ranked from highest to lowest, based on integrated scores.

Table 10. Integrated risk scores according to the weights determined by AHP

Process	Process steps	REBA	RULA	OWAS	MURİ	REBA (%)	RULA (%)	OWAS (%)	MURI (%)	Integrated score (%)
Sewing the face fabric	(1) Reach for the part	3	3	1	10	20	43	25	37	32
	(2) Sewing	5	4	2	11	34	57	50	41	45
	(3) Cutting	4	4	1	11	27	57	25	41	41
	(4) Reach for the machine	4	3	1	9	27	43	25	33	34
	(5) Drop the part	3	3	1	10	20	43	25	37	32
	(6) Change the thread and spool	2	4	1	9	13	57	25	33	35
Sponge laying	(7) Take the sponges	4	3	1	12	27	43	25	44	35
	(8) Take the bases	3	4	2	12	20	57	50	44	40
	(9) Reach for the glue gun (600gr)	2	3	1	10	13	43	25	37	29
	(10) Apply glue	3	3	1	10	20	43	25	37	32
	(11) Put down the glue gun	1	3	1	9	7	43	25	33	26
	(12) Stick the base to the sponge	3	3	2	11	20	43	50	41	34
	(13) Put the finished items aside	3	3	2	12	20	43	50	44	34
Priming or lining	(14) Take the sponge	4	3	1	11	27	43	25	41	35
	(15) Adjust the primer lining	2	3	1	12	13	43	25	44	30
	(16) Reach for the scissor	3	3	2	11	20	43	50	41	34
	(17) Cut the primer lining material	3	3	2	10	20	43	50	37	34
	(18) Reach for the stapler	3	3	2	9	20	43	50	33	33
	(19) Stapling	4	3	2	10	27	43	50	37	36
	(20) Reach for the knife	3	4	2	10	20	57	50	37	40
	(21) Open the mechanism	3	2	2	9	20	29	50	33	27
	(22) Put the finished items aside	3	3	2	10	20	43	50	37	34
Framework laying	(23) Take the frame	3	3	1	10	20	43	25	37	32
	(24) Take the cover	3	3	2	9	20	43	50	33	33
	(25) Put on the cover	3	3	1	10	20	43	25	37	32
	(26) Fix of the cover	5	3	1	11	34	43	25	41	38
	(27) Put the finished parts in the box	3	2	2	10	20	29	50	37	28
Wheel fitting	(28) Bring the materials to the table	3	2	1	10	20	29	25	37	26
	(29) Attach the wheel	4	2	1	9	27	29	25	33	28
	(30) Take the hub ring	3	3	2	12	20	43	50	44	34
	(31) Install the hub ring	4	2	2	9	27	29	50	33	30
	(32) Put the finished parts aside	5	4	1	9	34	57	25	33	43
Assembly process	(33) Take the bottom cover	1	4	1	9	7	57	25	33	32
	(34) Assemble the bottom cover	4	3	2	11	27	43	50	41	37
	(35) Take the mechanism	1	2	1	9	7	29	25	33	20
	(36) Assemble the mechanism	4	3	2	10	27	43	50	37	36
	(37) Leave the finished ones in the box	2	3	2	10	13	43	50	37	31
Packaging	(38) Take the legs	6	3	2	13	40	43	50	48	43
	(39) Put the legs in the box	4	3	2	11	27	43	50	41	37
	(40) Install the shock absorber	4	4	2	9	27	57	50	33	42
	(41) Close the box lids	6	3	2	10	40	43	50	37	42
	(42) Tape the box	7	5	2	13	47	72	50	48	58

The production processes of product A in the study consist of seven main stages: fabric stitching, frame upholstery, foam padding, lining, assembly, leg installation, and packaging. Each process also includes sub-processes, and a total of 42 processes were analyzed in the study. The physical strain experienced by workers during the production processes was analyzed using the REBA, RULA, OWAS, MURI, and AHP methods, and integrated risk scores were determined. The results are presented in Figure 2.

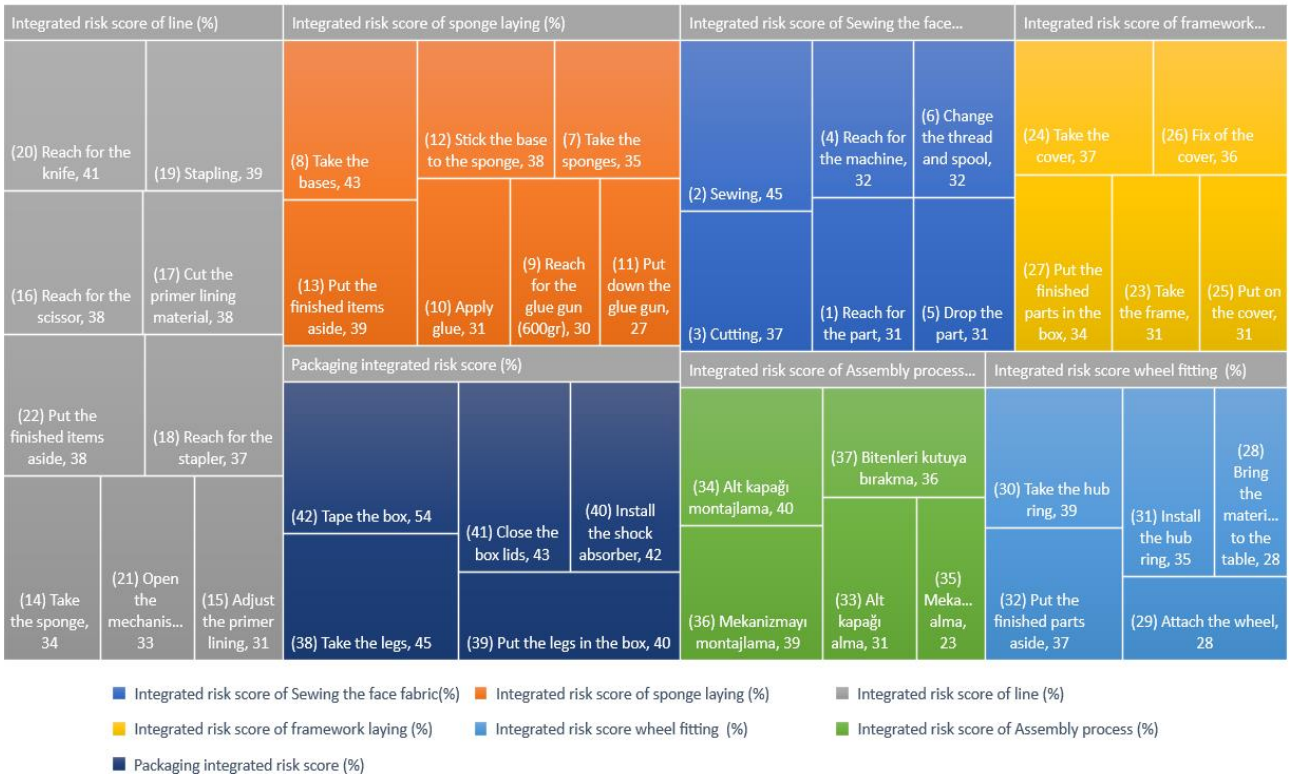

Figure 2. Integrated risk scores of processes

4. Conclusion and Recommendations

The data for the integrated ergonomic risk scores obtained using the AHP method are detailed in Table 10. From the data, the tasks with the highest risk levels were identified as box taping (58%), stitching (45%), placing finished parts aside (43%), retrieving legs (43%), closing box lids (42%), and Taking the Coasters (40%), in that order. Descriptions and recommendations related to the evaluated tasks are explained below.

BoxTaping: The worker performs the taping process of boxed materials by bending over on the ground with tape in hand. During this task, it is observed that the worker bends forward, while simultaneously twisting their torso and neck, extending their arms forward and outward, and maintaining an unbalanced position with their feet. These movements lead to associated risks.

Possible Measures:

- Adjustable workstations can be designed for placing boxes.
- Auxiliary tools (e.g., cutters, tape holders) can be utilized.
- Workers can be trained on proper working techniques (e.g., bending knees and keeping the back straight while working).
- Regular and sufficient breaks can be provided, along with regular stretching and tension-relief exercises.
- Task rotation can be implemented to avoid prolonged work in the same position.
- Frequently used items should be placed within easy reach

StitchingProcess: During this task, the worker operates a sewing machine while seated on a chair. During the process, workers are particularly exposed to risk factors related to back, neck, and wrist strain due to prolonged static posture.

Possible Measures:
- Chairs/seats with lumbar support and adjustable height can be used, along with footrests.
- Workers can be trained on proper working techniques (e.g., keeping the back straight while working).
- Fixtures that ensure easy access to auxiliary tools (e.g., needles, threads, etc.) can be utilized.
- Regular breaks can be provided to allow workers time to rest.
- Task rotation can be implemented to alternate workers between different duties.

Placing Finished Parts Aside: The worker lifts the assembled parts by hand and moves them to another location within the workshop to be packed. This process involves ergonomic risks such as back pain and excessive or repetitive strain on the knees and wrists due to lifting and carrying**.**

Possible Measures:
- Workers can be trained in proper lifting techniques, such as bending the knees and keeping the back straight.
- Finished parts can be carried with both hands to maintain body balance, and personal protective equipment, such as gloves, can be used.
- Workers can be provided with adequate and regular breaks.
- Tools like lift tables or scissor lifts can be used to elevate parts to waist height, reducing the need for bending.
- Surfaces where finished parts are placed should be designed to minimize bending at the waist.
- Safe weight limits should be established for lifting tasks, and mechanical assistance should be used for loads exceeding these limits.

Seat legs retrieval: The seat removes the legs from the apparatus where they were passed to fix them. While performing this operation, the amount of the feet is removed by bending down without bending the knees while the apparatus is small, and by lying down while the apparatus is excessive. During the procedure, the employee faces ergonomic risks such as bending forward on his back and bending forward at the waist when removing the legs, since the apparatus is far from the worker.

Possible Measures:
- Conveyor systems can be utilized to bring and transport the chair legs closer to the worker.
- Workers can be trained on proper lifting techniques, such as bending their knees and keeping their back straight while lifting and carrying objects.
- A job rotation system can be implemented to prevent workers from remaining in the same position for extended periods due to static posture.
- Stretching and flexibility exercises can be encouraged to allow muscles to recover and reduce the risk of injuries.
- Regular ergonomic assessments should be conducted to identify risk factors.

Closing Box Lids: In this task, the worker adds protective supports to the sides of the materials placed inside the box and then closes the lid. While performing this task, the worker is exposed to ergonomic risks such as leaning forward and sideways with their back, bending their neck, and rotating their arms forward and sideways due to the box height being insufficiently high, requiring them to work in a semi-bent posture.

Possible Measures:
- Boxes can be placed on pallets, carriers, or workbenches at waist height to minimize bending and reaching.
- Box lid closers or extendable tools that eliminate the need for bending can be utilized.
- Assistive tools should be positioned in easily accessible locations.
- Workers can be encouraged to bend by using their knees instead of their waist.
- Regular breaks and job rotation systems can be implemented.
- Comfortable and supportive footwear should be worn to reduce fatigue and maintain balance.

Taking the Coasters: In this task, the worker lifts plates weighing approximately 3-5 kg from boxes on the floor. During this process, the worker is exposed to ergonomic risks as they bend and rotate their back and lower back while lifting the materials.

Possible Measures:

- Workers can be trained on proper lifting techniques.
- Manual lifting equipment such as forklifts or lifting carts can be used to lift the bases.
- Adequate and regular breaks can be provided to workers, and/or job rotation can be implemented to prevent the repetition of the same movements.
- Safe weight limits for lifting should be established, and mechanical assistive devices should be used for loads exceeding these limits.
- Appropriate gloves can be provided to workers to reduce hand and finger strain.

This study analyzes processes in a labor-intensive furniture factory, considering 42 different work postures. As a result of analyses conducted using methods such as REBA, RULA, OWAS, and MUARI, risk scores for each job position were determined. Additionally, the weights of these scores were determined using the AHP method. The six job positions with the highest risk scores were identified, and detailed examinations were carried out for these positions, with improvement suggestions provided in detail.

The proposed solutions include measures that can be easily implemented and do not involve high costs, such as improving working conditions, making ergonomic adjustments, and ensuring the use of appropriate equipment. By implementing these measures, complaints related to musculoskeletal disorders and the risk of occupational diseases will be reduced, significantly increasing both work efficiency and employee satisfaction. The evaluations made in this study have objectively and systematically assessed the risk levels within the workplace and have played a guiding role in ergonomic improvements.

At every stage of production, employees perform tasks such as holding, lifting, carrying, packaging, and assembly. Repetitive execution of these seemingly simple tasks can lead to musculoskeletal disorders (MSDs) in areas such as the neck, back, arms, wrists, and knees. The main causes of these disorders are incorrect body posture, lack of planning, inappropriate task assignments without considering the workers' anthropometric characteristics, unsuitable workbench heights, and repetitive movements. Providing training to employees on handling and lifting processes, especially regarding ergonomics, will contribute to reducing MSDs. The results of this study demonstrate the critical importance of ergonomic adjustments in occupational health and safety. Such studies can make a significant contribution to the health and safety of employees in workplaces and can be applied to other similar businesses as well.

Conflict of Interest

All authors certify that they have no affiliations with or involvement in any organization or entity with any financial interest or non-financial interest in the subject matter or materials discussed in this manuscript.

Ethics Committee Approval

Ethics committee approval is not required.

Author Contribution

All authors contributed to this study. All authors have read and agreed to the published version of manuscript.

Acknowledgements

This study was derived from undergraduate students' theses.

5. References

[1] Esen, H. ve Fığlalı, N. (2013). Çalışma Duruşu Analiz Yöntemleri ve Çalışma Duruşunun Kas-İskelet Sistemi Rahatsızlıklarına Etkileri. Sakarya Üniversitesi Fen Bilimleri Dergisi, 17(1), 41-51.

[2] Öncü, E., Vayısoğlu, S.K., & Güven, Y. (2021). Akademisyenlerde Kas İskelet Sistemi Rahatsızlıkları Yaygınlığı, İş Gerilimi ve İlişkili Faktörler, Gümüşhane University Journal of Health Sciences, 10(2), 194-204.

[3] Akay, D., Dağdeviren, M., & Kurt, M. (2003). Çalışma Duruşlarının Ergonomik Analizi. Gazi Üniversitesi Mühendislik Mimarlık Fakültesi Dergisi, 18(3),73-84.

[4] Özel, E., & Çetik, O. (2010). Mesleki Görevlerin Ergonomik Analizinde Kullanılan Araçlar ve Bir Uygulama Örneği. Dumlupınar üniversitesi Fen bilimleri Enstitüsü Dergisi, 22, 41-56.

[5] Akın, G. (2013). Ergonomi. Alter Yayıncılık, Ankara.

[6] Coşkun, M. B., Sağıroğlu, H., & Erginel, N. (2015). İş İstasyonlarının Ergonomik Riskinin NIOSH Yöntemi ile Belirlenmesi. Mühendislik Bilimleri ve Tasarım Dergisi, 3(3), 365-370.

[7] Karabacak, N. (2016). Diş Hekimlerinin Çalışma Duruşlarının Ergonomik Analizi. Fen Bilimleri Enstitüsü, Yüksek Lisans Tezi. Selçuk Üniversitesi, Konya.

[8] Beliveau, P. J., Johnston, H., Van Eerd, D., & Fischer, S. L. (2022). Musculoskeletal Disorder Risk Assessment Tool Use: A Canadian Perspective. Applied Ergonomics, 102, 103740.

[9] Zengin, M. A., & Asal, Ö. (2020). Bina inşaatındaki çalışan duruşlarının farklı ergonomik risk değerlendirme yöntemi ile değerlendirilmesi. Gazi Üniversitesi Mühendislik Mimarlık Fakültesi Dergisi, 35(3), 1615-1630.

[10] Hawari, N. M., Sulaiman, R., Kamarudin, K. M., & Me, R. C. (2022). Musculoskeletal Discomfort Evaluation using Rapid Entire Body Assessment (REBA) and Quick Exposure Check (QEC) among woodworking workers in Selangor, Malaysia. Asian Journal of Applied Sciences, 10(5). 407-416.

[11] Erginel, N., Toptancı, Ş., & Ilgın, Acar. (2018). Bulanık REBA ile Bir Mobilya İmalat Firmasında Ergonomik Risk Değerlendirmesi. Mühendislik Bilimleri ve Tasarım Dergisi, 6, 92-101.

[12] Ekinci, E. B. M., & Can, G. F. (2018). Algılanan İş Yükü ve Çalışma Duruşları Dikkate Alınarak Operatörlerin Ergonomik Risk Düzeylerinin Çok Kriterli Karar Verme Yaklaşımı ile Değerlendirilmesi, Ergonomi, 1(2), 77-91.

[13] Akalp, H. G., Saklangıç, U., & Çırakoğlu, S. (2021). Zeytin Tarımında Çalışan İşçilerin Çalışma Duruşlarının REBA Yöntemi ile Analizi. Ergonomi, 4(2), 88-96.

[14] Koç, S., & Testik, Ö. M. (2016). Mobilya Sektöründe Yaşanan Kas-İskelet Sistemi Risklerinin Farklı Değerlendirme Metotları ile İncelenmesi ve Minimizasyonu. Endüstri Mühendisliği, 27 (2), 2-27.

[15] Polat, O., Mutlu, Ö., Çakanel, H., Doğan, O., Özçetin, E., & Şen, E. (2017). Bir Mobilya Fabrikasında Çalışan İşçilerin Çalışma Duruşlarının REBA Yöntemi ile Analizi. Süleyman Demirel Üniversitesi, Mühendislik Bilimleri ve Tasarım Dergisi, 5 (Özel sayı), 263-268.

[16] Costa, D. M. B., Ferreira, R. V., Galante, E. B. F., Nóbrega, J. S. W., Alves, L. A., & Morgado, C. V. (2018). Comparative Assessment of Work-Related Musculoskeletal Disorders in An İndustrial Kitchen. In Occupational Safety and Hygiene VI: Proceedings of the 6th International Symposium on Occupation Safety and Hygiene (SHO 2018), March 26-27, 2018, Guimarães, Portugal (p. 325). CRC Press.

[17] Kahya, E., Alpaslan, K., & Şenyüz, G. (2023). Bir Metal Sanayi İşletmesinde Ergonomik Risk Değerlendirme Yöntemleriyle Bütünleşik İş Yüklerinin Analizi. ESOGÜ Müh. Mim. Fak. Dergisi, 31(3), 848-861.

[18] Delice, E. K., Ayık, İ., Abidinoğlu, Ö. N., Çiftçi, N. N., & Sezer, Y. (2018). Ergonomik Risk Değerlendirme Yöntemleri ve AHP Yöntemi ile Çalışma Duruşlarının Analizi: Ağır ve Tehlikeli İşler için Bir Uygulama. Mühendislik Bilimleri ve Tasarım Dergisi, 6, 112-124.

[19] Hignett, S., & McAtamney, L. (2000). Rapid Entire Body Assessment (REBA). Applied Ergonomics, 31(2), 201 205.

[20] McAtamney, L., & Corlett, E.N. (1993). RULA: A Survey Method for The Investigation of Workrelated Upper Limb Disorders. Applied Ergonomics, 24(2), 91-99.

[21] Karhu O., Kansi P. & Kuorinka I. (1977). Correcting Working Postures in Industry: A Practical Method for Analysis, Applied Ergonomics, 8(4), 199-201.

[22] Ohno, T. (1988). Toyota Production System: Beyond Large Scale Production. Productivity Press, New York.

[23] Karaburun M. (2018). Çok Ölçütü Karar Vermede AHP ve TOPSIS Yöntemleriyle Silah Seçimi. Necmettin Erbakan Üniversitesi, Fen Bilimleri Enstitüsü Endüstri, Mühendisliği Anabilim Dalı Yüksek Lisans Tezi.

[24] Saaty, T. L. (1980). The Analytic Hierarchy Process. New York: McGraw-Hill.

[25] Atıcı, H., Gönen, D., & Oral, A. (2015). Çalışanlarda zorlanmaya neden olan duruşların REBA yöntemi ile ergonomik analizi, Suleyman Demirel University, Journal of Engineering sciences and Design 3:3, (SI), 239-244.

[26] Ülker, O. ve Burdurlu, E., (2012). Panel Mobilya İmalatında Kullanılan Bazı Makinelerde OWAS Yöntemi ile Eylemsel Duruş Analizi. Kastamonu Üniversitesi Orman Fakültesi Dergisi, 12(2), 291-300.

[27] Kahraman M. (2012). Ergonomik Risk Değerlendirme Yöntemlerinin Çok Ölçütlü Karar Verme Teknikleri ile Önceliklendirilmesi ve Bütünleşik Bir Model Önerisi, Yüksek Lisans Tezi. Gazi Üniversitesi, Ankara.

[28] Delice, E. K., Ayık, İ., Abidinoğlu, Ö. N., Çiftçi, N. N., & Sezer, Y. (2018). Ergonomik risk değerlendirme yöntemleri ve ahp yöntemi ile çalişma duruşlarinin analizi: ağir ve tehlikeli işler için bir uygulama. Mühendislik Bilimleri ve Tasarım Dergisi, 6, 112-124.

[29] Özdağoğlu, A. (2008). Bulanik Analitik Hiyerarşi Süreci Yönteminde Duyarlilik Analizleri: Yeni Bir Alternatifin Eklenmesi - Enerji Kaynağinin Seçimi Üzerinde Bir Uygulama, İstanbul Ticaret Üniversitesi Fen Bilimleri Dergisi 7(14), 15-34.

doi:10.55385/kastamonujes.1570731 KUJES 10(2):95-104, 2024

Kastamonu University
Journal of Engineering and Sciences
e-ISSN 2667-8209
http://dergipark.gov.tr/kastamonujes

Preparation and Properties of Foamable Ni-GNP/AlSi12 Precursor Materials

Kilani A. Mohamed Hassan[a], **Arif Uzun**[b,*]

[a] Department of Materials Science and Engineering, Institute of Science, Kastamonu University, Kastamonu, Türkiye
[b] Department of Mechanical Engineering, Kastamonu University, Kastamonu, Türkiye
***Corresponding Author:** auzun@kastamonu.edu.tr

Received: **October 20, 2024** ◆ Accepted: **December 20, 2024** ◆ Published Online: **December 25, 2024**

Abstract: In this study, nickel-coated graphene nanoplatelets reinforced AlSi12 precursor materials were produced by powder metallurgy method. For this process, Ni-GNP particles were added to the matrix material AlSi12 powders at different ratios (0%, 0.4%, 0.8% and 1.2% by weight). Then, the mixed powders were cold compressed and extruded at different ratios, and foamable precursor samples with diameters of 6 and 12 mm were produced. Microstructural analyses, density measurements and microhardness tests were carried out to evaluate the effects of Ni-GNPs on the properties of foamable precursor materials. Microstructure and surface analysis of Ni-GNP/AlSi12 precursor materials showed high density, uniform distribution of Ni, localized Si phases and surface oxidation due to reactivity of aluminum. It was revealed that the addition of Ni-GNP led to the formation of Al-Ni intermetallic phases, reduced the Al peak intensity and strengthened the graphene bond with the Al matrix. The relative density increased with increasing extrusion ratio, higher Ni-GNP content decreased the relative density but improved it significantly after extrusion. The maximum hardness was achieved in the precursor materials with the optimum graphene content of 0.4 wt%, while higher amounts led to aggregation, increased porosity and decreased hardness.

Keywords: AlSi12, Ni-GNP, powder metallurgy, microstructure analysis

Öz: Bu çalışmada toz metalurjisi yöntemi ile nikel kaplı grafen nanoplakçıklar ile takviyelendirilmiş AlSi12 öncü malzemeler üretilmiştir. Bu işlem için farklı oranlarda (ağırlıkça %0, %0.4, %0.8 ve %1.2) Ni-GNP parçacıkları matris malzemesi AlSi12 tozlarına ilave edilmiştir. Akabinde karışım tozlar soğuk olarak sıkıştırılmış ve farklı oranlarda ekstrüzyon işlemine tabi tutulmuş ve 6 ve 12 mm çaplara sahip köpürebilir öncü numuneler üretilmiştir. Ni-GNP'lerin köpürebilir öncü malzemelerin özellikleri üzerindeki etkilerini değerlendirmek için mikro yapısal analizler, yoğunluk ölçümleri ve mikro sertlik testleri gerçekleştirildi. Ni-GNP/AlSi12 öncü malzemelerin mikro yapısı ve yüzey analizi, yüksek yoğunluk, Ni'nin düzgün dağılımı, lokalize Si fazları ve alüminyumun reaktifliğinden dolayı yüzey oksidasyonunu gösterdi. Ni-GNP eklenmesinin Al-Ni intermetalik fazların oluşumuna yol açtığını, Al pik yoğunluğunu azalttığını ve grafen bağını Al matrisiyle güçlendirdiğini ortaya koydu. Artan ekstrüzyon oranı ile birlikte bağıl yoğunluk artmış, daha yüksek Ni-GNP içeriği bağıl yoğunluğu azaltmış ancak ekstrüzyondan sonra önemli ölçüde iyileştirmiştir. Optimum grafen içeriğinin %0,4 ağırlıkta olmasıyla öncü malzemelerde maksimum sertlik elde edilirken, daha yüksek miktarlar kümeleşmeye, gözenekliliğin artmasına ve sertliğin azalmasına yol açmıştır.

Anahtar Kelimeler: AlSi12, Ni-GNP, toz metalurjisi, mikroyapı analizi

1. Introduction

The production of aluminium foam by powder metallurgy starts with the mixing of starting powders, compaction of the powders and secondary processes such as rolling or extrusion. The materials produced after these process are called foamable materials. Therefore, foamable materials have an important place in aluminium foam production. The reason for this is that the physical and mechanical properties of foamable materials affect the properties of the foam structure. For example, low density foamable material produced by powder metallurgy method can exhibit lower expansion when subjected to foaming process. In this case, the density of the foam produced is high [1].

Melting methods, especially powder metallurgy, are used extensively in aluminium foam production [2-4]. In addition, there are many methods developed by researchers [5]. Foam production from foamable materials is mainly included in the powder metallurgy process. The mechanical and physical properties of foams do not only depend on the mechanical and physical properties of the foamable material. In fact, the chemical composition of the structure of the foamable material can also affect the properties of the final product, aluminium foam. In this respect, various ceramic reinforcements are suggested for the improvement of mechanical properties of aluminum foams. Especially the effects of nanoparticles have become a focus of research topics. Papantoniou and Manolakos [6] investigated the production and characterization of aluminum foam reinforced with nanostructured γ-Al_2O_3 using AA5083 plates. Foamable materials were produced by incorporating TiH_2 and γ-Al_2O_3 particles by friction stirring process and then foamed in a laboratory

oven. The researchers achieved a mean porosity of 70% and a plateau stress of 27 MPa in the foam structure they obtained. Wang et al. [7] used high energy ball milling (HEBM) and powder metallurgy techniques for the production of carbon nanotube (CNT) reinforced closed cell Al-Si composite foams. The starting powders for the production of Al-Si foams containing different CNT ratios (0.25%, 0.5% and 0.75%) were compressed under 500 MPa pressure and foamable materials were produced. It was determined that the inclusion of 0.50 wt% CNTs in the composite foams produced after foaming increased the fatigue strength by 54% compared to Al-Si foams, since it reduced the crack expansion rates and changed the failure modes. On the other hand, another study conducted by the researchers emphasized that CNT content can reduce the pore size and improve circularity. In particular, CNTs/Al composite foams with 1.0 wt% exhibited optimum compressive properties [8]. Gao et al. [9] observed improvement in mechanical properties by incorporating copper-coated carbon fibers (Cf) into aluminum foam. The researchers investigated the effect of Cf on bubble nucleation, growth, and foam stability in aluminum sandwich foams. In the study, the foamable interlayer was produced by powder metallurgy and rolling processes to form the sandwich structure before foaming. Pang et al. [10] produced foamable precursors using TiH_2 and Al_2O_3 powders with 7075 aluminum plates by friction stir process. Their analysis revealed that the rotation speed significantly affected the uniformity and density of precursors, while the welding speed had minimal effect. Rathore et al. [11] used an underwater method for friction mixing process which allows better mixing of foaming agent and stabilizer into the substrate for foamable precursor production.

Comprehensive research has been conducted on the production of aluminum foam with foamable precursor materials and the characterization of the produced foams. However, it has been observed that sufficient studies have not been conducted on the properties of foamable precursor materials. The produced foamable precursor materials are essentially a type of composite material. In our current research, Ni-coated GNP particles were selected as the reinforcement phase in the preparation of foamable AlSi12 materials by powder metallurgy method. The effect of Ni-GNP particles added to the AlSi12 matrix as reinforcement phase at different ratios on the physical properties and hardness changes of Ni-GNP/AlSi12 precursor materials was analyzed.

2. Experimantal procedures

2.1. Materials

In experimental studies, Al powder (99.8% pure - < 44 μm-round shaped) as matrix material from Buha powder company, Si powder (< 44 μm-sharp cornered) as alloying element from Acros Organics, TiH_2 powder (< 44 μm-sharp cornered) as foaming agent from Sigma Aldrich company and graphene nanoplatelets (GNPs) (99.9% purity - 3 nm size) as reinforcement element from Nanografi company were obtained. Figure 1 shows the scanning electron microscope (SEM) images of the powders used in the experimental study.

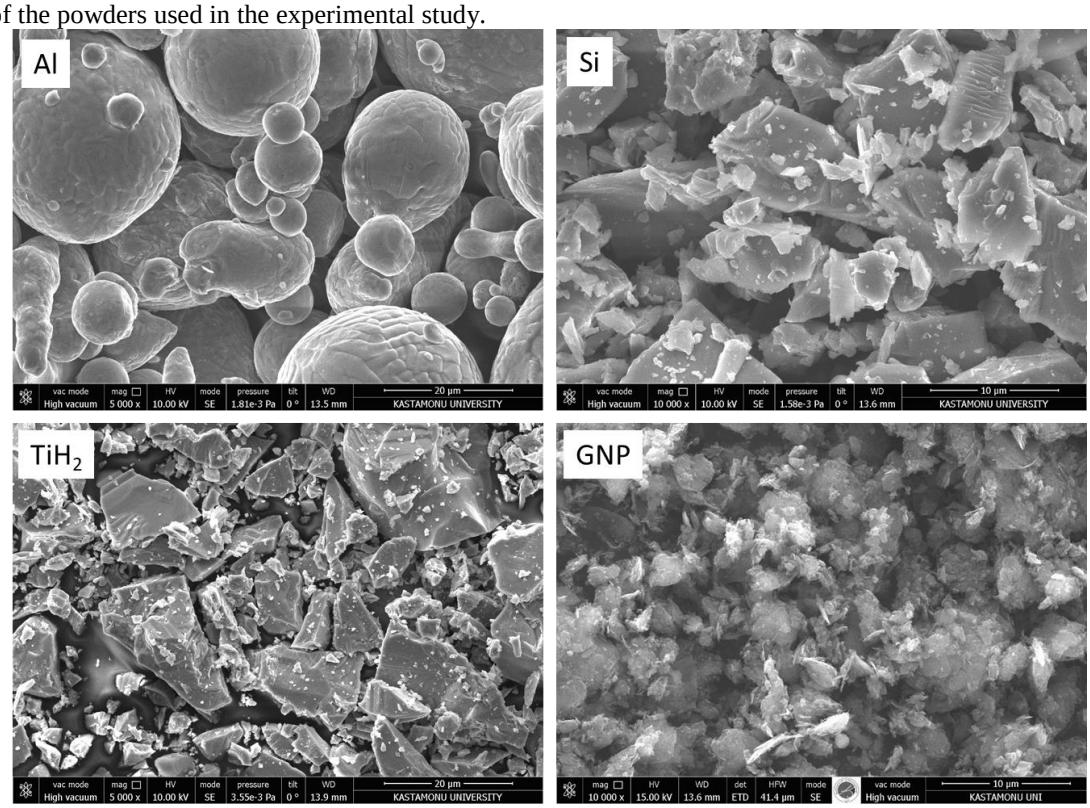

Figure 1. SEM images of the powders used in the experimental study

The chemical method was used for coating the GNPs with nickel. Sodium hydroxide (NaOH - 96%), nitric acid (HNO_3 - 68%), hydrochloric acid (HCl - 37.5%), tin(II) chloride (SnCl2 - 99%), tin (Sn - 99.5%), silver nitrate ($AgNO_3$ - 99.8%), ammonium hydroxide solution (28% NH_3. H_2O), nickel sulfate hexahydrate $NiSO_4 \cdot 6H_2O$ - 98.0%), ammonium chloride (NH_4Cl - 99.5%), disodium hydrogen citrate sesquihydrate ($Na_2HC_6H_5O_7 \cdot 1.5H_2O$ - 98.0%), boric acid (H_3BO_3 - 99.5%), sodium hypophosphite (NaH_2PO_2 - 99.0%) and distilled water were used in the preparation [12].

2.2. Production of Ni-GNP/AlSi12 Precursor Materials

GNPs were chemically coated with Ni before the production of Ni-GNP/AlSi12 precursor materials. The preparation of the Ni-coated GNPs consisted of five steps: (i) the GNPs were cleaned, (ii) the surfaces of the GNPs were roughened, (iii) the GNPs were sensitized, (iv) the GNPs were activated and in the final step (v) the coating process was carried out. After coating, experimental work continued by mixing the initial powders in a planetary ball milling device (PM-100, Retsch, Germany). For this process, 0 wt%, 0.4 wt%, 0.8 wt% and 1.2 wt% Ni coated GNPs, 1 wt% TiH_2 as foaming agent and 12 wt% Si as alloying element were added to the aluminum powders and mixed in a stainless steel container with a ball mixer for 60 minutes. Stainless steel balls with a diameter of 8 mm were added to the powder mixture to achieve a ball to powder ratio of 5:1 by weight. 0.3% stearic acid was added to the mixture to ensure effective dispersion of Ni coated GNPs, to prevent adhesion of the powders to the vessel walls and balls and to minimize the cold welding effect of the powder particles.

The mixed powders were compacted unidirectional in a steel mold under 600 MPa pressure using a hydraulic press. After compression, cylindrical billets with a diameter of 27 mm were produced (Fig. 2a) and these were placed in a steel mold and kept in an oven at 430ºC for 3 hours. Afterwards, the mold was removed from the oven and placed on a steel unit integrated into a vertical hydraulic press unit and extrusion process was carried out. The billets were extruded at two different extrusion ratios (1:5 and 1:20) to produce Ni-GNP/AlSi12 precursor samples with diameters of 6 mm and 12 mm (Fig. 2b).

Figure 2. Compressed block sample (billet) (a) and extruded Ne-GNP/AlSi12 precursor samples

2.3. Characterization

The densities (ρ_s) of Ni-GNP/AlSi12 precursor materials and Ni-GNP/AlSi12 foams were measured according to the archiment principle using a density kit integrated in a balance with a precision of 0.0001 g. The formula given in Equation 1 was used in the calculations.

$$\rho_s = \frac{m_{s_{air}}}{\left(m_{s_{air}} - m_{s_{water}}\right)} \times \rho_{water} \quad (1)$$

Where ρ_s is the density of the sample, ρ_{water} is the density of water at room temperature, $m_{s_{air}}$ is the weight of the sample in air and $m_{s_{water}}$ is the weight of the sample in water.

The theoretical densities (ρ_t) of the samples were calculated according to the mixing rule. Relative density (ρ*) values were obtained as the ratio of the experimental density to the theoretical density (Equation 2).

$$\rho * = {}^{\rho_s}/_{\rho_t} \times 100\% \quad (2)$$

Scanning electron microscopy (SEM) and integrated energy dispersive spectroscopy (EDS) were used for chemical composition and microstructural analysis of Ni-GNP/AlSi12 precursor materials. Metallographic evaluation of the prepared samples was carried out in a conventional way (grinding, polishing and etching). In addition, X-ray diffraction (XRD) device (Bruker) was used for phase determination. Measurements were performed in the range of 3 to 90 degrees and at a rate of 1.2 s/degree. The microhardness measurements of the Ni-GNP/AlSi12 precursor materials were performed on a Schimadzu (HMV-G) microhardness tester by applying a 300 g load for 10 seconds (HV0.3). The microhardness values were evaluated by averaging at least five measurements for each sample.

3. Result and Discussion

3.1. Microstructure of Ni-GNP/AlSi12 Precursor Materials

As seen in Figure 3, no obvious were observed in the microstructure photographs of the different composites. This indicates that the composites reached a high density after the extrusion process. On the surface of the composite materials with Ni-GNP addition, relatively black regions appeared. We think that these black regions are due to the condensation of Ni-GNPs as a result of agglomeration.

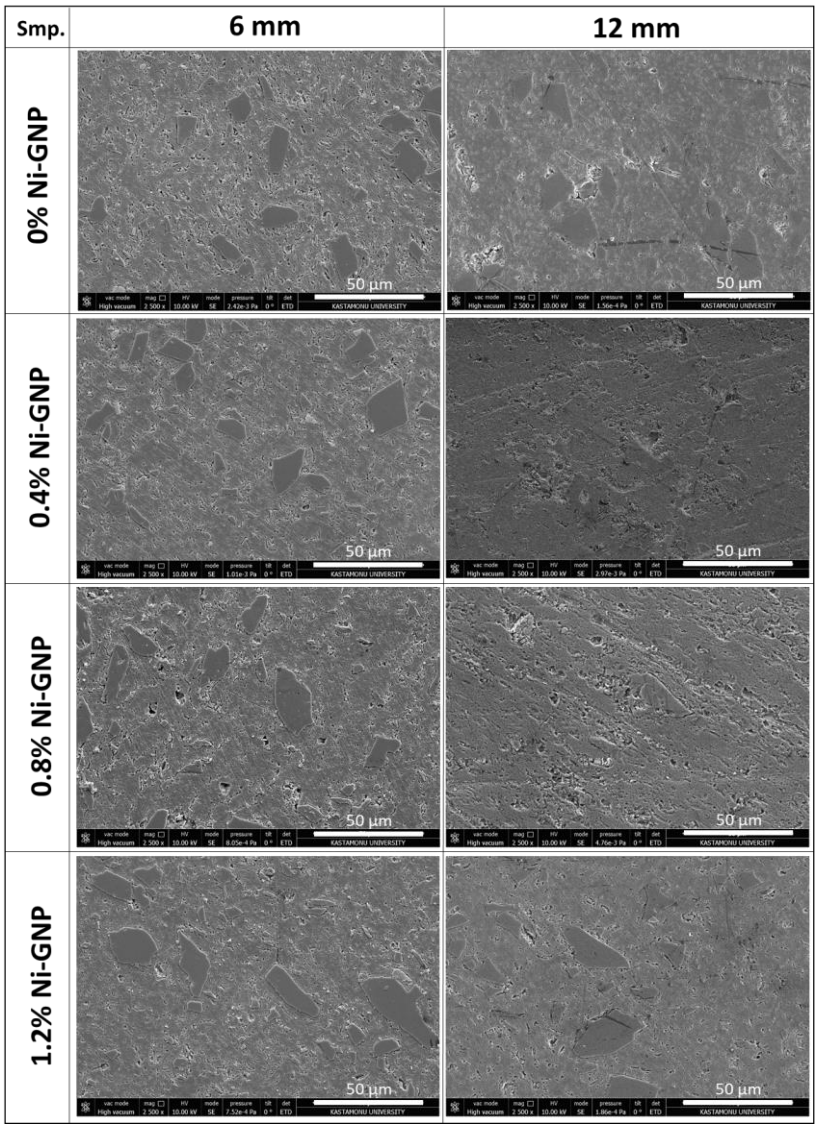

Figure 3. Microstructure photographs of Ni-GNP/AlSi12 precursor samples

Figure 4 shows the surface topography of the 1.2 wt% Ni-GNP/AlSi12 precursor material. The image reveals that the distribution of C and Ni elements in the EDS map of the composites is relatively uniform. Although the proportion of Ni

is less than 1%, it is observed to be homogeneously distributed in the structure with a yellow color in the mapping. In addition, the formation of localized Si phases was observed on the sample surface. The green dots indicate the element O, indicating that oxidation has occurred on the surface of the composites. The cutting, polishing, characterization and other processes of the composites were carried out in the absence of atmospheric control. Therefore, oxidation became inevitable due to the tendency of aluminum to oxidize easily.

The interplay between a homogeneous Ni-GNP distribution and localized oxidation significantly affects the final properties of the material [13]. While the uniform distribution of Ni-GNPs enhances mechanical, thermal, and electrical properties, localized oxidation presents challenges that could limit performance. Addressing these challenges through material design and process optimization will unlock the full potential of the composite for advanced applications.

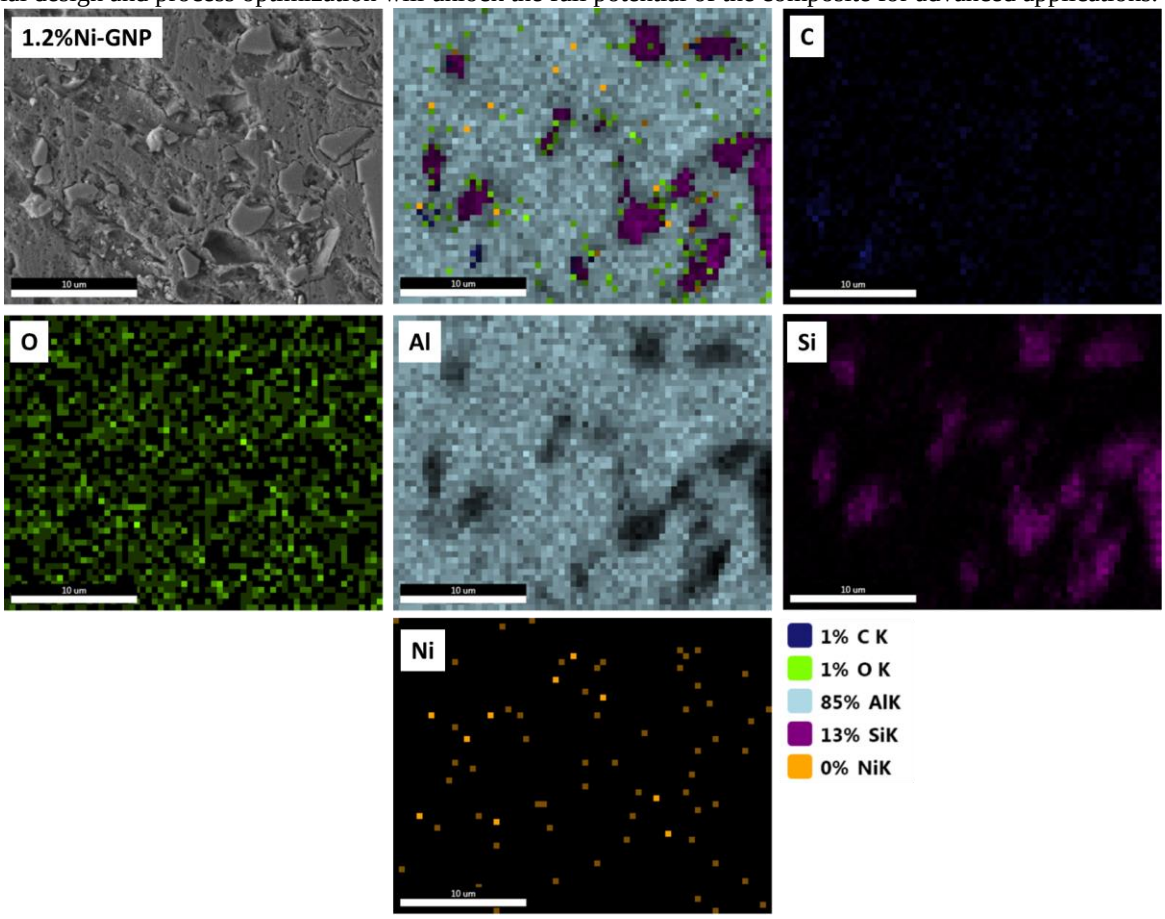

Figure 4. Surface topography and EDS map of the 1.2 wt% Ni-GNP/AlSi12 precursor material

3.2. XRD results

Figure 5 shows the XRD patterns of 0% Ni-GNP-AlSi12 and 2% Ni-GNP-AlSi12 samples. According to the XRD pattern of the 0% Ni-GNP-AlSi12 sample, Al (Bravais lattice: cubic, a = b = c = 4.040 nm) and Si (Bravais lattice: cubic, a = b = c = 5.430 nm) phases were detected. According to the XRD pattern of 2% Ni-GNP-AlSi12 sample, Al (Bravais lattice: cubic, a = b = c = 4.040 nm), Si (Bravais lattice: cubic, a = b = c = 5.420 nm), Al_3Ni_2 (Bravais lattice: hexagonal, a = 4.028; b = 4.028; c = 4.891 nm), Al_4Ni_3 (Bravais lattice: cubic, a = 11.480; b = 11.480; c = 11.480 nm) and C (Bravais lattice: hexagonal, a = 2.522; b = 2.522; c = 20.593 nm) phases were detected. The formation of Al_3Ni_2 and Al_4Ni_3 intermetallic between the Al matrix and the Ni coating demonstrates the effectiveness of nickel, which enables graphene to form a strong bond directly with the Al matrix. When the XRD patterns of 0% Ni-GNP and 2% Ni-GNP reinforced AlSi12 composites are compared, it is noticeable that the intensity of Al peaks decreases with the increase of graphene content. Al_3Ni_2 and Al_4Ni_3 phases are known to be brittle materials [14]. increase the strength of aluminum-based composites by acting as reinforcements within the matrix. These phases improve hardness and wear resistance, making the material suitable for high-load applications such as aerospace and automotive components.

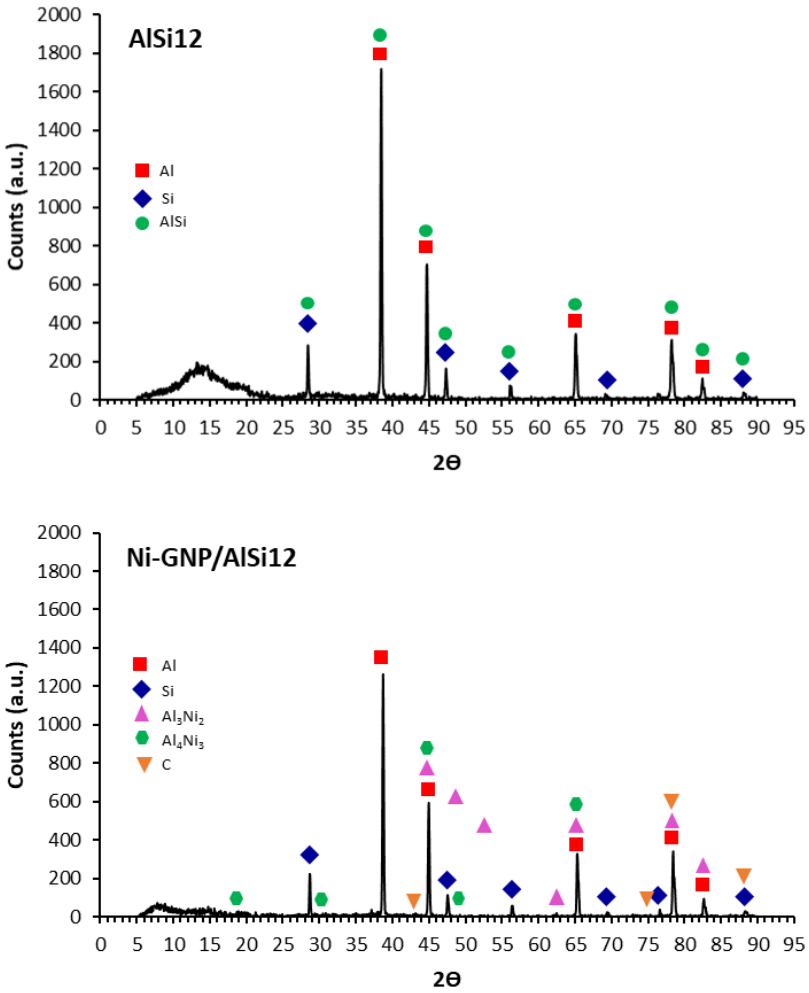

Figure 5. XRD patterns of 0% Ni-GNP-AlSi12 and 2% Ni-GNP-AlSi12 samples

3.3. Density Variation of Ni-GNP/AlSi12 Precursor Materials

In the production of Al-based composite materials, secondary processes such as extrusion, rolling and forging can be applied in addition to compression processes to obtain PM products with high density and low porosity [15]. However, the deformation that occurs in the preformed materials produced during these processes brings problems such as cracking. Abdel-Rahman and El-Sheikh [16] tried to explain the effect of relative density on the deformation properties of PM parts. According to the researchers, high stresses are needed for deformation of materials with high relative density.

Figure 6 shows the density change graph of Ni-GNP/AlSi12 precursor materials depending on secondary processing. The graph shows that the increase in the amount of particles decreases the relative density of the samples from 95.58% to 93.77% after pressing. On the other hand, this density difference of 1.81% decreased to 0.49% for samples with a diameter of 6 mm and 1.39% for samples with a diameter of 12 mm with extrusion. In both stages, the increase in the amount of Ni-GNP had a decreasing effect on the relative density of the samples. However, for the samples without Ni-GNP, the extrusion process increased the relative density value by 3.73% for the samples with a diameter of 6 mm and 3.55% for the samples with a diameter of 12 mm. With the increase in the amount of Ni-GNP (1.2%), this difference increased to 5.05% and 3.96%, respectively. Therefore, it can be said that extrusion processes increase the relative density values of foamable materials containing Ni-GNP.

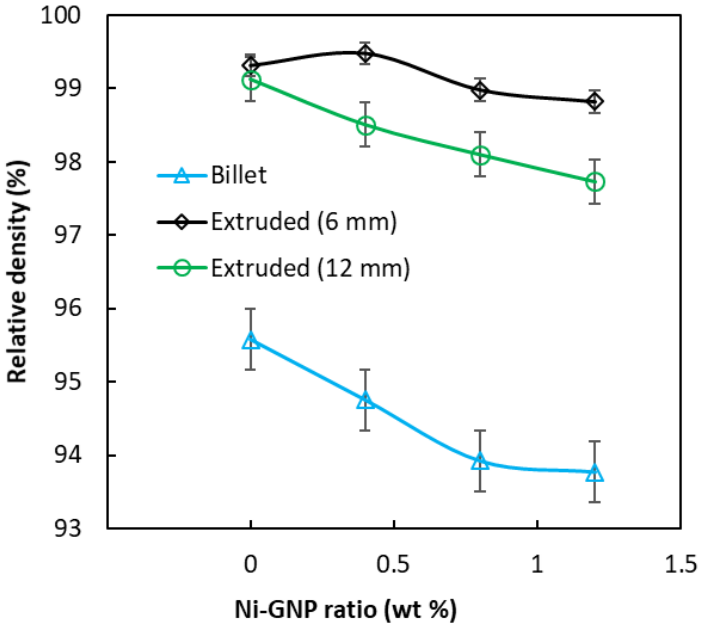

Figure 6. Density change of Ni-GNP/AlSi12 precursor materials

Table 1 shows the average density changes obtained in the samples as a result of the secondary processes applied. The increase in the deformation of the foamable materials due to the extrusion processes applied after the pressing process led to an increase in the relative density.

Table 1. Average density changes due to densification processes

Sample	Densification process	Density (g.cm^{-3})	Relative density (%)	Theoretical density (g.cm^{-3})
AlSi12	Billet	2.539	95.577	2.657
	Extruded (6 mm)	2.638	99.311	
	Extruded (12 mm)	2.633	99.123	
0.4% Ni-GNP/AlSi12	Billet	2.508	94.752	2.647
	Extruded (6 mm)	2.633	99.475	
	Extruded (12 mm)	2.607	98.504	
0.8% Ni-GNP/AlSi12	Billet	2.477	93.922	2.637
	Extruded (6 mm)	2.610	98.980	
	Extruded (12 mm)	2.587	98.097	
1.2% Ni-GNP/AlSi12	Billet	2.464	93.770	2.628
	Extruded (6 mm)	2.597	98.820	
	Extruded (12 mm)	2.568	97.728	

3.4. Hardness Changes of Ni-GNP/AlSi12 Precursor Materials

Graphene-reinforced aluminum composites exhibit improved stiffness compared to pure aluminum. Graphene, a two-dimensional allotrope of carbon, is known for its exceptional mechanical properties, including high strength and stiffness. Adding graphene to aluminum helps strengthen the composite by providing a reinforcing network within the metal matrix. If the graphene sheets are evenly distributed throughout the aluminum, they act as a barrier against dislocation movement and prevent deformation. This results in improved stiffness and resistance to plastic deformation [17, 18]. However, the specific relationship between the volume fraction of graphene nanolevels and the resulting hardness may vary depending on the composite system, production conditions and other factors. The effects of Ni-GNPs and extrusion rate on the hardness of aluminum composites are given in Figure 7. It is seen that the highest hardness values are obtained in the samples with a diameter of 6 mm for 0.4 wt% graphene content. However, it is seen that the specimens with a diameter

of 6 mm have higher hardness values compared to the specimens with a diameter of 12 mm. This is due to the fact that billet specimens with the same diameter are subjected to more plastic deformation. Thus, an increase in hardness is expected in denser specimens. The results show that the addition of GNPs up to 0.4 wt.% to pure aluminum increases the hardness of aluminum composites. The addition of graphene above 0.4 wt.% is thought to decrease the hardness of the composites due to the tendency of graphene to agglomerate. Therefore, the interaction between aluminum particles and GNPs is reduced by agglomeration. This leads to higher porosity and causes a decrease in hardness [19]. Studies highlight that excessive graphene content causes aggregation, leading to weaker interfacial bonds between the matrix and graphene particles [20]. Often, an optimum dispersion limit is formed, beyond which mechanical benefits are reduced due to poor stress transfer or pore formation [21].

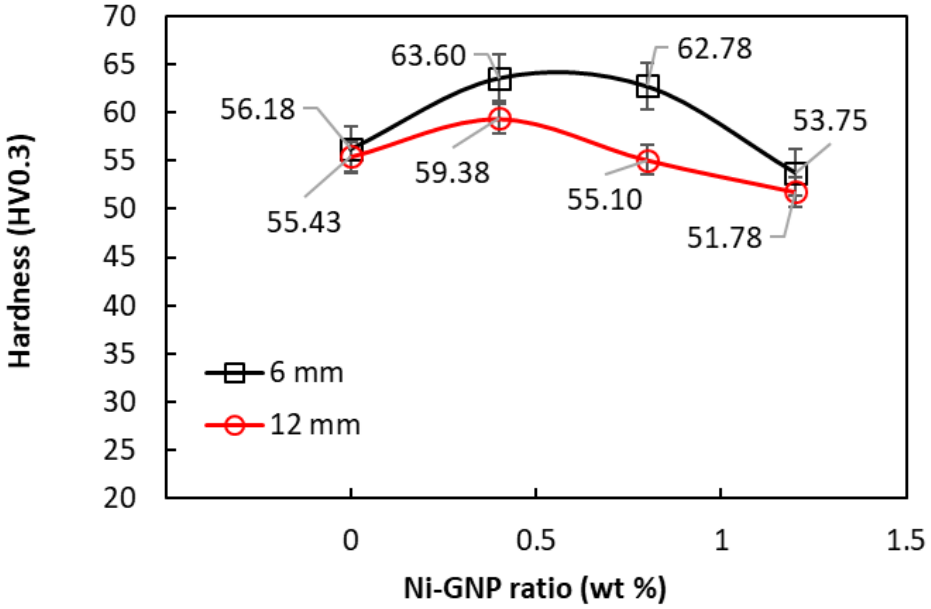

Figure 7. Hardness changes of Ni-GNP/AlSi12 precursor materials

4. Conclusion

It can be concluded that the addition of Ni-GNP to AlSi12 precursor materials significantly influences both the microstructure and mechanical properties of the composites. The microstructure analysis shows that the materials achieved high density after extrusion, with uniform distribution of Ni and C elements, although slight oxidation occurred on the surface. The presence of Ni-GNP contributed to the formation of intermetallic compounds (Al_3Ni_2, Al_4Ni_3) that strengthened the bond between graphene and the aluminum matrix, as demonstrated by the XRD analysis. The density of the composites was enhanced through secondary processes, such as extrusion, with Ni-GNP playing a key role in increasing the relative density, particularly in samples with higher Ni-GNP content. Additionally, the hardness of the composites was improved with the inclusion of graphene up to 0.4 wt.%, suggesting that the proper dispersion of graphene enhances the material's resistance to deformation. However, higher graphene concentrations resulted in agglomeration, leading to increased porosity and reduced hardness.

Ni-GNP/AlSi12 composites offer enhanced mechanical properties, particularly in terms of hardness and density, when optimal graphene content is maintained. However, controlling the dispersion of graphene is crucial to prevent negative effects like agglomeration, which can compromise the material's structural integrity. These findings highlight the potential of Ni-GNP as a reinforcing agent in aluminum composites, though further refinement in processing techniques may be needed to fully harness its benefits. Regarding industrial applications, the enhanced hardness and density of Ni-GNP/AlSi12 composites suggest their potential use in wear-resistant components, lightweight structural parts, and heat sinks in automotive and aerospace industries.

Conflict of Interest

All authors certify that they have no affiliations with or involvement in any organization or entity with any financial interest or non-financial interest in the subject matter or materials discussed in this manuscript.

Ethics Committee Approval

Ethics committee approval is not required.

Author Contribution

Conceptization: KMH, AU; methodology and laboratory analyzes: KMH, AU; writing draft: KMH, AU; supervisor: AU; proof reading and editing. All authors have read and agreed to the published version of manuscript.

Acknowledgements

Not applicable.

5. References

[1] Uzun, A., Asikuzun, E., Gokmen, U., Cinici, H., (2018). Vickers Microhardness Studies on B_4C Reinforced/Unreinforced Foamable Aluminium Composites. Transactions of the Indian Institute of Metals. 71:327-337.

[2] Ding, X., Qian, H., Su, G., Hu, X., Liu, Y., Peng, G., Wu, Y., (2024). Reinforcement effect of fly ash with different morphologies on aluminum foam prepared via powder metallurgy. Powder Technology. 119944**.**

[3] Zhiqiang, G., Yonglin, G., Guoyin, Z., Xiaoguang, Y., Feng, W., Jinwei, L., (2024). Foaming Behavior of AlMg4Si8 Matrix and Pure Al Matrix Precursors in Closed Cavities with Different TiH_2 Addition Levels. International Journal of Metalcasting. 1-16.

[4] Yuan, G., Li, Y., Hu, L., Fu, W. (2023). Preparation of shaped aluminum foam parts by investment casting. Journal of Materials Processing Technology. 314:117897.

[5] Kumar, M., Singh, R. K. R., Jain, V., (2023). Characterization of mechanical and metallurgical properties of AA6063 foam developed by friction stir precursor deposition technique. Journal of Adhesion Science and Technology, 37(18): 2608-2625.

[6] Papantoniou, I. G., & Manolakos, D. E., (2024). Fabrication and characterization of aluminum foam reinforced with nanostructured γ-Al2O3 via friction stir process for enhanced mechanical performance. The International Journal of Advanced Manufacturing Technology. 130(11), 5359-5368.

[7] Wang, S., Pu, B., Liu, G., Zhang, X., Sha, J., Zhao, N., Yang, X., (2024). Research on compression-compression fatigue properties of carbon nanotubes reinforced closed-cell aluminum matrix composite foams by reinforcement content design. Engineering Failure Analysis, 159:108117

[8] Wang, S., Yang, K., Xie, M., Sha, J., Yang, X., Zhao, N. (2024). Effect of carbon nanotubes content on compressive properties and deformation behaviors of aluminum matrix composite foams. Materials Science and Engineering: A, 898:146391.

[9] Gao, Q., Su, X., Feng, Z., Huang, P., Wei, Z., Sun, X., Zu, G. (2024). Preparation, bubbles evolution, and compressive mechanical properties of copper-coated carbon fibers/aluminum foam sandwich panels. Journal of Materials Research and Technology. 30:375-384.

[10] Pang, Q., Wu, Z., Hu, Z., (2022). The influence of process parameters on the preparation of closed-cell aluminum foam by friction stir processing. The International Journal of Advanced Manufacturing Technology, 120(3), 2489-2501.

[11] Rathore, S., Singh, R. K. R., Khan, K. L. A., (2021). Effect of process parameters on mechanical properties of aluminum composite foam developed by friction stir processing. Proceedings of the Institution of Mechanical Engineers. Part B: Journal of Engineering Manufacture. 235(12), 1892-1903.

[12] Guan, R., Wang, Y., Zheng, S., Su, N., Ji, Z., Liu, Z., Chen, B., (2019). Fabrication of aluminum matrix composites reinforced with Ni-coated graphene nanosheets. Materials Science and Engineering: A. 754:437-446.

[13] Taşcı, U., Yılmaz, T. A., Karakoç, H., Karabulut, Ş., (2024). Enhancing Wear Resistance and Mechanical Behaviors of AA7020 Alloys Using Hybrid Fe3O4-GNP Reinforcement. Lubricants. 12(6), 215.

[14] Kurapova, O. Y., Smirnov, I. V., Solovyeva, E. N., Konakov, Y. V., Lomakina, T. E., Glukharev, A. G., Konakov, V. G., (2022). The Intermetallic Compounds Formation and Mechanical Properties of Composites in The Ni-Al System. Materials Physics & Mechanics. 48(1), 136-146.

[15] Surappa, M. K., (2003). Aluminium matrix composites: Challenges and opportunities. Sadhana. 28(1-2), 319-334.

[16] Abdel-Rahman, M., El-Sheikh, M. N., (1995). Workability in forging of powder metallurgy compacts. Journal of materials processing technology. 54(1-4), 97-102.

[17] Tabandeh-Khorshid, M., Omrani, E., Menezes, P. L., Rohatgi, P. K., (2016). Tribological performance of self-lubricating aluminum matrix nanocomposites: role of graphene nanoplatelets. Engineering science and technology. an international journal, 19(1), 463-469.

[18] Şenel, M. C., Gürbüz, M., Koç, E., (2019). Fabrication and characterization of aluminum hybrid composites reinforced with silicon nitride/graphene nanoplatelet binary particles. Journal of Composite Materials. 53(28-30), 4043-4054.

[19] Gürbüz, M., Can Şenel, M., Koç, E., (2018). The effect of sintering time, temperature, and graphene addition on the hardness and microstructure of aluminum composites. Journal of Composite Materials. 52(4), 553-563.

[20] Ghodrati, H., Ghomashchi, R., (2019). Effect of graphene dispersion and interfacial bonding on the mechanical properties of metal matrix composites: an overview. FlatChem. 16:100113.

[21] Yang, S., Gao, X., Li, W., Dai, Y., Zhang, J., Zhang, X., Yue, H., (2024). Effects of the graphene content on mechanical properties and corrosion resistance of aluminum matrix composite. Journal of Materials Research and Technology. 28:1900-1906.